Modeling a Channel Migration Corridor for the 59-Mile Segment of the Missouri National Recreation River

Final Report

Stephen T. Lancaster, PhD* (Oregon State University)
Robert B. Jacobson, PhD (US Geological Survey)
Sky Coyote (consultant to OSU)

March 15, 2009

*Corresponding author: lancasts@geo.oregonstate.edu

Contents

Contents

Notes

Most of the 73 figures in this report have been encoded at 150 dpi in order to save space. This resolution should be quite sufficient for on-line viewing. Figures 41-46 have been encoded at 300 dpi for printing, as they contain more detail and represent the main results of this study. Figure 66 is also at 300 dpi.

Although some references to sources of information are inserted into the text, this is meant to be an informal report. There is a short bibliography on page 99 which lists the primary references used, and gives a short description of each. These items may be considered as interesting further reading for anyone who wishes to know more about this subject.

1.0 Abstract

This project represents an attempt to predict a 100 year migration corridor for the 59-mile segment of the Missouri National Recreational River from Gavins Point Dam to Kensler's Bend (approximately from Yankton, South Dakota, to Ponca, Nebraska). This prediction is based primarily upon the results of running multiple river simulations using the Johannesson-Parker 1989 meandering model. Several computer programs were written in Python (also using the WxPython and NumPy libraries) to digitize the banks of the Missouri River from USGS topographic maps and Google Earth satellite images, to calculate the river centerline and width, to digitize the river valley wall boundaries, to perform the meandering simulations while maintaining river points within the simulation boundaries, and to check for and remove loop cutoffs (switchbacks in the river which touch or cross one another). These programs were used to run many (3612) slightly different 100 year simulations in order to accumulate 2d valley coverage statistics showing the individual and aggregate locations of the various simulated rivers over time, and to perform a sensitivity analysis of river evolution with respect to input parameter values. This data will be useful in planning river management and land use during the next century, and in assessing the impact of the river on the proposed growth of structural and population development within the valley. In addition, a simple multiple-thread river model is presented as an example of future research on this topic.

2.0 Introduction

SUMMARY -- The initial objective of this study was to predict the lateral motion and migration of the 59-mile segment of the Missouri National Recreational River by simulating the evolution of the geometry of this segment using one or more currently published meandering models. The study would attempt to answer the following question: given the initial configuration of the river at the present day, how far from this configuration would the simulated river travel, and in which directions, during the next 100 years? However, this goal proved to be impossible to attain due to the inability of current 'state of the art' meandering models to adequately represent and predict the motion of the actual river in a single simulation, making use of digitized bank coordinates and measured physical values for input parameters. It was clear that to accomplish this goal would require the development of new models of river meandering and evolution which were beyond the scope of the present study.

Instead, we sought the simplest possible solution that still captured most of the physics of the river's migration, but making use of a large set of similar but slightly different simulations using the traditional methods to yield an aggregate probabilistic result. Thus, rather than attempt to predict the evolution of a single simulated river with great accuracy, it was decided to make use of a large set of simulations, each having moderate accuracy, to predict the evolution of a population of similar rivers, and to make statements about the likely evolution of a single river based on the behavior of this population. Specifically, the '100 year migration corridor' was to be determined from the fraction of this population of simulated rivers which reached and occupied various points within the river valley during the course of the simulation, and from the boundaries that were defined by the limits of these regions and the area they enclosed.

BACKGROUND -- The Missouri River is the longest river in the United States, estimated at 2,540 miles (4,090 km) for the total length of all reaches. From its origins in Montana and Wyoming until it joins the Mississippi River near St. Louis, the Missouri acquires about 1/6 of the total surface runoff water from rain

and snow in the continental U.S. During the past 200 years, the shape and behavior of the Missouri River has been changed considerably by human intervention aimed toward the development of flood control, navigation, irrigation, hydroelectricity, water supply, and recreation. While the Missouri River of 200 years ago was generally free-flowing and unpredictable, the river of today is tamed by 600 miles of reservoirs and 800 miles of artificial channels, and six dams which limit its flow and sediment content. However, in 1978, 59 miles of the river from Gavins Point Dam, near Yankton, South Dakota, to Ponca, Nebraska, were designated as a nationally protected area where the conditions and environment of the river would be maintained closer to its free-flowing and environmentally-friendly ancestry. In 1991, another 39 miles of the river from Fort Randall Dam to Running Water, South Dakota, were also included in this mandate, the two segments together being known as the Missouri National Recreational River.

The present study is concerned only with the 59-mile segment of the MNRR, which is considered to be the 'wilder' and 'more natural' of the two segments. This segment of the MNRR, on the South Dakota and Nebraska state border, remains closer to the shape, appearance, and behavior of 200 years ago than do other segments of the Missouri River, and it is relatively free to meander across the surrounding valley much as it did before human intervention and deliberate engineering. Although there are currently several flow regimes in this segment which have been altered artificially, part of the intent of the MNRR designation was to preserve the free-flowing condition as much as was practical to do so, given the often conflicting constraints and desires of the local population and various group entities which manage the river. There has been considerable success in this respect, as the 59-mile segment of the MNRR today has numerous islands and small secondary channels, submerged and surface sand bars (with and without persistent vegitation), and naturally eroding banks and surrounding topography similar to the historical river.

Land area adjacent to the MNRR is owned both publicly and privately in Nebraska and South Dakota. Many individuals and groups are engaged in activities intended to curtail or repair bank erosion, maintain ecological habitats for indigenous species (including those which are threatened or endangered), and generally improve recreational opportunities on the river. Nevertheless, these activities do not always coexist harmoniously, nor do they have the same goals in mind. For example, while about one third of the banks along the 59-mile segment of the MNRR have been artificially stabilized in some manner since 1978 --mostly to protect privately owned land--, during the same time period naturalists and ecologists have come to realize that channel migration and bank erosion are necessary for creating and maintaining the aquatic and riparian habitats of the river, and that curtailing or halting the meandering of the river would entail the destruction of many of these habitats and preclude the formation of new ones. Similarly opposing viewpoints exist concerning the costs and benefits of water level and flow rate, and potential alterations to bed geometry for purposes of recreation and navigation.

Most property adjacent to the MNRR is privately owned, while the remainder is divided among tribal, state, and federal entities. Managing the natural resources within and near to the river in a way that is amenable to all viewpoints is quite difficult. Currently, ecological habitats within and adjacent to the MNRR contain at least 237 bird species, 80 fish species, 17 reptile species, nine amphibian species, and more than 40 mammal species in addition to Homo Sapiens. Threats to these habitats and other natural resources include fragmentation and loss due to residential, agricultural, and other commercial development, pollution from agriculture, industry, and recreation, the construction and maintenance of artificial erosion-control structures, and the introduction of invasive species from other ecosystems, as well as disputed management issues concerning the control of water level, flow, and channel migration appropriate to different uses of the

river. In addition, shoreline areas are disappearing at an accererating rate as more primary dwellings, vacation homes, and other structures are built on desirable river-front property.

Before the construction of six major dams changed the natural variation in flow due to seasonal runoff, the Missouri River was prone to periodic flooding, bank erosion, and concomitant sediment transport and redeposition that lead to considerable temporal and spatial variation in the river channel, shallows, and surrounding floodplain. Although the river carries considerably less sediment volume today, it still retains the nickname "Big Muddy", and can be clearly distinguised from the Mississippi River where the two join in St. Louis, due to its higher sediment content. Historically, river migration, erosion, and sediment redistribution was responsible for sandbar formation and destruction which created transient habitats, washed others away, and created new ones elsewhere. This resulted in a constant turnover of rich and diverse populations of plants and animals within and along the banks of the river.

After 1944, as a result of the construction of dams, and the consequent regulation and attenuation of both the averge flow and its high seasonal variation, the Missouri River lost many of its most characteristic features, including braids, islands, sandbars, chutes, and the oxbow lakes formed from previously cutoff segments of the meandering river. These modifications have in turn been responsible for the loss of aquatic and riparian habitats along the river, and declines in ecosystem diversity, stability, and longevity have been the overall result. Since the natural flows, floods, and their associated ecological benefits have been somewhat curtailed, the relatively free-flowing segments of the MNRR have become particularly important, especially in so much as they are permitted to continue to meander uninhibited across the planform of the valley. There has been increased recognition of and interest in the importance of these segments in terms of their ability to resist habitat loss and further damage to the ecology of the river, and in preserving undisturbed areas which still remain.

This report is based on the hope that an improved understanding of the spatial and temporal variability of MNRR geometry and dynamics can contribute important information to those people who make decisions about the river and the management of its resources. Specifically, a quantitative prediction of channel migration that delineates the probable limits --both nominal and extreme-- of river motion during the next century should provide managers with necessary information to assess proposed intervention activities according to the inherent characteristics of the habitats and other resources contained within those regions. In the case of bank-stabilization decisions, for example, this prediction will delineate reaches in which channel migration rates are inherently higher or lower than the norm, and where there is more or less danger to the loss of surface area, sediment, or biomass. Such information can be used to determine where channel migration can be tolerated and where channel migration presents unacceptable risks or conflicts with other uses of the river.

An understanding of the process of river meandering is essential to an understanding of river processes in general. That general understanding is important for people whose work covers a broad range of spatial and temporal domains and their transitions on scales from the erosion of pasture land from year to year to the evolution of an entire river basin over geologic time, with the consequent changes in ecological communities and niches which are a function of these transitions. However, based on observations of the geometry of the MNRR made from maps and satellite photographs, and comparisons of this geometry to that produced by meandering simulations, we have found that important aspects of migrating behavior were not represented in or predicted by the currently published 'state of the art' models, especially the Johannesson-Parker 1989

model used in this study. This is primarily due to the fact that such models represent the river as an idealized single channel having only a centerline and width, and a trapezoidal channel cross-section, rather than their failure to include some essential aspect of the physics in their equations of motion.

Current meandering models do not take into consideration any of the 3-dimensional aspects of the topography of the river bed or banks and surrounding shallow areas, specifically the many islands and submerged and surface bars which are contained within the 59-mile segment of the MNRR. We feel that in order to accurately understand and predict the evolution of a river such as the MNRR, a model which is aware of this 3-dimensional topograpy and the multiple channels, chutes, and braids which contribute to the overall flow and migration of the river is essential. Although the development of a new meandering model of this type is beyond the scope of this project, we present the results of some initial attempts at multiple-thread simulations in the discussion section 5.4.3.1 later in this report which indicate the direction in which future research might go.

CONCLUSION -- The objective of this study was to develop a quantitative prediction of motion of the 59-mile segment of the MNRR that delineates migration domains and ranges which are amenable to potentially different management strategies. The main tool to accomplish this objective was the Johannesson-Parker 1989 meandering model, considered to be the nominal mathematical approach for such studies. Although this tool was not sufficient to develop a prediction based upon a single simulation of the river, we feel that it was sufficient to do so when employed in a novel way --specifically to generate a large population of simulations, each of which contributed a small part to the overall prediction. Nevertheless, the present work leaves some questions unanswered relative to the relationship between the river and its representation as a simple mathematical model. To answer these questions, the development of a multiple-thread meandering model more appropriate to the specific characteristics of the MNRR should be pursued as a subsequent project.

The Missouri National Recreational River preserves two segments of some of the last free-flowing portions of the once-wild Missouri River. The eastern 59-mile reach --with its wide, meandering channel, shifting islands and sandbars, and many small secondary channels-- contains some of the best natural aquatic and riparian landscape associated with the Missouri River along its entire length, and perhaps the last naturally preserved floodplain and wetland habitats on the river or anywhere on the eastern border of the Great Plains. The MNRR today represents a diverse and dynamic ecosystem whose future is uncertain. Both care and well-informed deliberation should be employed in its management and use for several generations to come.

2.1 Study location

The 59-mile segment of the Missouri National Recreational River is situated at (and defines) the eastern border between South Dakota and Nebraska. This reach of the river extends from Gavins Point Dam (at the eastern edge of Lewis and Clark Lake), near Yankton, South Dakota, south-eastward for approximately 95 river kilometers to the city of Ponca, Nebraska. The inlet at the dam is at longitude -97.480463 decimal degrees, latitude 42.850196 decimal degrees, and the 'outlet' at Ponca (an arbitrary point delimiting the south-eastern end of the river in this study) is at longitude -96.647947 decimal degrees, latitude 42.560457 decimal degrees.
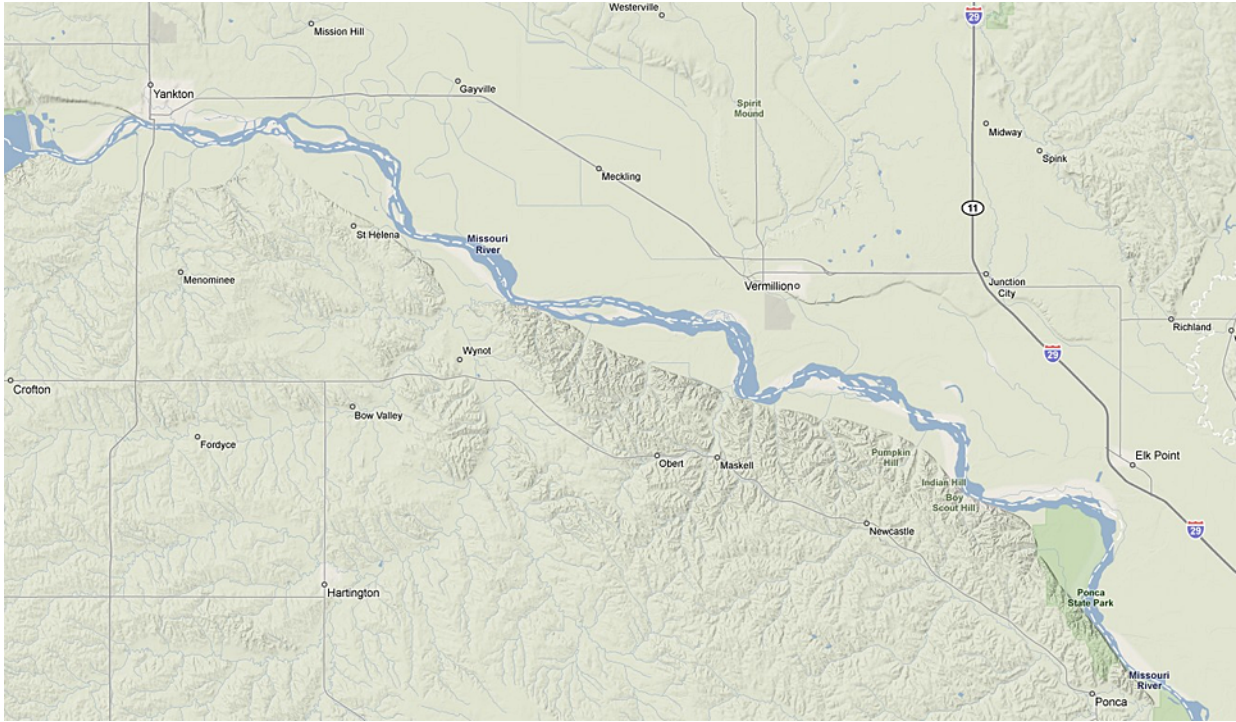
Figure 1: Map of study area from maps.google.com.

Figure 2: Satellite mosaic made from images at earth.google.com.
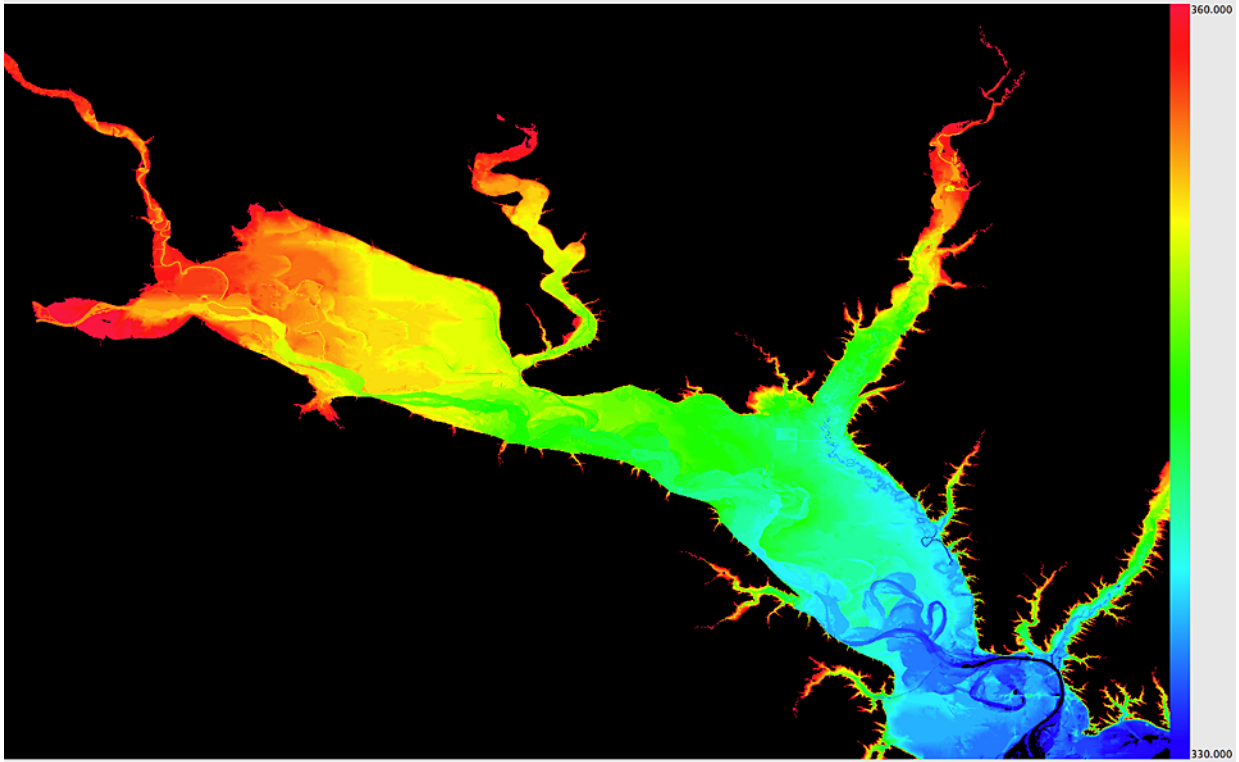
Figure 3: Elevation of study area from National Map.
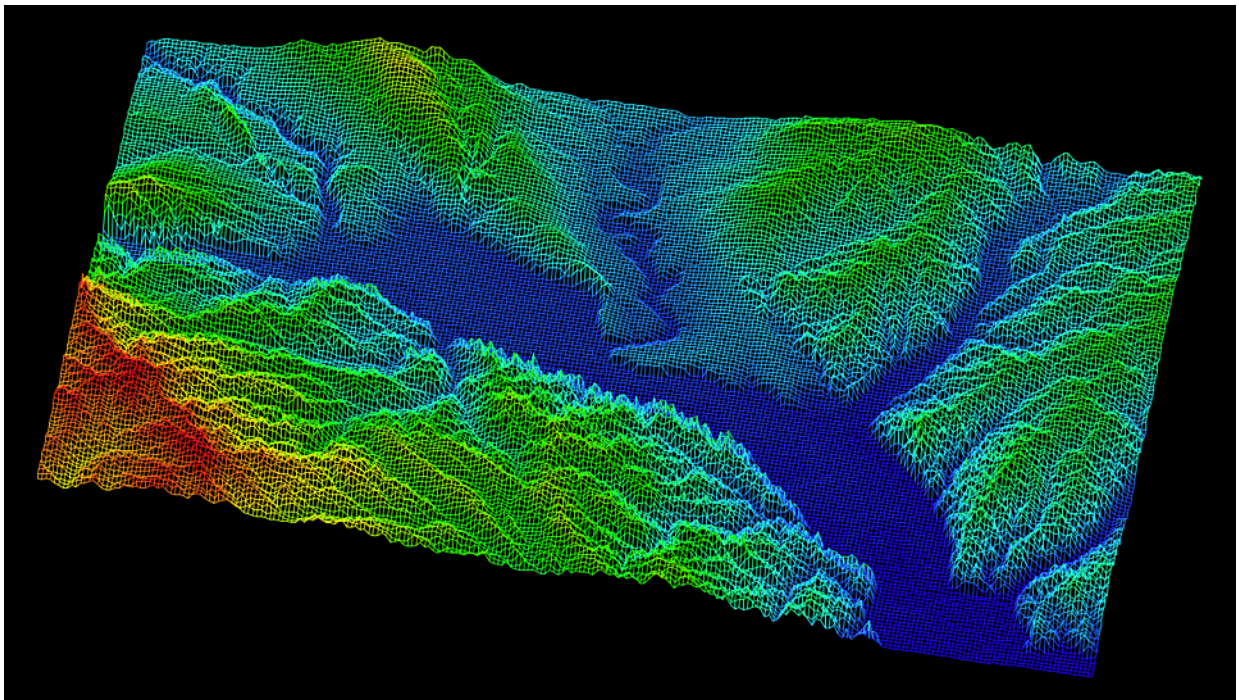
Figure 4: Study area in 3d using National Map Digital Elevation Model.

After leaving the concrete inlet at Gavins Point Dam, the river is relatively free to meander bewteen the southern wall of the valley (which rises above 1300' near the river and to over 1500' beyond it) and the

relatively flat plain to the north, before it enters the concrete channel wall and wing dikes of Kensler's Bend, and then continues on through Sioux City, Iowa. The inlet is at river mile 811 and an elevation of 354.76 m, while the outlet --almost 100 km away-- is at river mile 753 and an elevation of 336.40 m. The surrounding area is relatively flat to within 20 m. The extent of this valley, and the limit to the potential migration range of the river, was defined in this study by the approximate 1200' (365.76 m) topographic line. The maps and satellite images used in this study will be discussed in more detail in section 3.2.

2.2 Dynamics of river meandering

Meandering rivers and streams are familiar features of the Earth's landscape. The topography of meandering flows often consist of relatively flat valley or canyon floors, as in the case of the 59-mile segment of the MNRR. There are also meandering flows which incise vertically down into the surrounding landscape, creating terraces at different depths, but in this study we are concerned only with meandering motion which occurs in two dimensions primarily at a single depth near to the surface level. In these cases, channel migration tends to flatten the valley bottom over time by net erosion of the banks and deposition of alluvial sediment carried by the flow from upstream or other parts of the valley. Thus, the transport of sediment from one point to another, either along the downstream direction of flow, or cross-stream in the direction of channel migration, is an important function of the meandering process.

Although it is perhaps natural to expect that flowing water would prefer to travel in a straight line, this is actually not the case, and it is rare to find a river running in a straight line for very long. From above, rivers usually look like convoluted lines consisting of many loops which frequently change direction and curve back upon one another. The origin of the term 'meander' is reputed to be the name of the Menderes river in present-day Turkey, although the ancient Greeks knew this as Maiandros or Maeander. This river is characterised by a very convoluted path along the lower reach, and has a flat flood plain which is much wider than the currently active meandering zone.

Figure 5: Example of meandering river from en.wikipedia.org.

A 'meander' in general is a bend in a sinuous watercourse, although 'to meander' means simply to move in a somewhat erratic or inconstant manner, changing direction often. A meander is formed when the moving

water in a river erodes the outer banks and widens its channel. The material removed from the migrating bank is carried by the flow and made available for potential redeposition somewhere downstream. A river of any size may exhibit a meandering course, alternately eroding sediment from the outside bank of a bend and depositing it elsewhere (possibly on the inside bank), and then from the other bank as the newly formed meander causes a change in the direction of the bend. The result is a snaking pattern of loops as the stream wanders back and forth across its valley. Over time, meandering loops generally tend to migrate downstream with the flow.

When a meandering loop curves back upon itself sufficiently so that the channel intersects itself, the main flow of the river then takes a 'shortcut', excising the loop from the main stream, and an 'oxbow' lake is formed, named for the characteristic crescent shape of the now unmoving water remaining in the isolated basin. As additional bends form and are cut off, many oxbow lakes will be left behind as a legacy of previous locations of the river, and will eventually fill with vegitation and other biomass, or will dry up. However, rather than intersecting itself, a recurring loop may suddenly change direction again and continue to migrate, forming a 'compound bend' consisting of two or more sequential loops linked together.

These two mechanisms --cutting-off and compound bend formation-- are both important to the development of complex meandering stream patterns. Bends removed when the channel bypasses them by seeking a shorter path across their intersection lead to the main axis of the flow shifting to one side or another at different locations, and the channel course becomes erratic as the discarded loops are shed first from one side of the flow, and then from the other. In the absence of cutoffs, bends continue to grow and form compound bends, increasing the overall length of the river until they too are eventually excised. In this way, the length of a river will grow and then shrink again in bursts, as new bends and compound bends are formed which gradually increase the overall length, and are then cut off and removed all at once.
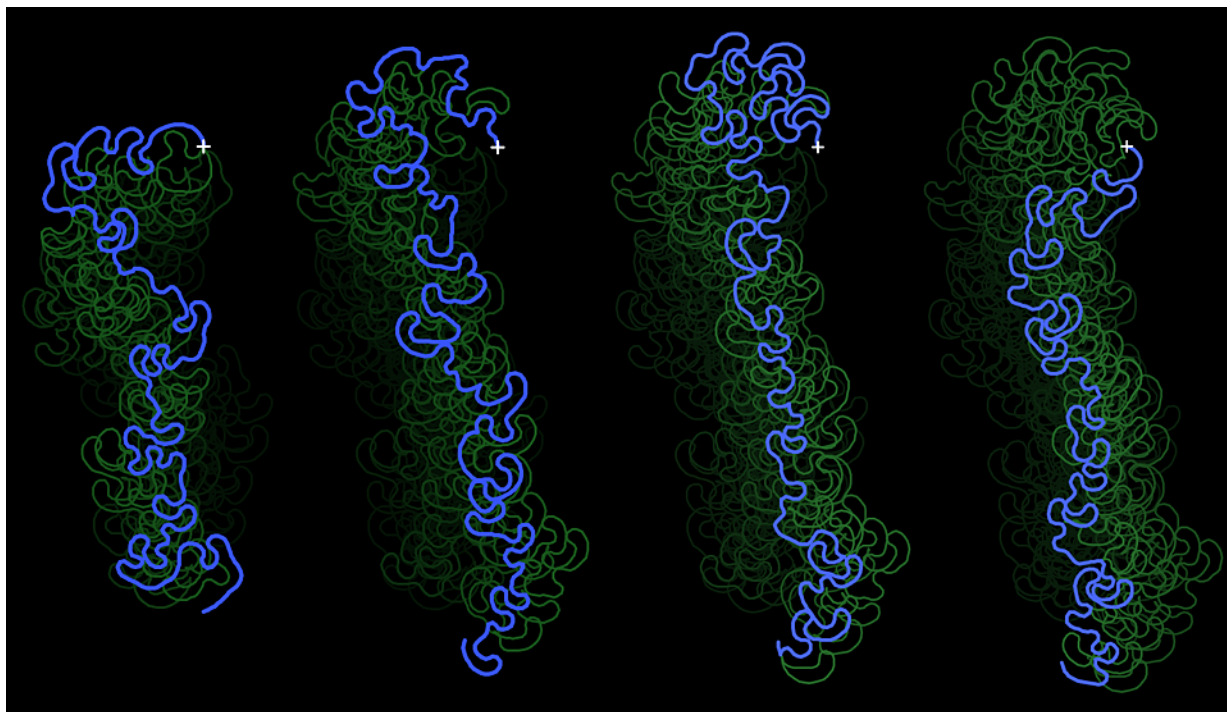

Figure 6: Evolution of meandering river shape.

The meander-generating process in each river is both dynamic and unique. River meanders develop throughout the years, and continue to change over long periods of time, perhaps never converging on a stable or quiescent pattern. The perpetual creation of meanders is a natural phenomenon which occurs similarly in rivers all around the globe, so that river meandering is one of the most predominant geometric phenomena on the surface of Earth. The physical processes encountered and created by meandering rivers have long intrigued scientists and engineers alike. Not only does the characteristic shape of river bends and beds give rise to a complicated two- or three-dimensional water flow field, but --equally important--, the flow field reshapes the bends and bed surface through the process of erosion, indicating the existence of a complex feedback loop between water flow and bed topography.

An intriguing observation about meandering geometry and dynamics is the similar basic shape of all meanders, despite the different geophysical locations, conditions, and material properties of rivers around the world, and that these similarities can be captured in mathematical models and computer simulations. One common, and possibly counter-intuitive, characteristic shared by meandering rivers all around the world, appears to be the adage that --similar to 'nature abhors a vacuum'-- 'flowing water abhors a straight line'. This observation is often considered surprising (although it should be familiar to anyone who has handled a wildly undulating garden- or fire-hose), and begs the question of why water conduits of any size become sinuous in the first place.

The answer appears to be that water flowing in a straight line is an example of an unstable equilibrium --similar to that of a pencil balanced upon its point-- which does not endure for long. An equilibrium is unstable because any slight perturbation away from that state causes additional perturbations of an increasing magnitude. In the case of a meandering river, what contributes to this instability is the observation that water (or any mass) flowing or moving through a conduit which changes in direction (as around a curve or bend) tends to act in a manner which exaggerates that change in direction, and therefore the shape of the curve over time. There are at least two possible explanations for this phenomenon, which lead to a general division bewteen the 'forced based' and the 'speed based' models of meandering.

This instability, and the positive feedback associated with it, can be demonstrated by a simple simulation of meandering in which the rate at which points on a river migrate laterally cross-stream to the direction of the flow is a simple multiple of the signed curvature of the river at that point. Curvature can approximately be considered as the relative amount the river changes direction in angle per unit of its length (where angles to the left are considered 'positive', and angles to the right 'negative'), although in this study curvature is calculated specifically as the inverse of the radius of a circle passing through every three sequential points of the river (see sections 3.4.1.1. and 3.4.1.2 for details). Thus, gentle bends in the river have a small curvature, sharp bends have a high curvature, and straight line segments have zero curvature.

Consider an 'almost straight' segment of a hypothetical river consisting of a set of equally-spaced sequential points arranged on a straight line to which has been added a slight (and potentially imperceptible) amount of random noise. Initially the curvature everywhere is essentially zero, and there is no meandering motion. However, anywhere randomness has made the points non-colinear (as would be expected on an actual river), there will be some non-zero curvature. Furthermore, in general the random nature of the non-linearity will make the sign of the curvature change from point to point along the length (i.e. first the river will bend very slightly to the left, and then very slightly to the right, etc...), and this is enough to begin the process of instability which leads ultimately to meandering dynamics. Shown below are a sequence of configurations

of a simulated river, at 0, 750, 770, 800, 820, and 900 steps.
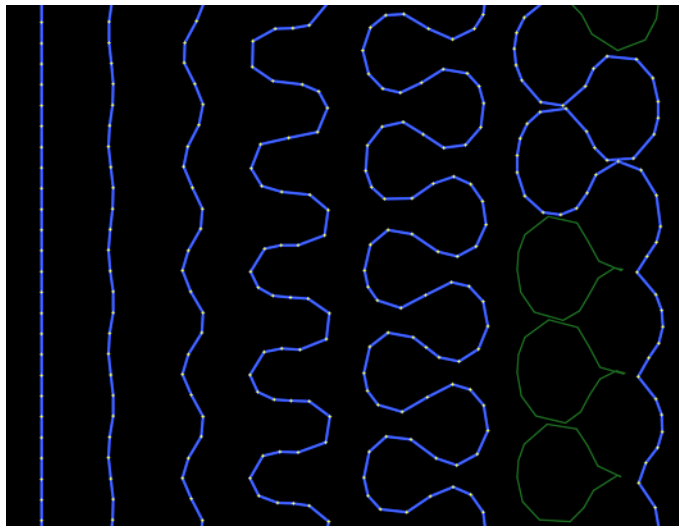
Figure 7: Non-colinear instability leads to meandering.

Although the river appears quite straight to the eye initially, small random variations in curvature eventually pull sequential points in opposite directions, as each point migrates in response to the signed curvature of the river at that position. As each point moves away from its neighbors, this increases the curvature, which increases its rate of migration in a positive feedback loop. As the points move further apart, new points are inserted between them, and the total length of the river increases. Eventually the process of migration stabilizes into the familiar meandering loop pattern as the curvature along finite lengths of the river changes more gradually and becomes similar in value at neighboring points. With time, the loops become large enough to intersect, and they are removed.

Therefore, once a sinusoidal channel exists, it undergoes a process during which the size and curvature of its loops increase due to the positive feedback of their motion, and then begin to slow to a near constant average rate of growth as that feedback becomes mixed or negative due to the similarity of loop curvature at neighboring points. There are two different, but not mutually inconsistent, kinds of physical explanation for the feedback which results in meandering motion. In the first kind, the change in bend size and curvature is the result of a lateral force which causes the change in direction as the flow goes around the bend (an acceleration), and this force in turn causes a change in the non-rigid geometry of the bend wall (a stress and strain). In the second kind, any difference in the speeds of flow near the inside and outside banks of a bend causes a differential erosion or deposition of material from the bend walls, resulting in the migration of the channel.

This study makes use of meandering models of the second kind, of which the Johannesson-Parker 1989 model is the primary method in the simulations which follow. The JP89 model expresses the bend near-bank flow speeds in terms of linear perturbations of the mean value at the center of the flow, in between the banks. In the model, the rate of erosion at the outer bank of a bend is proportional to the speed perturbation at that point. If the speed of the flow near the outer bank exceeds the centerline value by an amount u1b (in the case that u1b > 0), the outer bank will erode, otherwise it will deposit material. The amount of erosion or deposition is taken to be proportional to the magnitude of u1b. Material eroded from one bank of a bend is

simply assumed to be transported to and deposited on the other bank, so that both banks of the channel migrate at the same rate, and the width of the river does not change.

The JP89 paper presents an analytical model for calculating the lateral distribution of the averaged primary flow velocity (speed and direction) in meandering rivers. Their solution is actually quite complicated, and makes use of 2 coupled second-order differential or integral equations, which have subsequently been implemented in computer code by the autthors of this (MNRR) study. In terms of the mechanics of the model, the solution gives rise to a helical vortex about the midline of the flow, in the direction of the flow. This vortex creates a secondary flow in bends which is radially outward at the surface of the water, and radially inward near the river bed. This secondary flow powers a convective transport of primary flow momentum (and eroded sediment) leading to a significant outward redistribution of primary flow velocity (in other words, the flow is faster near the outer bank, and eroded sediment from the outer bank is moved to the inner bank by the vortex).

The JP89 paper attempts to accurately explain and quantify the phenomenon of redistribution of primary momentum by secondary flow at a linear level, in the simplest possible fashion. The helical vortex is explained as a transfer of momentum from the inside of the bend to the outside. As soon as the flow enters the bend, some of its linear momentum becomes angular. As the mass of the water goes around the bend, a centripetal force is added to gravity causing the surface of the water to tilt, elevating it on the outside of the bend. This additional volume of water is provided transversely from the inside of the bend, creating a radial surface flow cross-stream. The water then moves down to replace the subsurface water pushed radially inward at the end of the bend to re-establish a level surface. The result is a helical flow, and the greater the curvature, the greater the angular momentum transformed and the stronger the cross-stream secondary current.

Thus, the JP89 model makes use of force and angular momentum to create a speed-based meandering model. Increasing the curvature of the bend increases the force and concomitant change in angular momentum, which in turn increases the inclination of the water surface, the helical flow, and the amount of erosion occurring on the outside of the bend. This explains the positive, self-intensifying, feedback process described above: greater curvature results in more erosion of the bank, which results in greater curvature, more erosion, etc... The actual calculations of the JP89 model used in this study will be discussed in more detail in section 3.4.2.3.

The work performed on the JP89 and other models has done much to further the understanding of the meandering process, but a key question is left unanswered: that is, how important is the effect of the 3-dimensional topography of a specific river in 'steering' the evolution of meandering, in light of the success or failure of much simpler geometric or physical models? A new approach combining both the 3-d geometry and physical properties of actual river beds is called for to address otherwise unaccounted-for effects over long channel distances and migration times, where such rivers are not limited to simple bends with small curvature, and where there are complex feedback loops between flow velocity and bed topography.

Determining the essential physics required to accurately model a specific river's evolution might be considered a 'holy grail' of geophysical science. Different mathematical formulae attempt to relate the many variables of meandering geometry and dynamics in various meaningful ways, not necessarily with considerable success. In some cases, numerical parameters and functions can be established which affect the

shapes of similar meandering curves in a consistent way. Nevertheless, the space- and time-varying shape of a particular meandering river depends ultimately on the geometrical and physical characteristics which can be measured from it, not on the intricacies of mathematical equations.

In order to develop a new and useful meandering model, we must first address the proper interaction of the individual elements of the model: the 3-d motion of the flow, the 3-d geometry and material properties of the meandering channel, and the 3-d topography and material properties of the landscape where they meet. However, geometry alone is not enough. For a fuller understanding of the evolution of these elements, sediment input to the channel both upstream of the flow and from the surrounding landscape due to erosion and migration of the channel must also be addressed, as well as the deposition of that sediment on downstream banks and bed and its effect on the alteration of that geometry. However, a thorough treatment of this issue is well beyond the scope of the present work.

Good or bad mathematical models can be developed for physical phenomena, and they differ from one another in one respect by their ability to accurately represent properties of the phenomenon being investigated, and to predict observable changes in these properties over time. A good mathematical model or simulation of a river must help predict essential changes in the flowing path, the containing conduit, and the surrounding landscape, and by doing so allow human decision and intervention in order to manage resources that increase the benefit that the river carries as a source not only of commerce, but of the lives of the people, animals and vegetation around it.

2.3 Simulation strategy used in this study

The simple meandering models typically used to simulate the shape and motion of rivers cannot generate the specific detail which is unique to the Missouri River. Although the Johannesson-Parker 1989 model is considered to be the 'state of the art' in this field, it cannot simulate the multiple channels, the 2-dimensional 'braiding' patterns, nor the many chutes, islands, and sand bars (both submerged and above the water surface) which are integral features of the 59-mile segment of the MNRR. However, by performing a large number (3000+) of simulations initialized to the shape of the current river, and each using slightly different physical input parameters, we can generate a diversity of river shapes and dynamics that --although different from one another and from the precise shape of the actual river-- will, taken together, approximate what we think the river is likely to do during the next 100 years.

These aggregate results, although completely deterministic in nature, provide a probabilistic interpretation of what the single actual river might do, and where it might go, during 100 years. 'Target' areas within the river valley can be defined which correspond to towns, roads, airstrips, parks, and other geographic landmarks. The aggregate 100 year 2-dimensional coverage array can then be overlaid on these targets to see which of them are encroached upon by the river, to what degree, and when. Specifically, the 2-d coverage array indicates what fraction of all simulated rivers passes through any point (represented as 125 x 125 m square areas) within the valley at some time during the simulation. This array is calculated every 10 years, so that the potential progression of the river across the valley can be tracked over time.

A database was programmed to make use of information saved with each run of the simulation in order to track the course of every individual river over time to see when, and how much area of, each target it will

---

eventually reach and subsume. The database can also find examples of individual simulated rivers which reach and flood several designated targets at some time during the simulation, but which miss others. This information, along with the 2d coverage maps mentioned above, can be used to assess the relative danger from the river to specific locations within the valley at different times during the next 100 years. In addition, contour plots showing the percentage (e.g. 99%, 95%, 75%, 50%, 25%, 5%, 1%) of all simulated rivers reaching points in the valley indicate the relative danger of being overrun by the river during 100 years to towns and other regions lying on or inside these lines.

3072 different simulations were performed using the Johannesson-Parker 1989 meandering model. An additional 540 simulations were performed using a simpler model as a comparison. All 3612 simulations amassed over 16 Gb of 'raw' data, composed of individual binary files storing river shape coordinates, 2d coverage arrays, cumulative erosion, and other information at 10 year intervals, as well as images of each final river. Any piece of information from this data set can be retrieved and used for analysis by the database program, and additional images and image mosaics of the rivers can be created as desired. Analyses of these results contribute over 155 Mb of additional data. Software and tests performed previous to the full set of simulations bring the total project size to over 17 Gb. Some of this data is available online at the website listed below.

2.4 Link to companion website

This report, a 3-page summary of the project, 33 detailed project updates, a software archive, and selected data sets, are available online at:

```
http://www.skycoyote.com/sky/MNRR/
```

This site contains many additional images and calculation details, and the summary pages are suited to a non-technical audience who is not familiar with this research.

3.0 Approach & methods

The overall approach used in this study consists of the following steps, each of which will be discussed in more detail in the sections below:

1. Create mosaics manually pieced together from several USGS topographic maps and Google Earth satellite images which cover the 59-mile segment of the Missouri National Recreational River and surrounding valley from Gavins Point Dam to Kensler's Bend.

2. Digitize the longitude and latitude coordinates of the left and right banks of the river, and the valley walls at the 1200' topographic line, at 100 m intervals.

3. Calculate the river centerline and width at 100 m intervals from the digitized left and right banks.

4. Convert the longitude and latitude coordinates to isotropic x and y coordinates based on a zero origin at the Gavins Point inlet using oblate ellipsoid geometry and multiple tangential planes.

5. Generate a set of input parameter combinations of physical values intended to yield a range of realistic

behavior in the simulated river using the Johannesson-Parker 1989 meandering model.

6. Run many 'constrained' river simulations using the valley boundaries and river inlet endpoint as fixed positions which limit the motion of the river.

7. Accumulate quantitative statistics for river length at several resolutions, erosion rate, total area eroded, occupied area (2d coverage arrays) of the valley, and occupation duration for {x, y} points in the valley, for all simulations.

8. Combine the valley coverage arrays from all simulations, and from subsets of simulations derived from specific combinations of input parameters, to create a 'common coverage' array which delineates the '100 year migration corridor' of the aggregate river at from 99% to 1% confidence levels.

9. Overlay the common coverage array and contours on maps and satellite images of the study area.

10. Designate 'target' areas in the valley, and calculate the fraction of simulations which reach and pass these areas, and their times of acquisition during the course of the simulation.

3.1 Computer software used

All of the computer software created and used in this study was written in the Python language, version 2.5.2, which is available free of charge for most computer systems at www.python.org. Python is a high-level cross-platform object-oriented programming language which is run by an interpreter program usually written in the C programming language. Python is well known for its ease of use and rapid development time. In the opinion of the authors of this study, all new scientific software should be written using Python, if possible. Also used were the WxPython 2.8.8.1 (www.wxpython.org) and NumPy 1.1.1 (www.numpy.org) libraries for graphics/user-interface and vector numerical calculations, respectively. Both libraries are also available free of charge for most computer systems.

All software was developed and run under the Apple Macintosh OS X 10.5.5 'Leopard' operating system. Development was performed, and simulations were run, on an Apple iMac 2.4 GHz Intel Core-2 Duo with 4 Gb of Random Access Memory and on an Apple MacBook 2.0 GHz Intel Core-2 Duo with 2 Gb of RAM. However, all software should run fine, with no or only slight modifications (e.g. for binary file access), on any Unix or other operating system which supports Python.

3.2 Maps & satellite images used

A single mosaic was made from 24 1957-1996 USGS 7.5' topographic maps which were individually downloaded from store.usgs.gov. These maps were rasterized from PDF, rotated by from 1.1 to 1.65 degrees clockwise, layered on a single canvas, and aligned by hand in Adobe Photoshop. The overall map projection was polyconic. The completed mosaic was 9726 x 7154 pixels. This contains sufficient detail for digitizing the river banks to better than 10 meter resolution, although we have extracted coordinates only every 100 m.
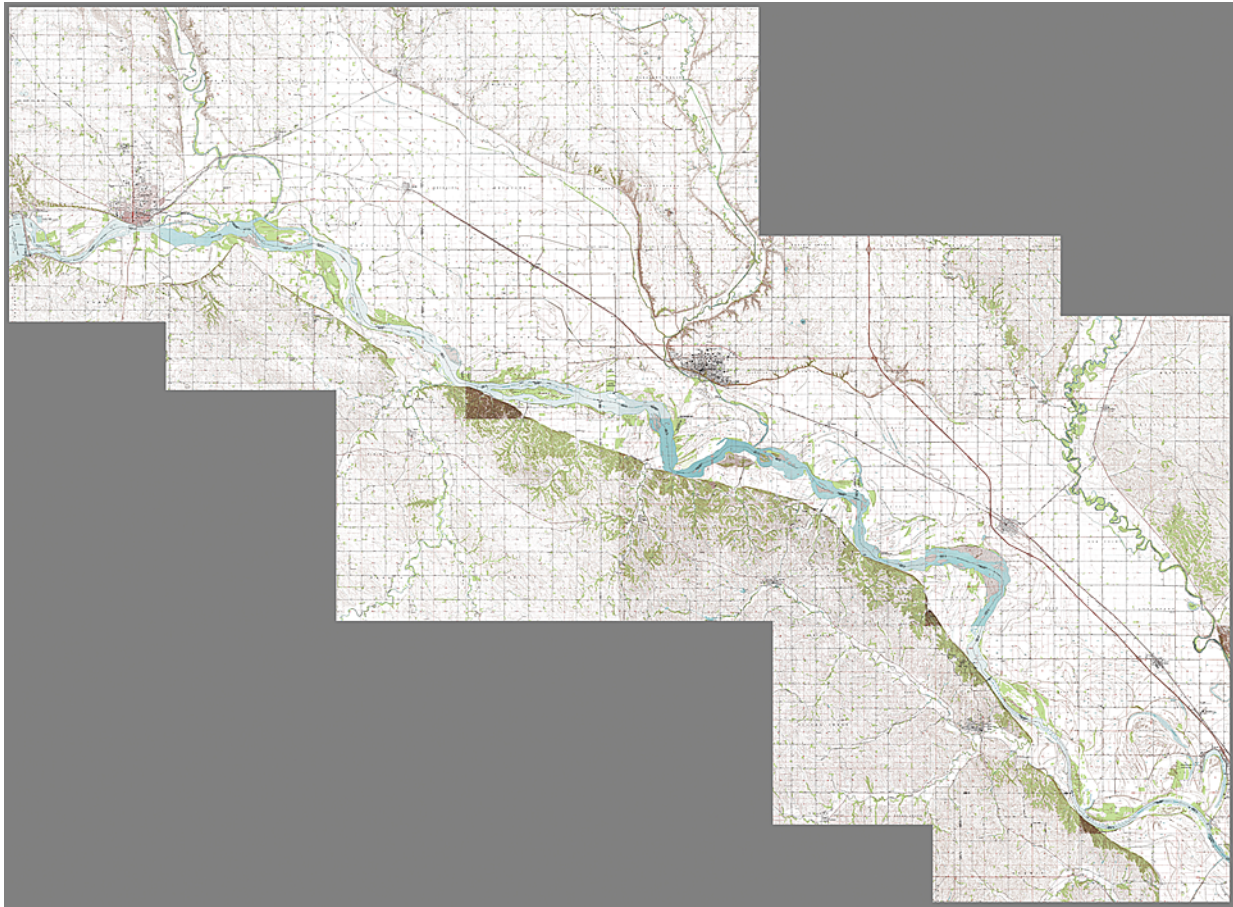
Figure 8: USGS topographic map mosaic.

A second mosaic was made from 17 Google Earth satellite images which were screen-captured at an 'altitude' of 20.17 km from earth.google.com using their free client program. These images were also assembled by hand in Photoshop. Although nothing is known about the actual projection used in these images, it is a reasonable assumption that they were also rectified individually via some form of digital image processing to create conic projections depicting a stationary 'birds-eye point of view'. This mosaic is shown in figure 2 in section 2.1.

By interpolating the satellite mosaic by 2x, and then independently adjusting the x and y scales to 103.5% and 103.05% respectively, the two mosaics can be overlaid and aligned at the same scale, even though the topographic maps were made at different dates from 1957-1996, and the satellite images were made much later (2006). Although both image sets were assembled by hand, the correspondence at both the Gavins Point Dam end of the river and the Sioux City end are quite good, and the alignment is virtually exact near the center of the mosaics. Since this provides a resolution of about 8.99 m/pixel and a visual error of at most a few pixels anywhere along the river, we feel that this alignment is sufficient for the 100 m discretization used in this study. While the position of the river can be seen to have changed in several places between the time the two image sets were acquired, the endpoints and other man-made features are the same in both.

Figure 9: Superimposed mosaics at Gavins Pt. and Sioux City ends.

3.3 Computer programs created for this study -- 3.3.1 Digitization of river coordinates

A simple Geographic Information System (GIS) program was written to semi-automatically digitize the coordinates of the river banks and valley walls from the map mosaic shown above, and to interpolate these coordinate paths to a resolution of 100 m using circular arcs (see section 3.4.1.1 for details). The meandering models described in section 3.4.2 below require a river centerline and width at all points as input, and the GIS program computes these based on the digitized bank coordinates (see section 3.4.1.3 for details).

This program is easy to use, and produces good results quickly. Program features include:

* A background image can be displayed as a guide.

* Points can be entered with the mouse on to multiple curves.

* Points can be added, inserted, selected, moved (by the mouse or keys), or deleted. Curves can be joined, split, or reversed.

* The current session can be saved to a binary file and restored so that digitization can continue at another time.

* All coordinates are in longitude and latitude decimal degrees. Coordinates reference landmarks (at least 2 required) which can be entered using known map positions.

* The display shows the longitude and latitude of the point at the window center, and the scale in meters/pixel at that point.

* Curve attributes (name, color, visibility, etc...) can be edited.

* The display can be zoomed in and out, and the background image and all points are rescaled accordingly.
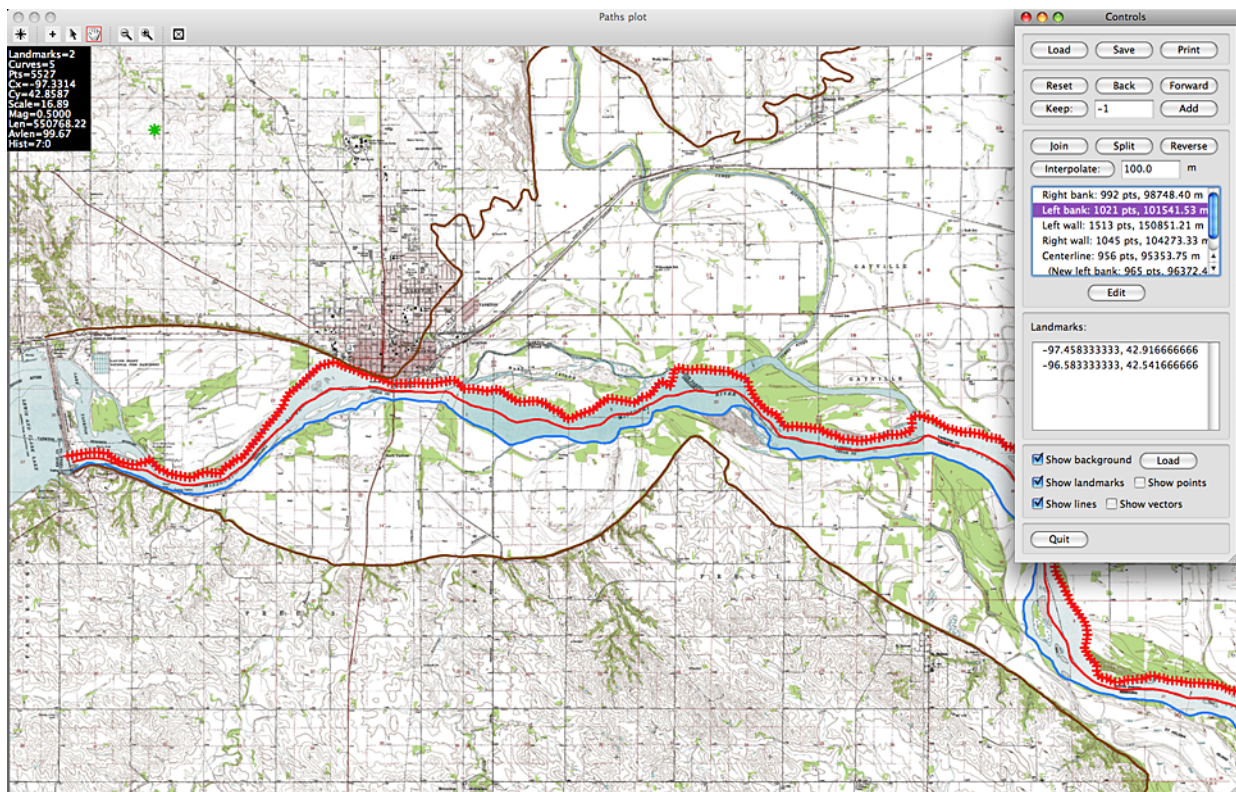
Figure 10: River digitization program.

The program has an unlimited undo and redo capability. The following operations automatically save a copy of the current data and settings in memory:

1. Adding a point.
2. Deleting points.
3. Moving points.
4. Joining paths.
5. Splitting a path.
6. Reversing a path.
7. Moving the background and points.
8. Zooming in or out.
9. Loading a new background.

Only the first of several contiguous additions, moves, or zooms is saved. In addition, the current state can be manually saved with a button at any time. Previous states can be visited by clicking another button, which in turn saves 'future' states for redoing, if desired. By saving all intermediate states, one can undo operations back to the beginning of the session, and then redo operations up to the end again. All past and future states are saved with the session file on disk, as well.

Points on each path can be resampled and interpolated at a designated resolution using circular arcs. After interpolation, points are evenly spaced and are placed on piecewise circular arcs (although distance is still calculated using the geodesic between each pair of points, as described on the next page). This has the effect of smoothing the curves, of ensuring that every point lies on a tangent to the river having a well-defined radius of curvature, and of maintaining a more continuous change of that curvature along each path.

Distances between points are calculated using oblate ellipsoid geometry:

$$M = M(\phi) = \frac{(ab)^2}{((a\cos(\phi))^2 + (b\sin(\phi))^2)^{3/2}}$$

$$N = N(\phi) = \frac{a^2}{\sqrt{(a\cos(\phi))^2 + (b\sin(\phi))^2}}$$

$$D \approx \sqrt{(Md\phi)^2 + (N\cos\phi d\lambda)^2}$$

Figure 11: Distance calculations from en.wikipedia.org.

where a = the equatorial radius of the Earth, b = the polar radius of the Earth, phi = the average latitude between 2 points, and lambda = the average longitude between 2 points (see http://en.wikipedia.org/wiki/Earth_radius for details).

The coordinates of points on individual curves can be printed or saved to a text file and then used as input to the meandering simulations:

```
2 landmarks
    -97.458333333000      42.916666666000
    -96.583333333000      42.541666666000
5 curves
5527 points
550768.22 meters

Right bank
992 points
98748.40 meters
  -97.480853994157     42.848401546880          0.000000
  -97.479737382918     42.848769328422        100.000011
  -97.478666896876     42.849205080022        199.999407
  -97.477633147690     42.849686487696        299.999598
  -97.476519822884     42.850059606317        399.997057
  -97.475298363029     42.850095419229        499.917122
  -97.474120963862     42.849851812300        599.889169
...
```

Table 1: Digitized river coordinates showing longitude, latitude, and river distance.

This program was used to perform a digitization of the 59-mile segment of the MNRR and surrounding valley from USGS topographic maps which were combined as described in section 3.2. River bank coordinates were entered by hand (using the mouse) about every 125-250 m, and then interpolated to 100 m by the program. The valley boundary was digitized at about half this resolution along the 1200' topographic line, and was then also interpolated to 100 m.

Note that:

    * The river banks were digitized from Gavins Point Dam to just below the city of Ponca, where the river begins to be bounded by the concrete walls and wing dikes of Kensler's Bend. The resulting lengths of the right and left banks were 98.748 km and 101.541 km respectively.

    * The valley 'walls' were digitized wherever obvious. Otherwise, the 1200' topographic line was followed (although not in as much detail as the river banks). Intersecting canyons which entered the valley were not digitized.

    * The valley is fairly flat throughout. The river falls from about 1170' at Gavins Point Dam to about 1100' below Ponca. Mid-river is at about 1140'. The 1200' elevation line was considered to be a likely boundary of the meandering river.

Figure 12: Digitized river and valley superimposed on a 1 km grid.

We have attempted to capture a 'reasonable' rather than 'exact' facsimile of the river from these maps, and have been constrained by the meandering models to digitize a single channel throughout the extent of the river, and a single left and right bank. Therefore, while we have not included chutes or other bifurcations in the main flow, we have included several islands. Ideally a later version of the simulation program can properly take these into account (see section 5.4.3.1 on multiple threads). We have also attempted to combine conflicting bank data from maps made at different times (most notably the Burbank/Ponca maps from 1994 and the Elk Point map from 1963).

In all cases, we have attempted to render a reasonable-looking whole, rather than paying particular attention

to the detail represented in the maps of one time period over another. Nevertheless, superimposing the resulting digitized banks over the satellite mosaic background indicates a good correspondence between the maps, the digitized banks, and the satellite images, although some features present in the maps no longer exist, and the river has clearly migrated during the intervening time.
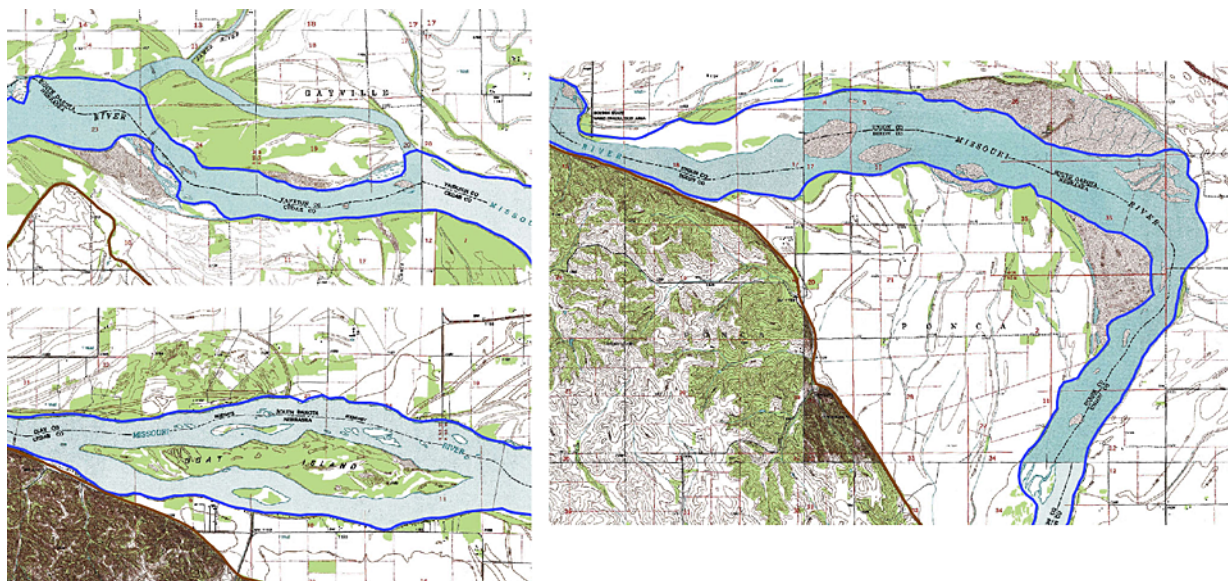
Figure 13: Omitted details and conflicts in digitization.
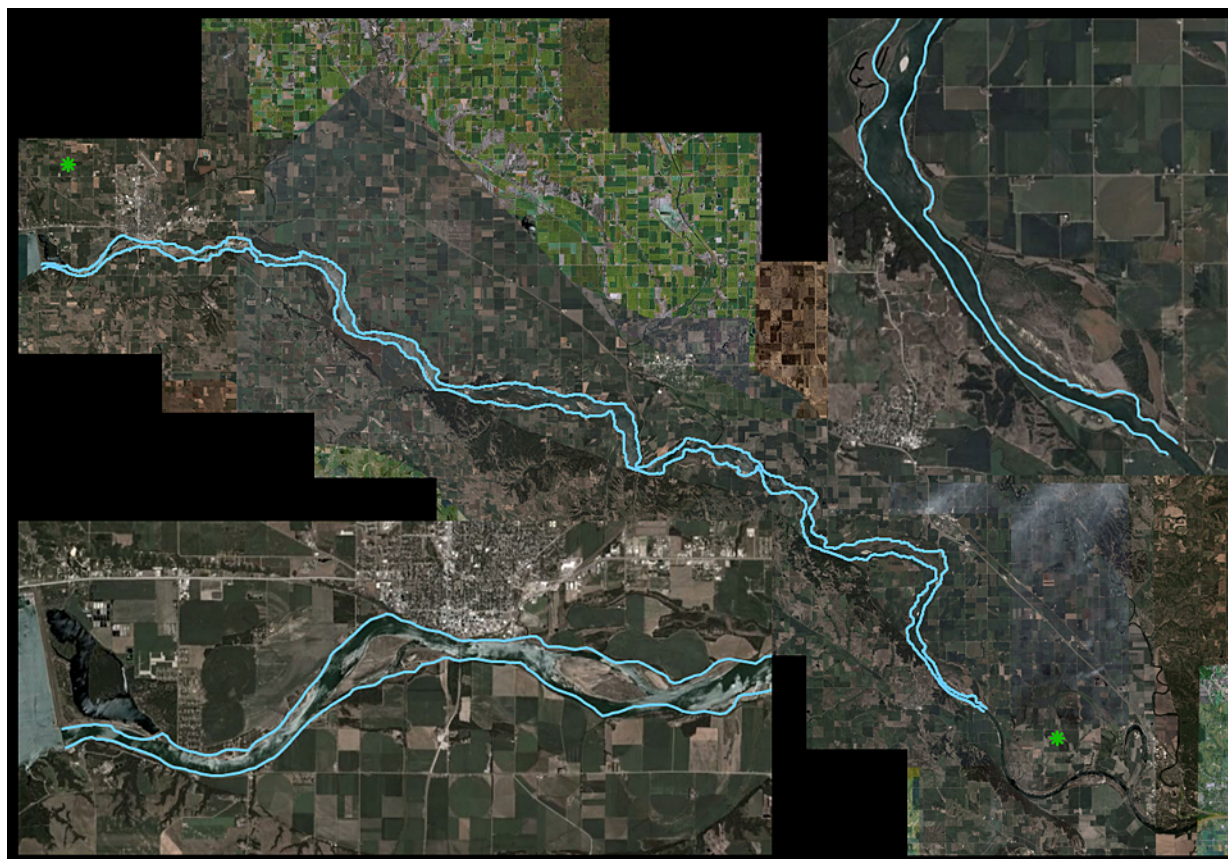
Figure 14: Digitized banks superimposed on satellite mosaic, and detail of both ends. Landmarks used are in green.

3.3.2 Tests of meandering methods

Another program was written to simulate and display the evolution of a meandering river as it migrates, using one of several different models. The program also accumulates the cutoffs which occur as the river loops back over itself. This program provides a convenient way to test new meandering models and observe results immediately. Physical parameters can be entered into the graphical user interface of the control window, and results can be viewed in the plot window as the simulation is running. The meandering calculations are performed in a separate thread of execution so that the user interface and plot animation does not block. The meandering code interface is modular, so that different models can be 'swapped in' as required without editing the rest of the code. The main program calls the meandering module, provides for updating and displaying the river coordinates, and for automatically interpolating new river points as they are required.
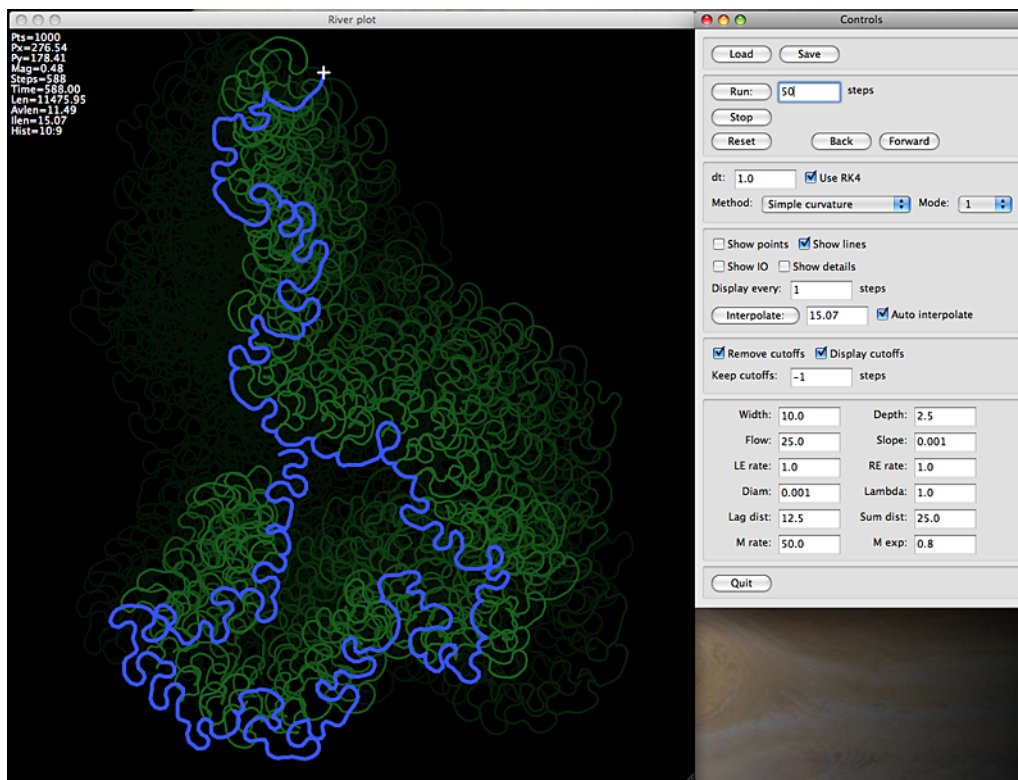
Figure 15: Stand-alone meandering test program.

One interesting feature of the program is that the interpolation of new river points is performed using circular arcs, rather than straight line segments, so as to preserve the existing curvature of the stream in new points (see section 3.4.1.1 for details). Thus, new points are created with a curvature similar to their surrounding points (rather than zero), and therefore the curvature does not increase erroneously at existing points. Another nice feature is that the state of the simulation is automatically saved at periodic intervals or whenever it is paused. Any number of intermediate states can be accumulated, and it is possible to go back to any previous state by clicking a button. The simulation can then be resumed from the past state (possibly using new input parameters), or it can be stepped forward again without having to recompute the intermediate configurations.

This program has been used to test both the Johannesson-Parker 1989 meandering model and other, simpler, models, as described in detail in section 3.4.2 below. The outcome of these tests indicate that it is both possible and fairly easy to generate the characteristic meandering looped shape of a river (which are sometimes called 'Kinoshita curves'), including the upstream asymmetry of their lobes, using a broad variety of methods and parameters, and not just from a complex physical model such as JP89. All models are ultimately derived from the curvature of the river, either 'local curvature': the inverse radius of a circle passing through a point and its two nearest neighbors, or 'effective curvature': the integral of local curvature along a finite segment of the river, usually upstream of the point to which it applies. Meandering models can be based on an algebraic equation of either force or speed, or on differential or integral equations (as is the JP89 model). Nevertheless, all can produce similar general qualitative behavior.

The program has the ability to accumulate excised cutoffs and display them in the plot, using different colors to indicate the age of the cutoff. Cutoffs can be kept for a certain number of additional steps and then discarded, or kept and displayed forever. Note that the cutoff plot does not necessarily show the full meandering range of the river, as the entire history of the main stream is not displayed, only the current stream and (possibly) all past cutoffs. Nevertheless, the main stream and accumulated cutoffs give a good indication of the extent of the planform at any time.

On the next page is a montage made of a single simulated river showing the main stream and the locations of all of the cutoffs accumulated during its evolution, starting from a nearly straight line with slight x and y perturbations, over the course of 17 intervals of about 100 steps each.

3.3.3 Simulation of a single river

The main program used in this study was written specifically to perform a single simulation of the 59-mile segment of the MNRR, although it could in principle be initialized by an appropriate input file to simulate a segment of any other single-channel river which has been digitized by the GIS program described in section 3.3.1 above. This program reads text files of inputs describing the shape of the river (the x and y coordinates of the centerline, and the width of the river at each point), and several name/value pairs of input parameters which control the simulation.

```
# coordinate files         # entries: 956
river center_xy.txt         # lon: max= -96.647947098400, min= -97.480463166501, range=  0.832...
left_boundary left_xy.txt   # lat: max=  42.865180960873, min=  42.560456749484, range=  0.304...
right_boundary right_xy.txt #              x               y               s               w
# river altitudes           # --------------- --------------- --------------- ---------------
high 354.76                        0.000000        0.000000        0.000000      337.607851
low 336.40                        94.166969       33.644584       99.996881      304.865654
# meandering method               189.301508      64.423559      199.986509      273.272731
method Johannesson-Parker_3       286.510982      87.703152      299.944607      251.233498
# physical parameters             385.890451      98.347114      399.892457      246.326393
depth 3.429                       485.858441      98.052150      499.860882      253.451750
flow 899.33                       585.583510      90.824070      599.847554      259.387774
diam 0.001                        684.138582      74.168666      699.800067      251.372569
ldist 1.0                         779.449051      44.191011      799.713756      227.240134
sdist 1.0                         871.661896       5.514147      899.709298      201.377192
# step time in years              963.311937     -34.488356      999.708949      186.790757
dt 0.1                           1056.491245     -70.770778     1099.702937      187.716638
etc...                      etc...
```

Table 2: Two input files to single-river MNRR simulation program.
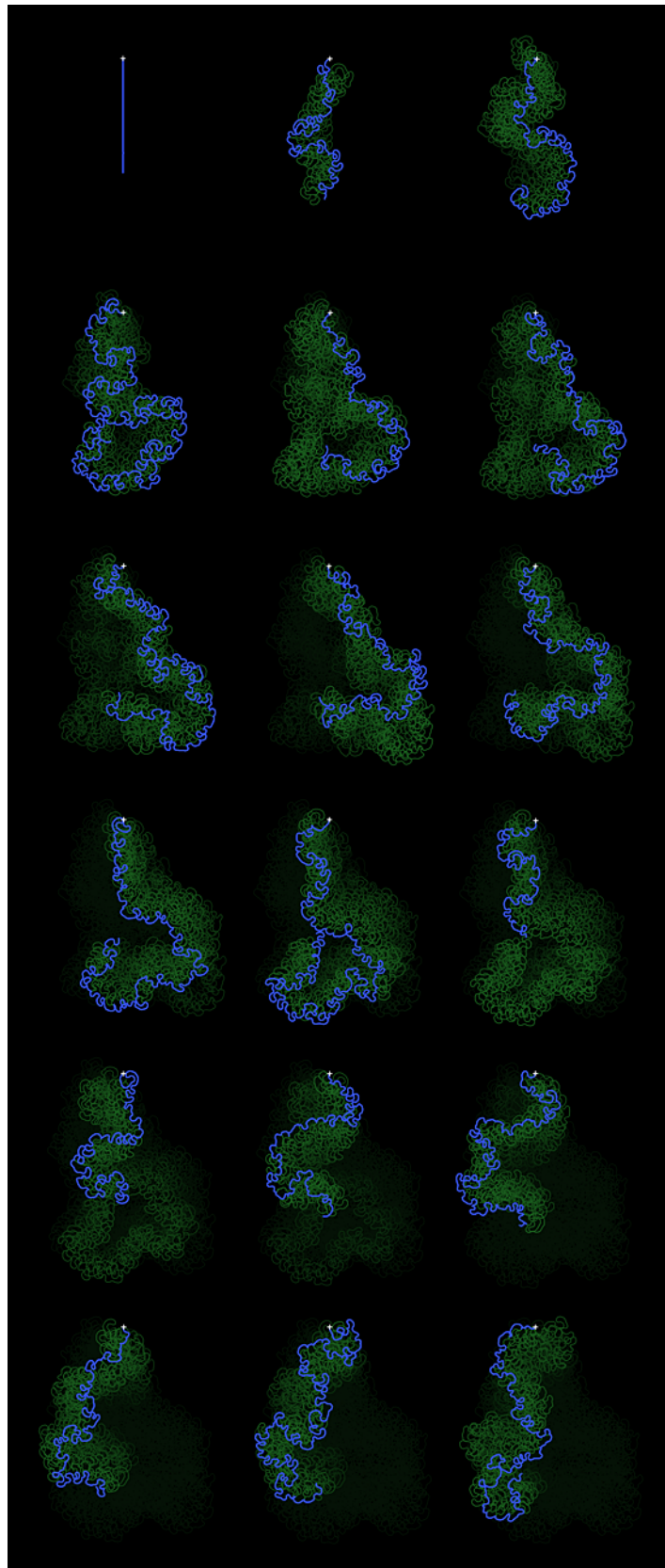
Figure 16: Evolution of simulated test river and cutoffs.

Features of the single-river MNRR program include:

* The valley boundary, river centerline, or filled width can be displayed on a background consisting of a 1 x 1 km grid or a selected image. The 2d coverage array, residence times, or cumulative erosion (see section 3.4.5 and 3.4.6 for details) can be superimposed on the river and background.

* The simulation can be saved to a binary file, reloaded, and continued at a later time.

* The coordinates of river points can be printed as text.

* The simulation can be run for any number of steps while saving 'snapshots' of the simulation at regular intervals for review. The simulation can be returned to any saved state and animated through a sequence of states either forward or backward in time, allowed to run forward with a new set of input parameters, or reinitialized from an external text file of coordinates and parameters.

* The simulation can make use of a number of different modular meandering models. Details of the data sent to and from the meandering module can be printed as a diagnostic.

* During the simulation, cutoffs can be detected and removed, saved and displayed, or discarded. The river coordinates can be checked against the valley boundary and maintained within the designated domain (see section 3.4.1.5 for details).

* The erosion rate can be calculated at each step, and the migration rate can be automatically adjusted to initialize the erosion rate to a specific value (see section 3.4.4 for details).

* Physical parameters controlling the simulation can be changed from the user interface, or imported from text files.

Default values of physical parameters used for the single-river MNRR simulation were set based on the following sources of information:

* A constant flow was estimated by averaging the Gavins Point Dam discharge quotes from Table 2 of [ref 1]. This value is consistent with the discharge plots in Figures 2 and 4 of the same source. This value was varied in the large population of multiple runs which were used in this study, as discussed in section 3.3.4 below.

* A constant depth was estimated from plots of the stream gauge heights at Yankton and Sioux City [refs 12, 13], and corroborated by the National Park Service website [ref 9]. This value will also be varied as discussed in section 3.3.4.

* The bed particle size was nominally set to a diameter of 1 mm, which is consistent with a medium sand basin. This value will also be varied as discussed in section 3.3.4.

* The water surface slope was calculated from the difference in the inlet elevation and the outlet elevation, divided by the current length of the river. The inlet elevation was estimated at 354.76 m, and the outlet elevation at 336.40 m, based on digital elevation data downloaded from the National Map website [ref 11].

* The effective curvature lag distance and sum distance (see section 3.4.1.2) were set to integrate

local curvature along an interval of one river width, one river width upstream from each meandering point. These values will also be varied as discussed in section 3.3.4.

* The river migration rate was adjusted so that the initial total erosion rate estimate (using 'unmeandered' river geometry) was close to 1.2 ha/yr/km, as quoted in Table 1 of [ref 1]. The initial erosion rate (and therefore the migration rate) will also be varied as discussed in section 3.3.4.

Two important caveats concerning the parameters and constraints of the simulation should be mentioned. As is discussed in section 3.4.1.6, the maximum width of the river in most simulations (and in all Johannesson-Parker 1989 simulations) was limited to one of several constant values (from 500-800 m) along its entire length from the inlet at Gavins Point Dam to the outlet at Kensler's Bend. In addition, while the inlet point of the river was fixed in place at all times during the simulation, the outlet was allowed to move freely (in accordance with the meandering model) as if the concrete walls and wing dikes below Ponca did not exist (see section 5.3 for discussion).

Different combinations of the various simulation parameters (e.g. width, depth, flow, bed particle size, curvature integration distances, etc...) yield an enormous variation in river shape. Some of the configurations are quite 'wild', and show far more activity than is expected of the real river over the same time period, usually by virtue of the initial erosion rate being set far higher than has been measured for the actual river. For this study, however, we are interested in more realistic simulations that are fairly 'tame', and have erosion rates which are commensurate with measured values. If these more realistic simulations are interpreted as the behavior of a 'nominal' or 'median' river, then a range of input values which encompass them could be expected to generate a population of rivers whose shapes and dynamics were representative of what was expected of the real river.

3.3.4 Multiple simulations framework

The strategy used in this study is based on the observation that none of the meandering models available to us nor any of the acceptable input parameter combinations will correctly genrate the geometry and dynamics which are specific to the Missouri River. This is trivially seen to be true since virtually all of the current river models (and especially the Johannesson-Parker 1989 model) simulate only a single channel, while the MNRR contains numerous bifurcations, chutes, islands, braids, and submerged and surface bars, making it an especially challenging subject to model. Therefore, an intelligent choice of many slightly different simulations, utilizing a carefully selected range of input values, is expected to better approximate, as a population, the likely behavior of the real river over the next 100 years than could any single simulation.

The selection of parameter choices to be used will be discussed in section 3.4.7. The ability to automatically perform mutiple simulations and accumulate aggregate planform/migration statistics is an enhancement of the single-simulation program discussed above. This program was modified to read and parse text files containing commands instructing the program to:

* Load a base model of river coordinates and settings.

* Reset the values of specific simulation parameters.

* Automaticaly vary the migration rate to initialize the erosion rate to a specified value.

* Run a 100 year simulation.

* Save the results to a binary file.

* Save an image of the final river configuration.

* Repeat the steps above for any number of different simulations.

* Skip over any number of already completed steps.

Here is an example of a partial command file used:

```
# MNRRSim command file          # 5001                          # 5002
                                *** 5001 ***                    *** 5002 ***
goto 5670                        load base.mnrr                 load base.mnrr
                                dt = 0.25                       dt = 0.25
# 5000                           runSteps = 400                 runSteps = 400
*** 5000 ***                     checkCutoffs = True            checkCutoffs = True
load base.mnrr                   displayEvery = 4               displayEvery = 4
dt = 0.25                        checkCutoffsEvery = 4          checkCutoffsEvery = 4
runSteps = 400                   wmax = 500.00                  wmax = 500.00
checkCutoffs = True              depth = 2.75                   depth = 2.75
displayEvery = 4                 flow = 800.00                  flow = 800.00
checkCutoffsEvery = 4            ldist = 1.0                    ldist = 1.0
wmax = 500.00                    sdist = 0.75                   sdist = 0.75
depth = 2.75                     mrate = 1.0                    mrate = 1.0
flow = 800.00                    initializeErosion 1.80         initializeErosion 2.40
ldist = 1.0                      run                            run
sdist = 0.75                     saveImage run5001.png          saveImage run5002.png
mrate = 1.0                      save run5001.mnrr              save run5002.mnrr
initializeErosion 1.20
run
saveImage run5000.png
save run5000.mnrr
```

Table 3: Multiple simulation command file excerpt.

This automation capability makes it possible to perform simulations spanning an n-dimensional grid of input parameter space in order to search for likely combination candidates (see section 3.4.7 below). Each 100 year simulation can take anywhere from several minutes to several hours to complete, depending on the resolution of the step size, the interpolation distances used, and other factors. Therefore it is essential to try to limit the different simulations performed to those expected to generate useful results. While sequences of simulations can be performed automatically by the program, the final river geometries must still be reviewed manually or semi-automatically using the database (see section 3.3.6 below) after all runs have been completed. Subsets of results which appear promising can then be used to refine the parameter search. This iterative process was used to find parameter ranges used for the large population of runs performed in this study.

Test runs to select combinations of input parameters usually took about 1-2 hours to perform, while the final runs used in this study took about 15-20 minutes each, using a dt of 0.25 years. While the total continuous time required for these runs (n = 3612) was in excess of 43 days, this was ameliorated by two factors:

1. Simulations were broken into groups and run simultaneously on 2 different computers (and in parallel on dual-core processors).

2. The command file syntax has a 'goto' command that allows a batch run to be stopped and resumed with a particular simulation at a later time.

Even so, completion of all simulations running 10 hours per day took about 35 days.

3.3.5 Graphics

All output graphics and user interface input were performed using the free WxPython cross-platform library (www.wxpython.org). Graphics were an integral part of all programs, rather than an additional post-processing step, so that it was possible to view the intermediate results of all simulations and other calculations in real time as they occurred, and to take immediate user action based on the evaluation of that output (e.g. to stop the simulation or change parameters and continue) without waiting for a long-running program to conclude. It would not have been possible to perform this study in the time period available without this interaction capability.

3.3.6 River database

The final major program to be written for this study was a 2-part database which was used to accumulate information about all simulations as a post-processing step, and to display and manipulate these results in both numerical and graphical form. This database has a programming and query syntax similar to the 'Structured Query Language' family of popular programs (e.g. 'MySQL' and 'PostgreSQL'), so we have elected to call it 'RiverSquirrel'.

First, a database creation program peruses all completed simulation files and accumulates several numerical results in 1- and 2-dimensions (including river length at several resolutions, number and length of cutoffs, sinuosity, erosion rate, coverage area and residence times, cumulative erosion, etc...), creating a large table of values. Then, a second database query program can perform the following operations on this table:

* Print entries and fields in any order.

* Sort entries about any field.

* Select subsets of entries using numerical relationships and combinations of 'and' and 'or' clauses.

* Plot the final or intermediate river for any input parameter combination.

* Accumulate and plot common coverage and average erosion as 2d arrays for subsets of entries.

* Plot mosaics of river coordinates on a background image, plus 2d arrays and contour lines as transparent overlays.

Individual queries (e.g. selecting and sorting) can also be chained together to form more complex operations. Once the database creation step has been performed, all query operations are quite fast to perform. Currently the query program uses a programming interface from Python, but it could easily be modified to read prepared text files, or to take interactive input from the terminal or over a web connection.

The database can track the course of every individual river over time, and can also extract specific examples of river behavior (such as the greatest and least river lengths, coverage areas, or erosion rates, or rivers which pass through specific points in the valley or other designated targets at some time during the simulation), and can plot histograms and trends in the behavior indicated by relationships between 2 or more input or output variables. See sections 4.2 to 4.6 below for several examples of using this database to extract, analyze, and display simulation results.

3.4 Calculations --
3.4.1 Discretization and interpolation -- 3.4.1.1 Interpolation via circular arcs

Both the river digitization program and the river simulation program represent curves (e.g. the river centerline) as paths parameterized by length, where points are placed on circular arcs rather than on line segments. What this means is that:

* A unique circle having a specific {x, y} center and radius is calculated to fit every three consecutive {x, y} points along each curve.

* New points added to the curve are placed somewhere on the perimeter of these circular arcs, rather than on straight lines connecting existing points.

* As the length of a curve grows (when the simulated river meanders), or the distance between points is changed (when a curve is interpolated), points are re-calculated and placed at equal distances along the total length of these circular arcs. Linear interpolation is used only if a set of three consecutive points is colinear (i.e. fits a circle of infinite radius).

Using circular arcs, rather than straight line segments, has the effect of preserving the curvature of the path in new points. New points are created with a curvature similar to their surrounding points (rather than zero, as would be the case with linear interpolation), and therefore the curvature does not increase erroneously at the existing points. As an example, consider a stream consisting of a single circular arc. If, as the stream lengthens, points are interpolated using straight line segments, the stream departs from circularity and existing points along the perimeter accumulate excess curvature. If circular arc interpolation is used, the circularity and constant curvature at each point is preserved.

In cases where the center or radius of arcs change along the path length of the curve, new points are placed using a weighted average of the previous and the next arc in the sequence, where the weights of the average are based on the fractional angular distance of the new point along both arcs. For example, a new point to be placed half-way between two existing points i and i + 1 would be placed at the average of 2 points, one on each of the arcs fitting points {i - 1, i, i + 1} and {i, i + 1, i + 2}).

Although all programs created for this study make use of circular arcs in their calculations, the graphics used to display points and curves is still based on drawing line segments, as the difference between the two representations is usually not discernable to the eye.
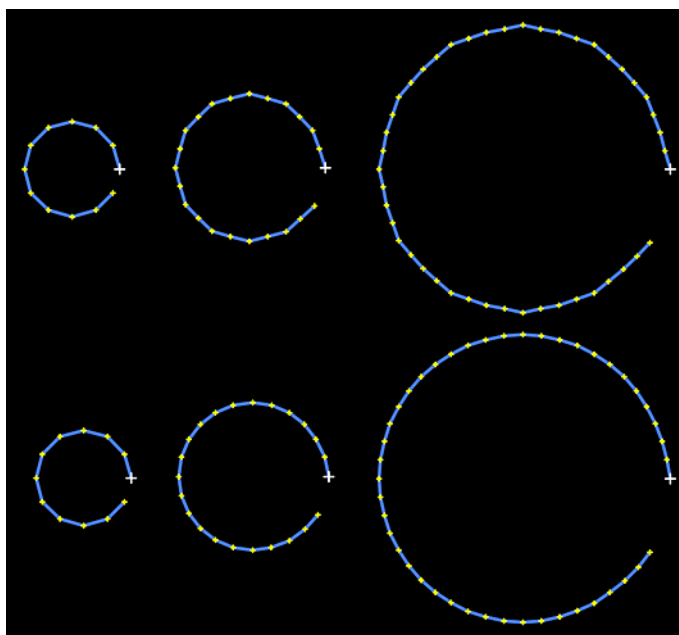
Figure 17: Growing circular path with linear interpolation (top) and arc interpolation (bottom).

3.4.1.2 Curvature and effective curvature

All of the meandering models described in section 3.4.2 below depend on the curvature at each point on the simulated river as their primary independent variable. In other studies, curvature is often calculated from the angle between the two vectors formed by three successive points on the river, so that the vectors are tangential to the flow between every two points. The curvature at a point is then estimated by the angular change in direction between the vector directly upstream of it and the vector directly downstream of it, and is proportional to this angle divided by the average length of the two vectors.

In this study, however, curvature is given directly as the inverse of the radius of the circular arc passing through each point and its two neighbors, as described in the previous section. Therefore, points which lie on small circles have large curvature, points which lie on large circles have small curvature, and points which are colinear have zero curvature. This has the effect of avoiding the spurious over-estimation of curvature which might otherwise be calculated by the vector method at places where the river changes direction suddenly, especially at the intersections of loop cutoffs or where the river encounters a boundary. The abrupt change in vector direction at excised cutoffs and at boundaries which limit the motion of the river might generate excessive curvature which could in turn cause excessive motion or discontinuities in the meandering calculations. The use of circular arcs to define curvature helps to curtail this anomalous behavior by distributing the change in direction over the circumference of the arc, rather than only at the vertex of a circumscribed triangle.

In addition to the local curvature C(i) calculated at every point in the river as described above, the meandering routines described in section 3.4.2 all make use of the 'effective curvature', Ce(i), which is simply an integral of the local curvature over some finite interval in the river, usually upstream. The location and the length of this integral is set by the two input variables ldist ('lag distance') and sdist ('sum distance'),

which are given in terms of the width of the river at the point to which they apply. These variables reflect the hypothesis that the migration of a particular point on the river is affected by the geometry of the river upstream of that point. The variables ldist and sdist control how far upstream, and over what interval, the local curvature is integrated and averaged to calculate the effective curvature used by the meandering models. Nominal values for both variables are 1 river width. By slightly changing these values away from unity in either direction, both the size and shape of the loops formed by the migration of the river can be altered, as well as the upstream or downstream asymmetry of those loops.

3.4.1.3 Centerline and width

Although the river has been digitized from the map mosaic as two curves representing the left and right banks, the meandering models require a single centerline and width at every point along that centerline as their input, and the migration displacements output by these models are applied to that centerline rather than to the banks individually. Therefore, it is necessary to calculate a centerline from the left and right banks, and to estimate the width of the river at each point on that centerline in a direction which is perpendicular to the downstream direction.

This is done automatically by the GIS digitization program after the left and right banks have been entered and interpolated on arcs as described above. In this case, the 'downstream' direction is defined as that which is tangential to the arc passing through each point on the resulting centerline, while the perpendicular 'cross-stream' direction is parallel to the radius of that arc. Thus, an additional benefit of using circular arc interpolation is that down- and cross-stream directions can be uniquely and robustly defined at each point on the river. The result is an 'idealized' river geometry that closely follows the actual river, but which can be described by a single smoothly varying curve and width at every downstream point. However, since the width is symmetric in both the left and right cross-stream directions, this representation eliminates some of the details of the individual banks.

The algorithm used to calculate the centerline is computationally intensive (but requires less than 5 minutes for two 100 km banks), and seems to work well for all parts of the river, including areas where the banks change direction and/or are highly curved. Although there are probably many ways that a centerline and width might be approximated, the algorithm used in this study is based on an iterative procedure which starts from a small set of corresponding pairs of points on both banks, and repeatedly adds additional pairs of points until all candidates have been exhausted. The basis of this calculation is the following definition of 'width', which can be taken as an axiom only for a certain set of points which meet the following criteria:

* The 'width' of the river is only well-defined for those corresponding points {L(i), R(j)} along the left and right banks L and R such that:

* For a given point L(i) on bank 1, the closest point on bank 2 is R(j), and for that point R(j) on bank 2, the closest point on bank 1 is also L(i). The width of the river at {L(i), R(j)} is then the distance between the two points, and the centerline is defined to pass halfway between them.

One might, in principle, imagine two surveyors walking along the left and right banks of the river, each holding an end of a rope which is stretched across the river between them. As they move along the banks,

sometimes the rope can be pulled tight and short between them, and sometimes it must be much longer, depending on both of their positions on the banks, and the actual width of the river. If the surveyor on the left bank stays at the same position while her partner on the right bank moves back and forth along the strand, they will discover a configuration where the rope is shortest between them. Similarly, if the surveyor on the right bank stays at the same position while her partner on the left bank moves back and forth along the strand, they will discover another configuration where the rope is shortest between them (and not necessarily the same configuration as before).

The constraint stated above says that if the two configurations just described are the same (both surveyors in the same positions when the rope is shortest from either side), then they have found a place where they can without doubt define the width of the river. Put another way: given the positions of the two surveyors, if the person on the left bank moves by any amount in either direction, the rope will by necessity become longer, and simultaneously, if the person on the right bank moves by any amount in either direction the rope will also become longer, then they have found a stable minimum distance between the two banks with respect to downstream distance, and can therefore uniquely define the width of the river at that point.

Application of this constraint yields surprisingly few mutually corresponding points along both banks, as in general the closest point R' to point L has as its closest point a different point L' not equal to L. However, this criterion can be applied iteratively, beginning with the set of corresponding points which are closest to one other, and then adding additional pairs of points in order of greater distance between them such that:

1. New {L(i), R(j)} combinations are selected as above from remaining points after all previously used {L(k), R(l)} pairs are excluded.

2. A new pair {L(i), R(j)} is added only if the line segment connecting L(i) and R(j) does not cross any previous line segments connecting already existing {L(k), R(l)} pairs.

In terms of the two hypothetical surveyors: as they move along the left and right banks and discover mutually minimal points as described above, they place stakes in the banks at their current positions and stretch ropes across them. Once they have found all such pairs of points, they begin to re-examine the points which are in between the points they have already found. In doing so, they look for new pairs of points which are mutually closest togther, such that in making their new measurements they do not move so far as to pass any already staked-out points (although they may re-use existing points paired with new points). As they find new corresponding pairs, they plant new stakes (if required) and stretch new ropes across them, such that none of the ropes cross one another (although some stakes may have more than one rope attached). Eventually, they will have exhausted all possible pairs of points. The centerline is then defined as the midpoint of each rope, and the width at that point is half the rope length.

This process is not necessarily one-to-one, as a point on one bank may be connected to several points on the opposite bank, as long as the two specified conditions hold. And, some points may not be connected at all, if they fail the conditions. In general, however, nearly all points on both banks will be connected to at least one other point, so that the resulting centerline is well represented. Nevertheless, some smoothing and re-interpolation of the centerline is useful as a post-processing step. The centerline point coordinates and widths are then printed to the terminal or a file, and used as input for the meandering simulations.
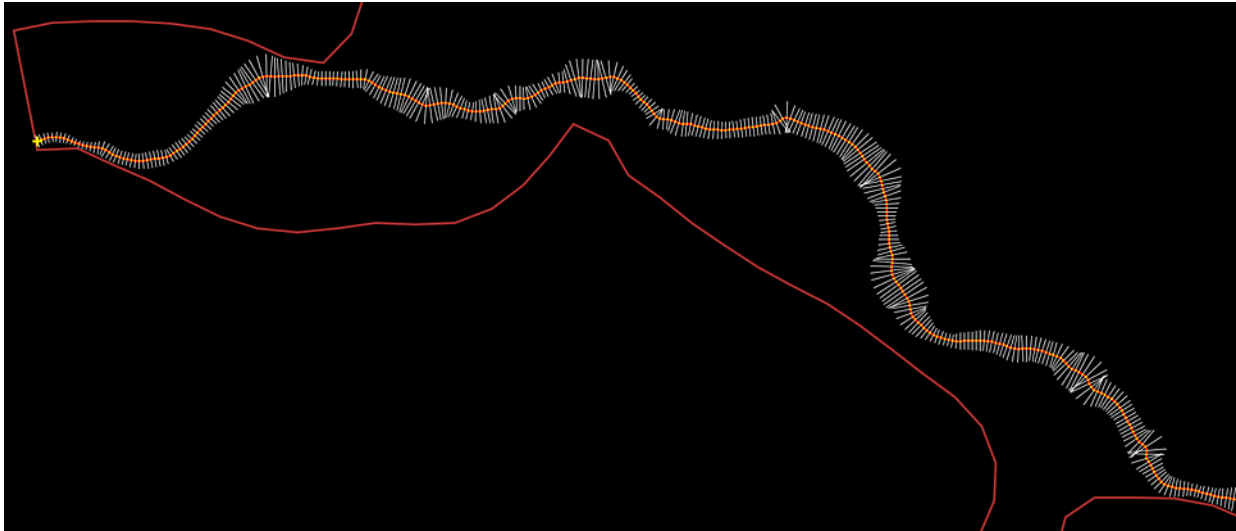
Figure 18: MNRR centerline, points, and widths.

3.4.1.4 Conversion to {x, y} coordinates

The river and valley coordinates digitized from the map mosaic are in terms of longitude and latitude angles on the surface of an oblate ellipsoid. However, the meandering model code requires inputs in terms of x and y coordinates in meters which are part of the same rectangular planar surface. In general, it is not possible to perform this transformation uniquely, although it is possible to approximate it for sufficiently small planes which are tangent to the ellipsoid surface at discrete points of interest. Since the river is represented by a 1-dimensional curve which extends primarily in a west-to-east direction from its inlet to its outlet, this approximation can be performed at each point on the river centerline without too much loss of accuracy.

A small utility program was written to convert the river {longitude, latitude} coordinates into {x, y} coordinates that are part of the same plane. Although this is not a complicated calculation, it is somewhat subtle and merits a little discussion. The MNRR bank coordinates, and the calculated centerline, were digitized as {longitude, latitude} pairs from USGS topographic maps. These maps were made using polyconic projections, and are themselves nearly equivalent to tangential planes at the center of the projection. During the digitization process, points were converted from screen coordinates to {longitude, latitude} using two landmark reference points at {-97d27m30s, 42d55m} and {-96d35m, 42d32m30s} which straddle the river in both north/south and west/east directions. The longitude and latitude of digitized points were calculated by bi-linear interpolation between the two landmarks using separate scales for longitude and latitude that were assumed to be constant across their bounding rectangle. Although this is not strictly correct, it is sufficiently accurate for use in this study, as will be shown below. Ideally, several landmarks along the path of the river should be used, with local longitude and latitude interpolated from the closest of these for each point on the river.

The river simulation needs x and y coordinates in meters, and all must reference the same origin (arbitrarily defined as the inlet at Gavins Point Dam). This is impossible for points on an oblate spheroid which are not all on the same geodesic, especially as the length of the river is over 95 km. Nevertheless, a good approximation can be performed using the small-distance calculations of figure 11, and one or more small

XY planes tangential to the surface of the Earth. The range of longitude and latitude from the beginning to the end of the river is 0.83 degrees and 0.30 degrees respectively, so the distortion incurred by this approximation is not too large. However, it is not isomorphic, due to the difference in radius between a circle of longitude (great circle) and a circle of latitude (not a geodesic) at the latitude of the river (about 43 degrees).

We transformed coordinates to x and y first using a single tangent plane at the midpont in longitude and latitude at {-97.064, 42.713} degrees using two separate scales for converting delta-longitude to delta-x and delta-latitude to delta-y, measured from small changes in these angles (0.000001 radian) at that point. Angular differences of 1 micro-radian at this point produce linear distances of 4.694 and 6.365 meters respectively, yielding scales of 81919.690 and 111087.144 m/deg. Calculating x and y for the river using this constant scale yields values from {0.0, 0.0} meters at the inlet to {68199.458, -32186.265} meters at the outlet and a total length of 95402.556 m, which is close to the 'actual' centerline length of 95353.747 m given by the GIS program.

We also transformed to x and y using different scales calculated at each centerline point along the length of the river, which correspond to using a set of many small XY tangent planes, each situated on the centerline at the midpoints between each of the 100 m digitized points. Each set of scales was calculated as above, and the pair for pts i and i+1 were used to calculate the delta-x and delta-y distance in meters bewteen those two points, from the beginning to the end of the river. Transforming in this way yields values from {0.0, 0.0} m to {68143.168, -32186.223} m and a total length of 95353.747 m, which is 'exact' to within less than 1 mm. The final x and y values for the single-plane vs. multiple-plane transform differ by about 56 m in x and 4 cm in y.

As a comparison, we also performed a transform using an isomorpic scale in x and y derived from the Euclidean distance in longitude and latitude between the river inlet and outlet (as if the river was on a flat surface and delta-x = c * delta-longitude and delta-y = c * delta-latitude for some constant c).
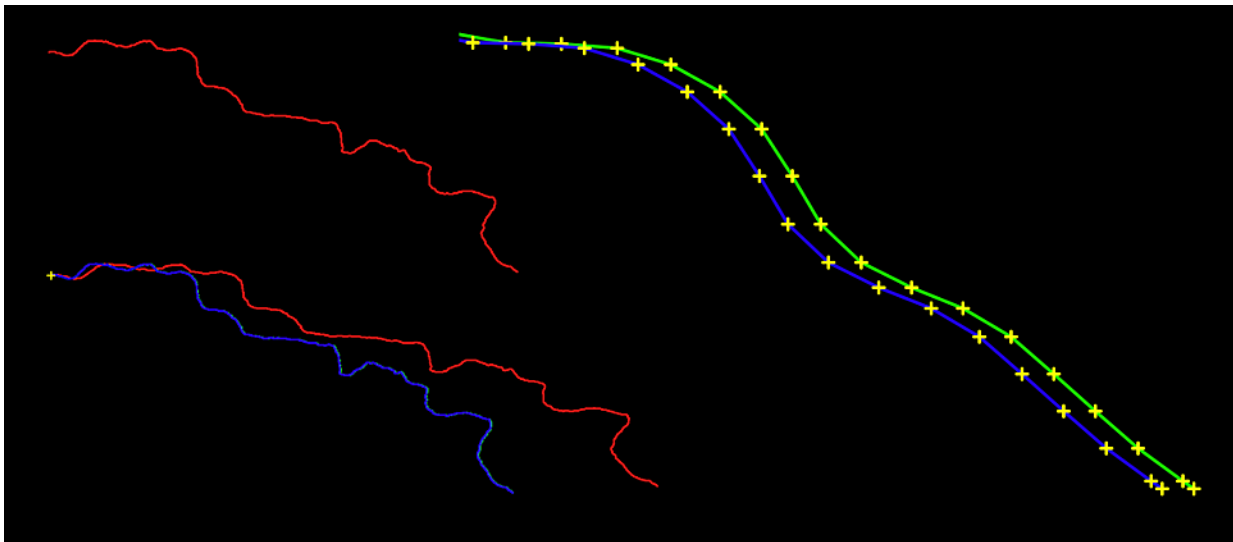
Figure 19: (Top) Original lon/lat coords; (bottom) transform to x/y via isomorphic scale (red), single plane oblate scales (green), multiple planes (blue); (right) details of outlet end.

3.4.1.5 Boundary checks

The boundary of the MNRR valley was digitized at approximately the 1200' topographic line. The simulated river is constrained to remain within this boundary, and to approach it no closer than 1/2 the width of the river at any point. The location of the inlet point at Gavins Point Dam is also fixed in place, as are points on the first half kilometer of the river. Points on the next 800 m of the river have their motion damped by a negative power of 2 in the sequence {1/256, 1/128, 1/64, 1/32, 1/16, 1/8, 1/4, 1/2} multiplied by the displacement generated by the meandering model.

The downstream end of the river is free to move in accordance with the output of the meandering model, although in reality the tail of the river is constrained by the artificial channel and wing dikes of Kensler's Bend. This end of the river was left free so that the length and shape of the simulated river could grow without limits other than those imposed by the topographic boundary, and that therefore the 'migration corridor' defined by that motion would represent an 'upper bound' to that of the river constrained at both ends. Tests performed with the outlet fixed in place did not differ substantially from those in which it was free to move, and so the decision was made to always permit this motion.

The boundary forms a closed irregular polygon around the river. All river points are checked after each migration step to ensure that:

1. They are within the boundary.

2. They are at least 1/2 river width from all boundary points and edges.

Points which are in violation of either of these constraints are moved according to the following procedures:

1. Points too close to but inside of the boundary are moved away from the boundary along a vector perpendicular to the nearest edge until they are 1/2 river width away.

2. Points which have moved outside the boundary are moved inside it along a vector perpendicular to the nearest edge until they are 1/2 river width away.

Thus, the boundary forms a 'hard' limit to the motion of the river, and does not otherwise affect the migration rate. This process allows the river banks to become very flush along the boundary perimeter, respecting the current river width. The boundary was originally digitized at a resolution of 100 m, but that was found to make the boundary-checking code too slow (and, most of the simulation program time was spent in boundary checks at each step). The boundary resolution was subsequently reduced to 1 km per edge, which is sufficient for containing the river geometry (which is digitized at 100 m) within the valley, but is fast enough for practical purposes.

3.4.1.6 River width

After having digitized the MNRR geometry and performed preliminary tests with the meandering models, we have observed the following:

1. The digitized river has a minimum width of 186.79 m, maximum of 1647.97 m, mean of 747.84 m, and

standard deviation of 337.62 m. We do not believe this to be an accurate representation of the active meandering width of the flow, and in general believe that the observed bank-to-bank surface width is a serious over-estimate of the submerged sediment-carrying conduit width, especially around islands and bars, and in shallow areas.

2. The Johannesson-Parker meandering model, discussed in section 3.4.2.3 below, cannot make use of the full width of the river. Specifically, this model causes numerical over- or under-flow in the exponential terms of the equation for u1b at widths over 800 m and/or flows below 800 m^2/s.

3. The behavior of the meandering river is quite different at different widths. In general, a wider river migrates much more slowly and produces fewer, larger, features, while a narrower river is quite active and produces many smaller features. Since this has an effect on the overall valley coverage of the river, we have elected to make maximum river width one of the parameters which was varied to generate the different simulations used as part of this study.

When we originally plotted the distribution of digitized river widths, it showed a distinctive 'tail' at widths over 1531 m, suggesting that we had erroneously included too many large features from the maps. We made the assumption that the tail of this distribution was spurious, and was due to islands and other artifacts included in the digitization. If these points are neglected, the adjusted histogram and cumulative distribution is basically unimodal, and more reasonable. The median width (at 50% cumulative distribution) is 693.15 m. We have tried a constant 'effective' width of 400 m in some simulations, which is only as wide as about 18% of the measured values, but this has produced unrealistic behavior. Therefore we have used a minimum maximum width of 500 m in the full set of simulations, while 800 m was the maximum permitted by the JP89 model at all flow values.

When initializing the simulations based on a maximum river width, we made an additional modification to 'soft clip' the width to the maximum value, rather than simply truncating all widths greater than the cutoff value. This has the effect of maintaining variation in the river width in its widest parts, rather than replacing the widest parts (which comprise a significant fraction of the overall river) by a smooth channel of constant width.
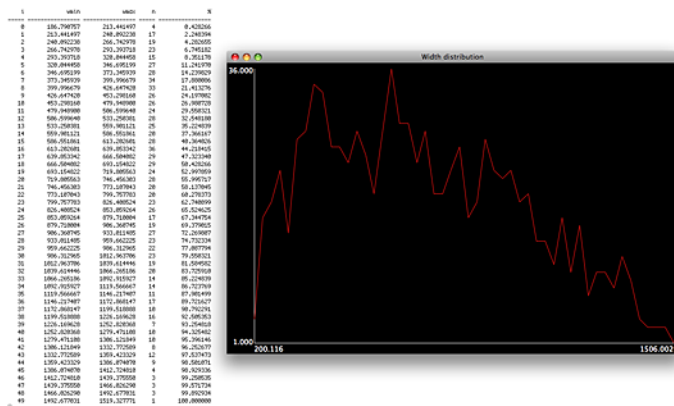
Figure 20: Distribution of river width using 50 bins, after widths over 1531 m are discarded.

1379.50 768.91
1387.22 769.50
1389.80 769.78
1391.70 769.84
1408.24 771.06
1413.54 771.44
1418.49 771.80
1435.57 772.97
1441.18 773.35
1453.87 774.18
1460.36 774.60
1476.52 775.61
1480.89 775.87
1483.18 776.01
1519.33 778.08
1535.16 778.93
1560.95 780.25
1578.78 781.11
1592.68 781.75
1595.92 781.90
1596.79 781.94
1608.05 782.44
1609.26 782.49
1614.32 782.71
1615.75 782.78
1622.72 783.07
1623.51 783.11
1627.77 783.29
1627.96 783.29
1634.41 783.56
1637.12 783.67
1637.68 783.69
1638.50 783.73
1641.43 783.85
1641.83 783.86
1643.31 783.92
1647.97 784.11

Figure 21: Attenuation of river widths to 800 m.

3.4.2 Meandering motion

There appear to be 3 general requirements for the onset of river meandering, irrespective of the specific model or equations used:

1. The migration rate depends, as its primary variable, on the local curvature or a derived function of the local curvature, at each point on the river, in the minimal form a * f(C(s))^b for some constants a and b. Meandering models fall into two general classes based on the type of function of curvature used:

   I. So called 'force based' models, which relate migration to physical quantities such as mass, acceleration, and force.

   II. So called 'speed based' models, which relate migration to the speed of the flow or the difference between the speeds of flows near the two banks of the river.

2. The curvature or derived quantity must be spatially smoothed (integrated) over some finite interval of the river.

3. The curvature or its derived quantity is usually calculated upstream of its point of application, and therefore has a delayed action on the downstream migration of the river.

The last 2 requirements can be satisfied by having the function f() perform a spatial integration of curvature (e.g. by averaging the upstream curvature along some finite interval of the river). In the meandering models used in this study, this is accomplished via the 'ldist' and 'sdist' variables of the effective curvature calculation, which control how far upstream, and over what distance interval, in river widths, this integration is performed.

In this study, we have used three different, but related, curvature- and speed-based meandering methods:

1. Simple curvature.

2. Circumferential speed.
3. Johannesson-Parker (as specified in their 1989 paper).

These three methods are described in the sections below.

3.4.2.1 Simple curvature (SC)

In this method, the migration rate of the river is simply proportional to the signed effective curvature calculated for each point:

```
Rm = a * Ce(s)^b
```

The constant b is usually set to 1.0, and a is empirically determined by adjusting it until the initial erosion rate (see section 3.4.4) becomes a specific value. Curvature is considered to be 'positive' in sign wherever the river bends to the left, and 'negative' in sign wherever the river bends to the right. At each point on the river, the cross-stream direction is given by the radius vector of the circular arc passing through the point (which is perpendicular to the flow), and has a positive sign toward the left bank, and a negative sign toward the right bank. The migration displacement of a point is in the opposite direction of the sign of its curvature, along the cross-stream left-pointing vector, scaled by the simulation timestep:

```
dxy = -Rm * left_vector * dt
```

Simulations based on simple curvature tend to produce small circular loops which may be realistic for smaller streams, but are considered unrealistic for wider, faster flows, as they are not based on any physical parameters of the river, but on geometry alone.
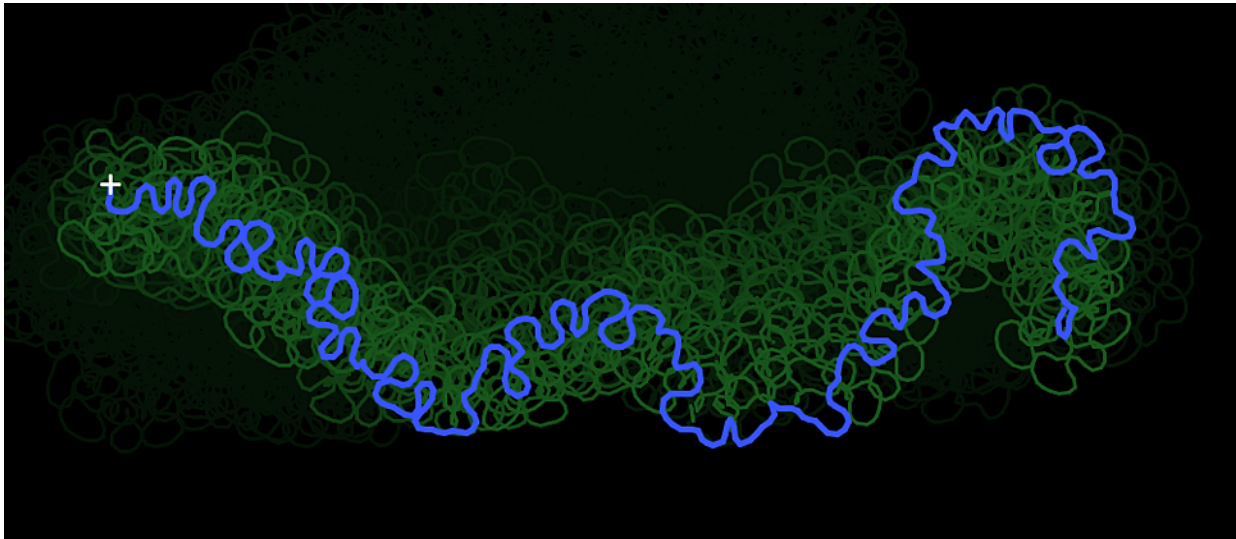
Figure 22: Simulation based on curvature alone.

3.4.2.2 Circumferential speed (CS or sigma)

This simplest speed-based method approximates the channel at each point by a circular arc of non-zero width, and calculates the migration rate as proportional to the excess speed of the flow on the circumference of the outside bank in the bend, as if each radial element of the flow was rigid and traversed the bend at the same angular rate, so that small volumes situated at the larger radius of the outside bank moved faster to cover the longer distance in the same amount of time as those near the inside bank.

In this case the migration rate is given by:

```
Rm = a * excess_speed
```

where

```
excess_speed = flow / (width * depth) * ((radius + width / 2.0)
               / radius - 1.0)
      radius = 1.0 / Ce(s)
```

for a given flow (in m^3/s), width, depth, and effective curvature. This excess speed, which is greater than the average speed at the center of the flow, is thought to erode more material from the outside bank, while the below-averge speed at the inside bank causes material to be deposited. Thus, there is an overall migration of the channel toward the outside of the bend. This hypothetical transfer of material from the outside bank to the inside bank is the basis of channel migration in all the speed-based methods. The circumferential speed method produces more realsitic meandering geometry and loop shape than that due to curvature alone, as it is also based on the physical parameters of width, depth, and flow, as well as curvature. Examples of CS meandering motion are shown in figures 6, 15, and 16.

3.4.2.3 Johannesson-Parker 1989 (JP89 or u1b)

The JP89 meandering model is based on several physical input values, including width, depth, flow, bed grain size, and water surface slope, as well as the effective curvature at each point along the river. This model makes use of 2 coupled second-order differential or integral equations of the stream distance variable s, the latter of which have been implemented by one of us (Coyote) specifically for this study. The JP89 method modifies the circumferential speed method described above to produce a more complicated expression for the speed perturbation u1b at the outside bank of a bend which includes linear terms from the secondary part of the flow which is perpendicular to the stream direction. The implementation we are using is based on the integral equations 45 and 46 from the Johannesson-Parker 1989 paper:

$$\sigma_s(\phi) = \sigma_s(0)e^{-(\delta/r)\phi} + \frac{\delta}{r}e^{-(\delta/r)\phi}\int_0^{\phi} e^{(\delta/r)\phi'}\sigma(\phi')d\phi'$$

$$u_{1b}(\phi) = [u_{1b}(0) + \chi_{20}\sigma(0)]e^{-2\phi/r} - \chi_{20}\sigma(\phi) + \frac{1}{r}[\chi_{20}(F^2 + 2)$$

$$- 1]e^{-2\phi/r} \int_0^\phi \sigma(\phi')e^{2\phi'/r}d\phi' + \frac{1}{r}(A + A_s)e^{-2\phi/r} \int_0^\phi \sigma_s(\phi')e^{2\phi'/r}d\phi'$$

Figure 23: JP89 integral equations.

These equations form a second order initial value problem. Their details, and the meanings of the various symbols involved, are not important for this study, with the exceptions being to note that sigma is the curvature, and phi is the downstream distance. Thus, these equations involve exponential functions of both the positive and negative stream length, which causes them to overflow or underflow if implemented in their stated form for rivers greater than a few km in length, depending on the other input variables. However, knowing the values of sigma and u1b at the start of the river (for phi = s = 0):

```
sigma_0 = abs(Ce) * (width / 2.0)
  u1b_0 = sigma_0
```

allows one to iteratively calculate them for all other values downstream without performing the entire distance integration at each point. In our implementation, we calculate only one term of each integral equation for each point on the river, and then reset sigma_0 and u1b_0 to the values from the previous calculation. This produces the same values for u1b as evaluating the full intergals, but reduces the magnitudes of the integrands due to the exponential terms (as phi is never larger than the distance between points), and thus permits calculations for long rivers. It is also a bit faster to perform that the full intergals.

If the ratio of outer bank speed to center speed in a bend is (radius + width/2) / radius, as it is in the circumferential speed method of the previous section, then the excess speed at the outer banks is given as:

```
u1b = ((radius + width / 2) / radius - 1)
    = (width / 2) * (1 / radius)
    = b * C_tilde
    = sigma
```

This is why the circumferential speed method is also called the 'sigma' method, as it is a simpler version of JP89 where the cross-stream contribution to the outside bank speed perturbation is not included.

To test these implementations, we simulated a circular channel using the constant-flow parameters listed in run F2 of Table 2 in the JP89 paper [ref 4]. According to figure 5 of the paper, the observed values of u1b for this channel should be about 0.2 (that is, about 1.2 times the center speed). The circumferential speed method produces output yielding a constant u1b value of 0.111 at all points along the curve. The JP89 method (using both the full integral and our modification) produced identical results which started at 0.111 and increased over the length of the channel until yielding limiting values of about 0.18. Although this is not exact, it is much closer than the value calculated from sigma alone.

However, the JP89 calculation does not yield a constant value for u1b immediately, but requires a 'start up' period, and produces the final u1b value asymptotically after a finite delay in stream length. This appears to be a general characteristic of the JP89 model, and was also seen in the other river simulations used in this study. This may not represent a problem in the JP89 model per se, as a time or phase delay is often associated

with coupled second order systems such as electrical signal filters or mechanical systems invloving masses and springs.

Two other potential problems with the JP89 model appear to be:

1. Values of u1b range from far less than 1 to many times 1, whereas they are expected to be near to and just greater than 1 for realistic bends and curvatures. Nevertheless, this does not appear to adversely affect the meandering behavior of the simulations, and it is automatically compensated for by the river simulation program by adjusting the migration rate factor down until the desired erosion rate is obtained, irrespective of the 'raw' u1b values.

2. There appears to be an inherent numerical instability to the JP89 model that often causes regions of low curvature, or where the curvature changes sign, to degenerate into oscillations or unbounded random motion. This instability appears to be in addition to the innate instability of straight flowing segments which leads to normal meandering behavior. Resonance at particular frequencies is often a property of coupled second order systems such as band-pass filters. In the present case, this behavior might be more akin to a system of masses connected by springs which absorb energy at a specific set of frequencies. In the JP89 simulations used in this study, we have taken several numerical steps to attempt to damp this behavior, such as smoothing and reinterpolating the output of the JP89 meandering module before applying the meandering motion to the river points. However, some resonances continue to appear, generally for slower flows in wider rivers. This subject will be mentioned again in section 4.6.1 below.

Most of the simulations shown in the remainder of this report use the JP89 method.
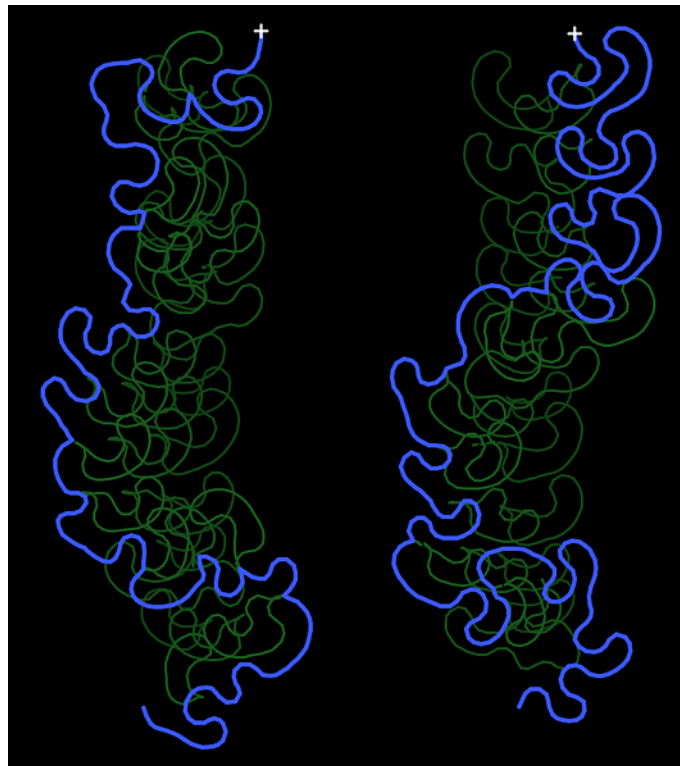
Figure 24: JP89 simulations.

3.4.3 Limitations to meandering methods

The Johannesson-Parker 1989 meandering model used in this study is clearly not adequate to accurately represent a river like the MNRR, primarily because:

1. It reduces the geometry of the river to a single idealized channel defined by a centerline and width at every point and having a trapezoidal cross-section, rather than the multiple irregular channels and braids of the MNRR which contain numerous shallows, islands, chutes, and submerged and surface bars.

2. It does not track the transport of sediment within the flow from where it is eroded from the banks or bottom to where it is eventually deposited downstream. The JP89 method in particular makes the simplistic assumption that material eroded from one bank of the channel is immediately carried to and deposited on the opposite bank, so that the rate of migration is the same for both banks, and the width of the channel does not change.

The JP89 method only accepts physical inputs in a fairly narrow range of values, otherwise the values of the exponents of s computed in the integral equations either underflow of overflow. In general, the JP89 method 'prefers' fairly narrow streams with fairly high flow rates. To use the JP89 method with the MNRR over a simulated period of 100 years, we have, for example, had to limit the maximum width to 800 m, the minimum flow to 800 M^3/s, and the minimum depth to 2.75 m. In addition, we have been unable to find a set of initial conditions which produce migration behavior that is very similar to the MNRR, as seen in the maps and photos. Specifically, the JP89 method does not produce loops and other features that closely resemble those seen in the MNRR without some manual supervision concerning the values of certain input parameters.

We have attempted to create JP89 simulations having loops similar in size and shape to those seen in the 1890 maps of the MNRR, some of which currently exist as oxbow features in the 1957-1996 maps and 2006 satellite images. This does not present too great a difficulty, as it is generally only a matter of picking the proper lag and sum distances used for calculating the effective curvature, the nominal distance being approximately one river width. However, one disadvantage to bigger loops is that the river may tend to 'hug' the valley wall for long periods and distances, as there is less variation in curvature to make it change direction and migrate away from the wall. Thus, loop size involves a tradeoff between similarity to reality and the potential stagnation of the straighter segments which are near to the boundary.

We have also found that artificially 'clipping' the river width to a maximum value of 800 m or less creates simulations which are more active and more closely resemble the shape of the MNRR, with activity increasing for smaller widths. This observation corroborates our hypothesis that a narrower channel is more representative of the actual meandering width of the river, especially in segments where we have disregarded islands, shallows, or multiple channels in the digitization. We believe that the water surface and observed bank width are a deceptive kind of 'event horizon' which hide from view the fast-flowing, narrow, submerged conduits which are actually responsible for sediment exchange and the migration of the overall river. One potential consequence of this hypothesis is that there might be a second meandering planform beneath the visible surface planform, and that the surface width of the river may be just the 'hull' or 'envelope' of the range of this more active submerged planform. We examine this possibility further in the multiple-thread simulations of section 5.4.3.1.

3.4.4 Erosion rate

The erosion rate, in hectares per year per kilometer of river length, is the primary independent variable governing the migration rate of the simulations in this study. In the equations for migration shown in section 3.4.2 above, the exponent b is set to a value of 1.0, and the constant factor a is determined empirically by setting the initial erosion rate of the river to a specific value, which has been determined by observation of the actual river, and is nominally estimated at 1.2 ha/yr/km.

In all simulations, the erosion rate is determined after each time step in a dynamic way that involves the motion of every point on the river, rather than statically as the difference between the final remaining dry surface area and the initial surface area. In particular, the surface area eroded between any two points on the river during a particular time interval is estimated as the area swept out by a quadrilateral whose vertices consist of the locations of the river points i and i + 1 at times t and t + dt. The total area eroded by the river during a single time step is the sum of the individual areas calculated between every two consecutive points. The yearly erosion rate at that time in the simulation is therefore this total are divided by the length of the river, divided by the time step. Because the discretization of the river is finite, this estimate is an upper bound of the actual rate of erosion.

Therefore, whenever points of the river are in motion, they are considered to be eroding surface area from the surrounding plain. The JP89 meandering model makes the assumption that all material eroded from one bank of the river will be immediately deposited on the other bank, but this is not a realistic assumption. Although some of this material may be deposited on the opposite, or the same, bank, it is most likely to do so only after being carried somewhere downstream by the flow, possibly out of the simulation domain. The present study makes no attempt to estimate the fraction of sediment redeposited within, or carried beyond, the simulation domain, and therefore considers all material removed by the migration of the river to be eroded and lost, again making this estimate an upper bound.

Furthermore, even if the average motion of a finite segment of the channel is negligible over some time period, and the surface area at the banks does not appear to change, the discrete motion of individual points within that segment --no matter how small-- will continue to erode material. At present, it is assumed that there is an inexhaustible supply of erodable material, and that all erosion is limited to the surface and due only to the lateral migration of the channel. These are unrealistic assumptions, but they do not affect the outcome of this study. In more realistic simulations, computational bookkeeping to track and balance the transport of mass and volume of eroded and potentially redeposited material would be required.

The initial erosion rate of a river can be automatically set to a specified value by the simulation program by varying the migration rate using a binary search. This is done at the start of every simulation in the large population of runs used in this study. On the next page is typical output of setting the initial rate to 1.2 ha/yr/km. In this case, the migration rate was changed from 1.0 to a final value of 51.197 after 25 steps. This is very quick to accomplish, as only the meandering and erosion calculations need to be performed each step, without the usual boundary or cutoff checks, or re-interpolation of the river. Once initialized, the migration rate factor is held constant for the duration of the simulation. Although the initial erosion rate is set to a known value, this value may increase or decrease at any time during the course of the simulation, and no additional attempt is made to hold it at a constant value.

```
 0: mrate =   1.000000, erate =  0.023441     13: mrate =  51.250000, erate =  1.201228
 1: mrate =   2.000000, erate =  0.046881     14: mrate =  51.125000, erate =  1.198299
 2: mrate =   4.000000, erate =  0.093762     15: mrate =  51.187500, erate =  1.199763
 3: mrate =   8.000000, erate =  0.187523     16: mrate =  51.218750, erate =  1.200496
 4: mrate =  16.000000, erate =  0.375041     17: mrate =  51.203125, erate =  1.200130
 5: mrate =  32.000000, erate =  0.750061     18: mrate =  51.195312, erate =  1.199946
 6: mrate =  64.000000, erate =  1.500036     19: mrate =  51.199219, erate =  1.200038
 7: mrate =  48.000000, erate =  1.125059     20: mrate =  51.197266, erate =  1.199992
 8: mrate =  56.000000, erate =  1.312550     21: mrate =  51.198242, erate =  1.200015
 9: mrate =  52.000000, erate =  1.218805     22: mrate =  51.197754, erate =  1.200004
10: mrate =  50.000000, erate =  1.171932     23: mrate =  51.197510, erate =  1.199998
11: mrate =  51.000000, erate =  1.195369     24: mrate =  51.197632, erate =  1.200001
12: mrate =  51.500000, erate =  1.207087     25: mrate =  51.197571, erate =  1.199999
```

Table 4: Automatic initialization of erosion rate.

3.4.5 Area coverage & residence time

Every simulation accumulates a 2-dimensional array showing how long the river stays in any one place as it moves across the valley during 100 years. This array is initially acquired at a resolution of 500 x 500 m squares for all areas within the valley boundary, but is interpolated to a resolution of 125 x 125 m as a post-processing step. This data is saved at 10 year increments during the course of the simulation. At the end of every step of the simulation, all grid squares which contain any points of the river (including both the centerline and the left and right banks as determined by the width of the river), are incremented by the value of dt. Since the river is discretized at a resolution of 100 m, and the maximum half-width of the river used in the simulations is 400 m, a 2-d array with a resolution of 500 m is sufficient to capture all points on the river, and a final resolution of 125 x 125 m is large enough not to miss any points.

At the end of the simulation, this array shows the total amount of time during 100 years that the simulated river occupied every point in the valley, although this is not necessarily contiguous time. Incremental times occupied during 10 year intervals can be calculated by subtracting one array from another. All values of this array which are non-zero show the maximum extent of the range of migration during this time. Cutoffs (excised intersecting loops) are included in this array, as well as the active migrating channel. Note that this array may conatin lacunae --that is, areas of zero occupancy contained within an area of non-zero occupancy, indicating that the river has at some time curved back upon itself, but not sufficiently to acquire the intermediate area between loops.

We expect that the accumulation of these arrays for several thousand different simulations will enable the calculation of aggregate time and location statistics that will indicate with different quantifiable levels of confidence the potential migration range of the single actual river, and which can be used to generate the probability curves (as contours of the common coverage array) at different fractional values of all simulated rivers, which will then define the overall 'migration corridor' of the river as a function of time.

3.4.6 Cumulative eroded area

The dynamic erosion calculation performed in section 3.4.4 above is also acquired in a 2-dimensional array at 10 year intervals for every simulation, indicating how much surface area and sediment each river erodes from the valley, and where. Arrays accumulated for every simulation will also be combined to estimate the average cumulative erosion of the single river as a function of time and location.

3.4.7 Generation of multiple simulation parameter combinations

The key to the success of the strategy used in this study is the ability to generate an intelligently chosen set of different simulations. The ability to automatically generate and run many different simulations from a single program is provided by the ability to read and parse command files as discussed in section 3.3.4 above. However, the choice of the input variables used, and the ranges and value combinations of those variables, was made by first manually running and reviewing the results of several different potential combinations of those variables before a final selection was chosen for the automated runs.

Because, by carefully optimizing the code of the simulation program, we were eventually able to run 100 year river simulations in a reasonable amount of time (about 15-20 minutes each), we were able to explore some of these paramater combinations for the Johannesson-Parker 1989 and other speed-based meandering methods (e.g. circumferential speed) in preparation for the large set of runs we wished to perform. We searched for a set of initial simulation parameters which yielded meandering behavior similar to that of the actual MNRR, as was observed in the maps and satellite images. Based on tests with individual combinations of the input parameters used by the JP89 model, we chose 7 different parameters to use as the systematic variable inputs to the large set of simulations:

wmax: The maximum width of the river. The width at each point was estimated automatically from the digitized bank coordinates using the procedure described in section 3.4.1.3, and then 'clipped' to one of several maximum values using the procedure described in section 3.4.1.6.

depth: The depth of the river (a constant at all points).

flow: The volume of the flow in m^3/s, also a constant over the simulation time.

diam: The bed particle size in m; the same everywhere.

ldist: The effective curvature lag distance (in river widths), as described in section 3.4.1.2.

sdist: The effective curvature summation distance (in river widths), also described in section 3.4.1.2.

erate: The initial erosion rate, in ha/yr/km, as described in section 3.4.4.

By slightly varying each of these 7 individual parameters in nested sequence, a distribution of simulations could be generated. For example, by choosing 5 nearby values of each of the parameters, 5*5*5*5*5*5*5 = 78125 slightly different simulations could be performed, which would require about 2.6 years to complete. Unfortunately, this number was far in excess of the time we had available (1 year for the entire project).

Therefore, we needed to somehow select a subset of these parameter combinations that would produce useful results in the time that was available to us (a few weeks).

We decided to perform this selection in what seem both a logical and a semi-automated way. A small Python program was created to generate a command file which designated 25 different test simulations, each ranging through one of the 5 by 5 sets of combinations of values of two of these parameters as inputs, and holding the other 5 parameters at constant, nominal, values. This would allow us to see the effect on the simulation of changing two of the input variables at the same time, and would generate a 2-dimensional matrix of results for us to review. We paired the following input variables together in each of the 25 element matrices, in order to generate a set of 11 such matrices (and a total of 275 simulations):

1. ldist and sdist	5. flow and depth	9. erate and flow
2. wmax and flow	6. flow and diam	10. erate and depth
3. wmax and depth	7. depth and diam	11. erate and diam
4. wmax and diam	8. erate and wmax	

During a period of several weeks, we ran and evaluated the final 100 year river configurations of each of these sets of 5 x 5 simulations, frequently varying the combination of parameter values used in one set of simulations based on the results of a previous set of simulations (and often repeating sets of simulations with new values), in order to narrow down the search for a starting point to use in the large set of runs we wished to perform as the basis of the present study. In evaluating each set of simulations, we looked for combinations of parameters which generated 'reasonable' or 'possible' looking configurations of the MNRR, and we acknowledge that this evaluation was based primarily on our own subjective interpretation of the resulting geometry and dynamics as it compared to the actual river. We also looked for parameter combinations which clearly generated 'unreasonable' geometry or behavior, as these were much easier to detect. Such combintions of parameters, and derivatives based upon them in conjunction with other parameters, were removed from further consideration.

Here is a summary of our observations:

* As with all the curvature-based methods, an enormous variation in river geometry can be produced, including considerable variation in loop size and shape. This is based primarily on different combinations of the variables 'ldist' and 'sdist' which control the integration calculation responsible for effective curvature. Setting sdist < 1.0 river width generally produced less active rivers with smaller features, and left fewer excised cutoffs behind. Setting sdist > 1.0 generally produced more active rivers with larger features, and more cutoffs. In addition, larger values of sdist tended to elongate the shapes of loops, and also affected the direction toward which they 'leaned', making more asymmetric loops which pointed farther upstream.

* Variations in ldist away from 1.0 river width had little effect on the geometry or dynamics of the rivers. However, values of ldist < 0.75 or > 1.25 widths tended to generate unstable river features, consisting of oscillations or discontinuities bewteen points. It is not known whether this was a property of the JP89 model equations or of actual meandering behavior (although the latter seems physically unlikely). Nevertheless, for this reason we elected to fix ldist at a constant value of 1.0 river width for all future simulations. This seems reasonable, as we would expect the upstream effect on river migration to originate at a distance of on the order of 1 width, and to vary in length about that distance based on the speed of the

flow.

* The response of the JP89 model to variations in maximum river width was much as expected. Narrower rivers tended to be more active, and produce more but smaller features, and more cutoffs. Wider rivers tended to be considerably less active, and produce fewer, but much larger, features, and fewer cutoffs.

* The response of the JP89 model to increased flow is somewhat counter-intuitive. Although the loop size does increase, the overall activity and erosion rate decreases with increased flow. The migration rate must therefore be increased in order to create an initial erosion rate of a specified value, and that erosion rate then generally decreased over the remainder of the simulation time, whereas with other meandering methods the erosion rate usually increases with time as the river increases in length and sinuosity.

* Either decreasing the depth of the river or increasing the bed grain size appear to have the effect of making the river more active, with larger, more elongated features, although decreasing the depth also magnifies the differences in activity seen between the smaller and larger grain sizes. The equations we are using to calculate the 'scouring constant' A in the JP89 model are appropriate for a river bed composed of medium sand rather than gravel, so we would expect the grain sizes to be on the order of from 0.5 to 1 mm.

* The response of all simulations to variations in intial erosion rate was as expected: higher erosion rates were consistent with greater river activity, larger features, and rivers which ranged farther from their original positions. There was no perceptible correlation between initial erosion rate and any of the other 6 input variables, so that we consider the space of input combinations to be 6-dimensional, rather than 7-dimensional, and changes in erosion rate correspond to similar changes in river activity for all other variables, as if erosion rate was a 'gain control' on the overall rate of river migration.

The nominal initial erosion rate as measured for the MNRR is close to 1.2 ha/yr/km, as reported in [ref 1]. However, most of the 'interesting' river simulations have erosion rates far in excess of this value. Simulations limited to realistic erosion rates are considerably less dramatic, with far fewer cutoffs, but still consume planform area. We decided to use initial erosion rates of from 1x to 3x the measured value, so as to bracket the possible range of motion of the simulated river considering a potential upper bound due to unknown factors whch might occur during the next 100 years.

By examining the combinations of input parameters used in the different test simulations, and the final configurations of the rivers generated from those test matrices, we have found that the 'wilder' rivers tend to be narrower, shallower, have higher rates of flow, larger bed grain size, depend on more upstream geometry, and have higher initial erosion rates --which is consistent with expectation. By evaluating the simulations performed with distinct paired combinations of input values, especially {wmax and depth}, {flow and diam}, and {ldist and sdist}, (that is, for 3 orthogonal 2-dimensional subspaces of the 6-dimensional parameter space), we decided on the following discrete values of these parameters as the inputs to the full set of simulations:

```
Maximum attenuated width: 500, 600, 700, 800 m
                   Depth: 2.75, 3.0, 3.25, 3.5 m
                    Flow: 800, 1000, 1200, 1400 m^3/s
   Bed particle diameter: 0.0005, 0.00075, 0.001, 0.00125 m
                   ldist: 1.0 only
                   sdist: 0.75, 1.0, 1.25 local widths
     Initial erosion rate: 1.2, 2.4, 3.6 ha/yr/km
```

When taken in all combinations, this yields 4x4x4x4x1x3x3 = 2304 total runs, requiring an estimated 33.6 days to complete. While the runs were in progress, we decided to add an additional intermediate value of the erosion rate at 1.8 ha/yr/km, increasing the total number of runs using the JP89 meandering model to 3072. We also decided to use one other meandering method to compare and contrast the aggregate results. The circumferential speed method is essentially a simpler version of JP89 based on the same idea, but without making use of the perturbation in far bank speed due to secondary cross-stream flow.

Figure 25: JP89 response to variation in width.

Figure 26: JP89 response to variation in depth.

Figure 27: JP89 response to variation in flow.

Figure 28: JP89 response to variation in diameter.

Figure 29: JP89 response to variation in sdist.

3.4.8 Common area coverage and definition of migration corridor

Every simulation run accumulates the 2-dimensional area coverage and residence time arrays discussed in section 3.4.5. These arrays show both the maximum extent of the river in 2d, and also the total amount of time spent by the river (although not necessarily contiguous time) at any point in the valley. These arrays can be combined in a binary way for the set of all simulated rivers, or for subsets of rivers having specific values or ranges of input parameters, to yield the 'common coverage array' for that set. This array is calculated as follows:

1. From the coverage and time array of each simulation, a binary function is calculated such that if an element $c(i, j)$ of the coverage array is greater than zero (indicating that the simulated river spent at least one dt of time at that point in the valley), then $b(i, j) = 1$; otherwise $b(i, j) = 0$.

2. All of the binary functions for each simulation are summed, element by corresponding element. The resulting array of values indicates the 'common coverage' of the set of river simulations summed, in that the value of an element $cc(i, j)$ is equal to the number of simulated rivers in the set which occupied that point in the valley for at least one dt of time during the simulation.

3. The elements of the common coverage array are then normalized to be in the range 0.0 to 1.0 by dividing each element by the total number of rivers in the set. This process yields an array with real (floating-point) values, although the minimum difference between any two values can be no less than $1/3072 = 0.000326$, in the case that all rivers in the full population of simulations are combined.

Contour plots of the common coverage array will then show the range and extent of motion of different fractions of the simulated rivers in the population, and the area contained within those extents which has at some time been occupied by that fraction. For example, contours drawn for values of the common coverage at a level of 0.5 indicate how far 50% of all simulated rivers in the population have traveled from their original location. Similarly, contours can be drawn at different levels of this array indicating how far 99%, 95%, 75%, 25%, 5%, and 1% of all rivers in the population have traveled.

In this way, the common coverage array provides a probabilistic interpretation of the potential migration of the actual river. The value of an element of this array at any (x, y) point in the valley indicates the relative likelihood that the actual river will eventually reach and occupy that point at some time during the next 100 years. This value goes from 1.0 (100% likelihood) for all points occupied by the original river position, to 0.0 (0% likelihood) for those points which are never reached by any simulated river in the population, and which are outside all contour lines.

The 'migration corridor' can then be defined as the subset of the common coverage array for which all elements have values greater than or equal to some constant, perhaps 0.95 for a 95% confidence level. This corridor will be different for different confidence levels, and at different times during the 100 year simulation (the common coverage array can be calculated every 10 years). However, for a sequence of confidence levels ordered L1 > L2 > L3... the range and enclosed area of the correspondng sequence of migration corridors follows the reverse order: MC1 <= MC2 <= MC3... We believe that this provides a realistic and accurate picture of what the actual 59-mile segment of the MNRR might do during the next 100 years.

3.4.9 Target areas in simulation domain

Using the GIS program described in section 3.3.1, 'target' areas were defined within the MNRR valley at a resolution of 500 x 500 m squares which correspond to towns, roads, airstrips, parks, and other geographic landmarks. These coordinates can be used by the database program described in section 3.3.6 to compare them to non-zero elements of the coverage area and residence time arrays of each river simulation, described in section 3.4.5. The intersection of a non-zero element of the coverage array and one of the coordinates of a designated target area indicates that part of that target has been reached and occupied by that particular river.

Information about which rivers intersect the grid cells contained in any of the targets at any time during the simulation is accumulated by the database program, and an 'average incursion' or 'probability of invasive danger' over the entire 100 year period is calculated for each target area, indicating which of them are encroached upon by the aggregate river, and to what degree. The percent of target coverage, given by the number of grid cells of each target occupied by a particular river, divided by the total number of cells for that target, is averaged for all rivers in the database to yield an aggregate 'danger score' for that target.

For this study, 13 target areas were defined:

1. Elk Point (17 squares)
2. Gayville (2 squares)
3. Harold Davidson Field (5 squares)
4. Jefferson (6 squares)
5. Meckling (2 squares)
6. Mission Hill (4 squares)
7. Ponca state park (75 squares)
8. Richland (3 squares)
9. Vermillion shore (17 squares)
10. Volin shore (3 squares)
11. Westfield (3 squares)
12. Yankton (east shore) (14 squares)
13. Yankton (along SD50) (18 squares)
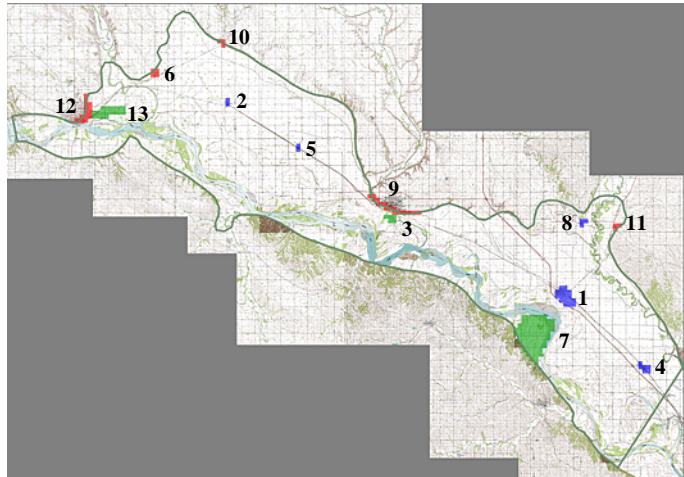
Figure 30: Location of target areas within the simulation boundary.

Since the coverage arrays for each simulation are saved at 10 year intervals, the database can determine the first time that any river reaches a specific target, if at all. These times can again be averaged together for all simulated rivers which reach designated targets to yield the probable average time of arrival of the actual river. The combination of average percent coverage and average arrival time of the aggregate river at each target, along with the contour plots of the 2d coverage maps described above, showing the percentage (99%, 95%, 75%, 50%, 25%, 5%, 1%) of all simulated rivers reaching points in the valley, can be used to assess and rank the relative danger faced by each target during the next 100 years (and at 10 year intervals before then). Targets lying on or inside specific contour lines have a well-defined, quantifiable, chance of being overrun by the river during the next 100 years.

The database program can also find examples of individual rivers which reach and occupy one or more designated targets during the entire simulation, or at some specific time during the simulation (at a resolution of 10 years), but which miss other targets.

3.4.10 Comparison of 2 meandering models

85% of the river simulations used in this study were performed using the Johannesson-Parker 1989 meandering model, which is based on the solution of 2 integral equations. Most of the simulated rivers shown in this report have been produced using this method. However, as a comparison, 540 simulations (15%) were perfomed using the much simpler, and less 'physical', circumferential speed meandering model, which is based on the difference in speed of flow at two different radii around river bends. Comparisons of the results of these two different models will be shown in section 4.6. below.

A total of 3612 river simulations were performed, using slightly different values of the 6 input parameters {maximum width, depth, flow, grain diameter, curvature summation distance, and initial erosion rate} each time, so as to generate a range of river shapes and behaviors. 3072 simulations were performed using the Johannesson-Parker 1989 meandering model, and another 540 were then performed using the simpler Circumferential Speed method, for use as a comparison to the JP89 results.

We originally planned on using 3 different values of the initial erosion rate at 1x, 2x, and 3x the nominal measured rate of 1.2 ha/yr/km, which yielded a total of 2304 distinct parameter combinations. However, because the runs were progressing well ahead of schedule, we decided to perform an additional 768 simulations using the same combinations of the 5 variables {wmax, depth, diam, flow, sdist}, but with an additional initial erosion rate of 1.8 ha/yr/km. This is partly because many of the simulations decreased their erosion rates during the simulation time (so that several ended with erosion rates well below 1.2 ha/yr/km), but also because after viewing the initial results we felt that an intermediate value between 1.2 and 2.4 ha/yr/km was needed, whereas there was less discernable difference between runs started at 2.4 and 3.6 ha/yr/km. This yielded a new total of 3072 distinct simulations.

During each simulation, the following 1-dimensional data was saved after each time step:

    * The length of the river at resolutions of 100, 2500, 5000, 7500, 10000, and 12500 m.
    * The total area coverage.
    * The current erosion rate.
    * The total cumulative erosion.

In addition, the following 2-dimensional data was saved at 10 year intervals:

    * The coverage and residence time of the river at each 500 x 500 m grid square.
    * The cumulative erosion in hectares per each 500 x 500 m grid square.

After all simulations were complete, the 2d coverage and residence time arrays were converted to binary (in which all elements $c(i, j) > 0$ became 1) and summed for all rivers to yield the common coverage array for the aggregate river. This array was then plotted transparently on both the topographic map and satellite image mosaics of the valley as a background to indicate its location and extent. These plots show the percentage of all river simulations which passed through various points in the valley, such that those points were occupied for at least one time step by at least one river of the population of simulations. Contour lines at 99%, 95%, 75%, 50%, 25%, 5% and 1% were displayed on these plots to indicate the range of migration of different fractions of the simulated rivers. We feel that these limits realistically define the probable range of motion of the actual river at a given confidence level, and suggest that together they be designated as the '100 year migration corridor' for the river.

We also wrote a simple database program to collect, manipulate, and display the results of any simulation, in both numerical and graphical form. This database has a programming and query syntax similar to some other common programs which make use of 'structured query language', such as 'MySQL' and 'PostgreSQL'. Initially this databse was sufficient to perform rudimentary searches and display subsets of results as text and images, but its interface and capabilities have evolved considerably over time as the simulation data were

analyzed. The database consists of two separate programs:

1. A database creation program which peruses all simulation files and accumulates numerical results, creating a large table of values which are saved in a binary file.

2. A database query program which can print entries and fields in any order, sort entries about any field, select subsets of entries using logical and numerical relationships, and plot any specific simulated river plus the 2d common coverage or average erosion arrays on a map or satellite mosaic background.

Using the database, we were able to calculate the common coverage array, and therefore the probable migration corridor, for specific subsets of the entire population of simulations to show, for example, the variation in coverage and migration with respect to river width, depth, flow, or other input parameters, or with respect to output variables such as total length, final erosion rate, or number of cutoffs. We can also plot the distributions of initial and final input and output variables, or any 2- or 3-dimensional relationship and linear trend between them.

Finally, using target areas defined within the 500 x 500 m grid, the database program can track the locations of all rivers over time to determine if and when these targets are reached, the fractional amounts they are covered by each river, and can use this aggregate information to estimate the probable danger to each of them from the actual river during the next 100 years.

4.2 Examples of simulations

Using the database, we can sort the resulting simulations based on extreme values of one of several output values to see what combinations of input parameters generated them. For example, on the pages that follow are examples of the longest and shortest rivers, the longest and shortest rivers when cutoffs are also included, rivers with the highest and lowest final erosion rates, and rivers with the greatest and least final coverage areas.

Looking at the combinations of input parameters which produced these examples confirms the general observation which was made in section 3.4.7: the longest, most active, rivers with the farthest migration ranges and coverage areas tend to be narrower, shallower, have higher flows, larger bed grain size, depend on more upstream curvature, and have higher initial erosion rates. In all these cases, the same river (#191) is the longest, is the longest including cutoffs, has the highest final erosion rate, and has the greatest final coverage area, indicating that this particular combination of input parameters is especially synergetic. Note also that while the shortest river has a high initial erosion rate (3.6 ha/yr/km), the shortest total length river has a low initial erosion rate (1.2 ha/yr/km). This suggests that a more active river is not necessarily a longer river, as it may produce more cutoffs which attenuate its length.

As the extreme cases tend to be represented by rivers having initial erosion rates of either 3.6 or 1.2 ha/yr/km, we have repeated the database queries limited to those rivers having initial erosion rates of 2.4 ha/yr/km for comparison. Following the two sets of extreme cases are several examples of more nominal rivers which are all within 0.1 standard deviations of both the average final length (164.20 km) and average final erosion rate (2.05 ha/yr/km).

```
Sorting by length...
Top 5 entries:
    i                file           length   maxwidth0              depth               diam               flow              sdist             erate0
----- -------------------- ---------------- ----------- ------------------ ------------------ ------------------ ------------------ ------------------
    1           run0191.mnrr    245477.926265         500           2.750000           0.001250        1400.000000           1.250000           3.600000
    2           run0375.mnrr    242306.678435         500           3.000000           0.001250        1400.000000           0.750000           3.600000
    3           run0539.mnrr    236444.152114         500           3.250000           0.001250         800.000000           1.250000           3.600000
    4           run0551.mnrr    235817.205567         500           3.250000           0.001250        1000.000000           1.250000           3.600000
    5           run0327.mnrr    234978.637504         500           3.000000           0.001000        1400.000000           0.750000           3.600000

Bottom 5 entries:
    i                file           length   maxwidth0              depth               diam               flow              sdist             erate0
----- -------------------- ---------------- ----------- ------------------ ------------------ ------------------ ------------------ ------------------
    1           run2987.mnrr    125995.557520         800           3.500000           0.001000         800.000000           1.250000           3.600000
    2           run2319.mnrr    124709.513316         800           2.750000           0.000500        1000.000000           0.750000           3.600000
    3           run2551.mnrr    123554.555611         800           3.000000           0.000750         800.000000           1.000000           3.600000
    4           run0679.mnrr    122863.106785         500           3.500000           0.001000         800.000000           1.000000           3.600000
    5           run3035.mnrr    121111.733427         800           3.500000           0.001250         800.000000           1.250000           3.600000

Sorting by totalLength...
Top 5 entries:
    i                file      totalLength   maxwidth0              depth               diam               flow              sdist             erate0
----- -------------------- ---------------- ----------- ------------------ ------------------ ------------------ ------------------ ------------------
    1           run0191.mnrr    776135.792425         500           2.750000           0.001250        1400.000000           1.250000           3.600000
    2           run0539.mnrr    662674.920443         500           3.250000           0.001250         800.000000           1.250000           3.600000
    3           run0155.mnrr    649278.177699         500           2.750000           0.001250         800.000000           1.250000           3.600000
    4           run0347.mnrr    637204.392931         500           3.000000           0.001250         800.000000           1.250000           3.600000
    5           run0359.mnrr    575770.123505         500           3.000000           0.001250        1000.000000           1.250000           3.600000

Bottom 5 entries:
    i                file      totalLength   maxwidth0              depth               diam               flow              sdist             erate0
----- -------------------- ---------------- ----------- ------------------ ------------------ ------------------ ------------------ ------------------
    1           run2340.mnrr    132885.307239         800           2.750000           0.000500        1400.000000           0.750000           1.200000
    2           run3024.mnrr    132281.982556         800           3.500000           0.001250         800.000000           0.750000           1.200000
    3           run2976.mnrr    130642.757137         800           3.500000           0.001000         800.000000           0.750000           1.200000
    4           run2928.mnrr    127935.465352         800           3.500000           0.000750         800.000000           0.750000           1.200000
    5           run2880.mnrr    126171.706677         800           3.500000           0.000500         800.000000           0.750000           1.200000

Sorting by erate...
Top 5 entries:
    i                file            erate   maxwidth0              depth               diam               flow              sdist             erate0
----- -------------------- ---------------- ----------- ------------------ ------------------ ------------------ ------------------ ------------------
    1           run0191.mnrr        10.922526         500           2.750000           0.001250        1400.000000           1.250000           3.600000
    2           run0179.mnrr         8.472486         500           2.750000           0.001250        1200.000000           1.250000           3.600000
    3           run0183.mnrr         7.848543         500           2.750000           0.001250        1400.000000           0.750000           3.600000
    4           run0383.mnrr         7.526362         500           3.000000           0.001250        1400.000000           1.250000           3.600000
    5           run0959.mnrr         7.511476         600           2.750000           0.001250        1400.000000           1.250000           3.600000

Bottom 5 entries:
    i                file            erate   maxwidth0              depth               diam               flow              sdist             erate0
----- -------------------- ---------------- ----------- ------------------ ------------------ ------------------ ------------------ ------------------
    1           run2112.mnrr         0.666959         700           3.500000           0.000500         800.000000           0.750000           1.200000
    2           run2881.mnrr         0.659446         800           3.500000           0.000500         800.000000           0.750000           1.800000
    3           run2928.mnrr         0.657151         800           3.500000           0.000750         800.000000           0.750000           1.200000
    4           run2880.mnrr         0.619784         800           3.500000           0.000500         800.000000           0.750000           1.200000
    5           run2884.mnrr         0.609788         800           3.500000           0.000500         800.000000           1.000000           1.200000

Sorting by cArea...
Top 5 entries:
    i                file            cArea   maxwidth0              depth               diam               flow              sdist             erate0
----- -------------------- ---------------- ----------- ------------------ ------------------ ------------------ ------------------ ------------------
    1           run0191.mnrr       795.000000         500           2.750000           0.001250        1400.000000           1.250000           3.600000
    2           run0187.mnrr       666.250000         500           2.750000           0.001250        1400.000000           1.000000           3.600000
    3           run0379.mnrr       659.250000         500           3.000000           0.001250        1400.000000           1.000000           3.600000
    4           run0959.mnrr       647.500000         600           2.750000           0.001250        1400.000000           1.250000           3.600000
    5           run0183.mnrr       643.250000         500           2.750000           0.001250        1400.000000           0.750000           3.600000

Bottom 5 entries:
    i                file            cArea   maxwidth0              depth               diam               flow              sdist             erate0
----- -------------------- ---------------- ----------- ------------------ ------------------ ------------------ ------------------ ------------------
    1           run0600.mnrr       205.000000         500           3.500000           0.000500        1200.000000           0.750000           1.200000
    2           run0576.mnrr       204.500000         500           3.500000           0.000500         800.000000           0.750000           1.200000
    3           run2112.mnrr       204.000000         700           3.500000           0.000500         800.000000           0.750000           1.200000
    4           run2928.mnrr       204.000000         800           3.500000           0.000750         800.000000           0.750000           1.200000
    5           run2880.mnrr       200.500000         800           3.500000           0.000500         800.000000           0.750000           1.200000
```

Table 5: Database entries sorted by river length (m), total river length (including cutoffs), final erosion rate (ha/yr/km), and total coverage area (km^2). The top (greatest) and bottom (least) five entries are shown for each variable. Note that the same river (#191) is the #1 entry in all categories, and that another river (#2880) is both the shortest total length river and has the least coverage area.

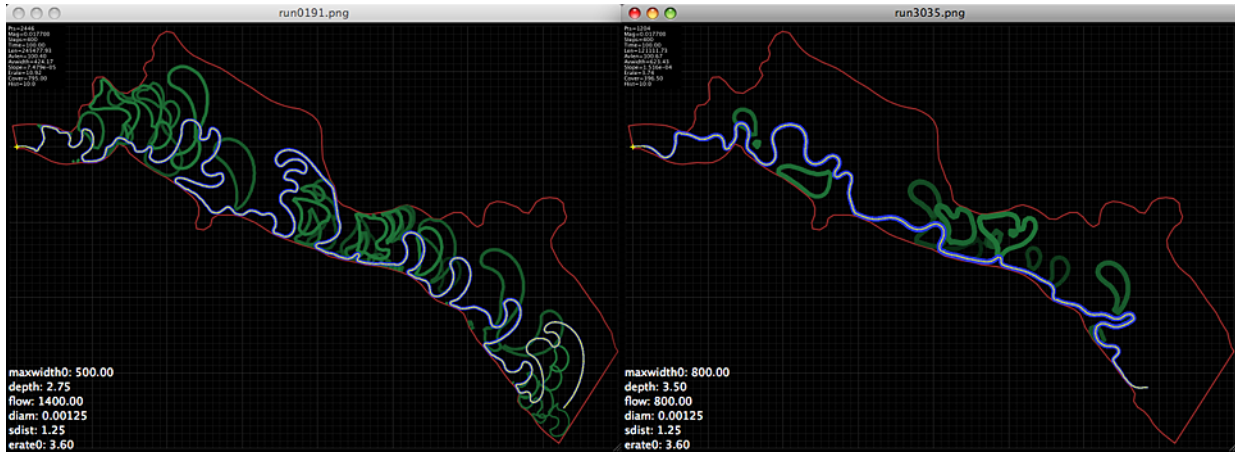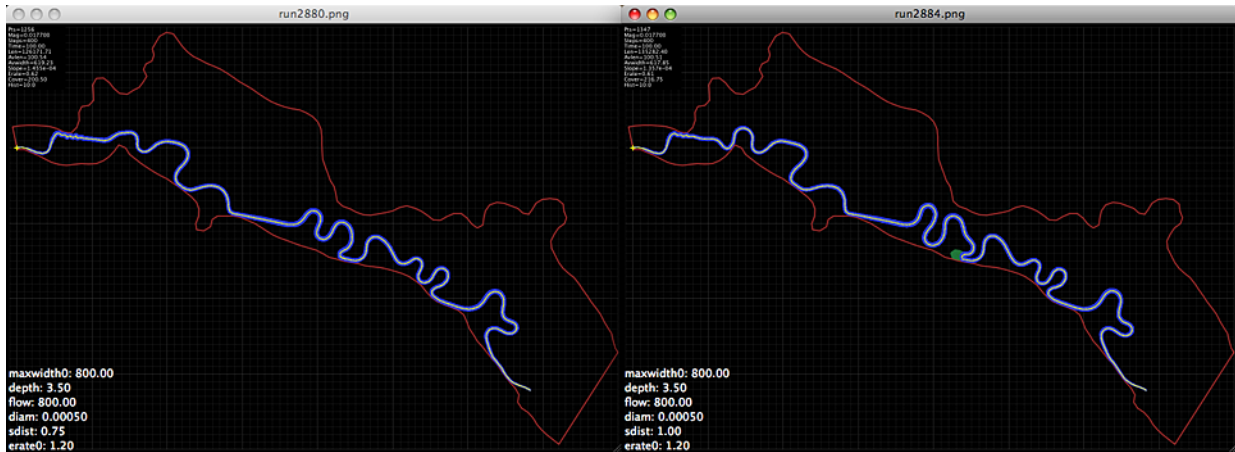Figure 31: The longest (left) and shortest (right) final rivers.

Figure 32: The shortest total length river (left), and the river with the least final erosion rate (right). The shortest total length river is also the river with the least coverage area.

Figure 33: The longest river (left) and the river with the greatest coverage area (right) limited to simulations with an initial erosion rate of 2.4 ha/yr/km.

```
Sorting by length...
Top 5 entries:
    i               file          length   maxwidth0            depth             diam             flow            sdist           erate0
----- -------------------- ---------------- ---------- ---------------- ---------------- ---------------- ---------------- ----------------
    1         run0762.mnrr   220512.623320        500         3.500000         0.001250      1400.000000         1.000000         2.400000
    2         run0570.mnrr   218235.866511        500         3.250000         0.001250      1400.000000         1.000000         2.400000
    3         run0250.mnrr   216965.783899        500         3.000000         0.000750       800.000000         1.250000         2.400000
    4         run0170.mnrr   215421.138754        500         2.750000         0.001250      1200.000000         0.750000         2.400000
    5         run0938.mnrr   214921.609066        600         2.750000         0.001250      1200.000000         0.750000         2.400000

Bottom 5 entries:
    i               file          length   maxwidth0            depth             diam             flow            sdist           erate0
----- -------------------- ---------------- ---------- ---------------- ---------------- ---------------- ---------------- ----------------
    1         run2962.mnrr   130524.833905        800         3.500000         0.000750      1200.000000         1.250000         2.400000
    2         run2650.mnrr   129958.402499        800         3.000000         0.001250       800.000000         1.250000         2.400000
    3         run2654.mnrr   129849.268584        800         3.000000         0.001250      1000.000000         0.750000         2.400000
    4         run2846.mnrr   128518.146455        800         3.250000         0.001250      1000.000000         0.750000         2.400000
    5         run2754.mnrr   128056.962374        800         3.250000         0.000750      1000.000000         1.000000         2.400000

Sorting by totalLength...
Top 5 entries:
    i               file     totalLength   maxwidth0            depth             diam             flow            sdist           erate0
----- -------------------- ---------------- ---------- ---------------- ---------------- ---------------- ---------------- ----------------
    1         run0154.mnrr   425008.636556        500         2.750000         0.001250       800.000000         1.250000         2.400000
    2         run0346.mnrr   400103.824484        500         3.000000         0.001250       800.000000         1.250000         2.400000
    3         run0166.mnrr   371653.760388        500         2.750000         0.001250      1000.000000         1.250000         2.400000
    4         run0538.mnrr   371592.172177        500         3.250000         0.001250       800.000000         1.250000         2.400000
    5         run0106.mnrr   364112.064029        500         2.750000         0.001000       800.000000         1.250000         2.400000

Bottom 5 entries:
    i               file     totalLength   maxwidth0            depth             diam             flow            sdist           erate0
----- -------------------- ---------------- ---------- ---------------- ---------------- ---------------- ---------------- ----------------
    1         run2114.mnrr   175049.778210        700         3.500000         0.000500       800.000000         0.750000         2.400000
    2         run2690.mnrr   174856.316840        800         3.250000         0.000500       800.000000         0.750000         2.400000
    3         run2930.mnrr   172084.264124        800         3.500000         0.000750       800.000000         0.750000         2.400000
    4         run2978.mnrr   171111.130693        800         3.500000         0.001000       800.000000         0.750000         2.400000
    5         run2882.mnrr   165564.747279        800         3.500000         0.000500       800.000000         0.750000         2.400000

Sorting by erate...
Top 5 entries:
    i               file           erate   maxwidth0            depth             diam             flow            sdist           erate0
----- -------------------- ---------------- ---------- ---------------- ---------------- ---------------- ---------------- ----------------
    1         run0154.mnrr        4.437586        500         2.750000         0.001250       800.000000         1.250000         2.400000
    2         run0958.mnrr        4.387906        600         2.750000         0.001250      1400.000000         1.250000         2.400000
    3         run0166.mnrr        4.210558        500         2.750000         0.001250      1000.000000         1.250000         2.400000
    4         run0190.mnrr        4.180796        500         2.750000         0.001250      1400.000000         1.250000         2.400000
    5         run0382.mnrr        4.121625        500         3.000000         0.001250      1400.000000         1.250000         2.400000

Bottom 5 entries:
    i               file           erate   maxwidth0            depth             diam             flow            sdist           erate0
----- -------------------- ---------------- ---------- ---------------- ---------------- ---------------- ---------------- ----------------
    1         run2930.mnrr        1.033187        800         3.500000         0.000750       800.000000         0.750000         2.400000
    2         run2894.mnrr        0.988216        800         3.500000         0.000500      1000.000000         0.750000         2.400000
    3         run2882.mnrr        0.988040        800         3.500000         0.000500       800.000000         0.750000         2.400000
    4         run2690.mnrr        0.928975        800         3.250000         0.000500       800.000000         0.750000         2.400000
    5         run1346.mnrr        0.913626        600         3.500000         0.000500       800.000000         0.750000         2.400000

Sorting by cArea...
Top 5 entries:
    i               file           cArea   maxwidth0            depth             diam             flow            sdist           erate0
----- -------------------- ---------------- ---------- ---------------- ---------------- ---------------- ---------------- ----------------
    1         run0178.mnrr      494.750000        500         2.750000         0.001250      1200.000000         1.250000         2.400000
    2         run0166.mnrr      487.500000        500         2.750000         0.001250      1000.000000         1.250000         2.400000
    3         run0154.mnrr      479.250000        500         2.750000         0.001250       800.000000         1.250000         2.400000
    4         run1726.mnrr      479.000000        700         2.750000         0.001250      1400.000000         1.250000         2.400000
    5         run0382.mnrr      478.500000        500         3.000000         0.001250      1400.000000         1.250000         2.400000

Bottom 5 entries:
    i               file           cArea   maxwidth0            depth             diam             flow            sdist           erate0
----- -------------------- ---------------- ---------- ---------------- ---------------- ---------------- ---------------- ----------------
    1         run1346.mnrr      281.000000        600         3.500000         0.000500       800.000000         0.750000         2.400000
    2         run2978.mnrr      277.250000        800         3.500000         0.001000       800.000000         0.750000         2.400000
    3         run2930.mnrr      274.000000        800         3.500000         0.000750       800.000000         0.750000         2.400000
    4         run2114.mnrr      272.750000        700         3.500000         0.000500       800.000000         0.750000         2.400000
    5         run2882.mnrr      262.000000        800         3.500000         0.000500       800.000000         0.750000         2.400000
```

Table 6: Database entries limited to simulations having an initial erosion rate of 2.4 ha/yr/km, sorted by river length (m), total river length (including cutoffs), final erosion rate (ha/yr/km), and total coverage area (km^2). The top (greatest) and bottom (least) five entries are shown for each variable. Note that the same river (#154) is the #1 entry by total length and by final erosion rate, and that another river (#2882) is both the shortest total length river and has the least coverage area.

Figure 34: The longest river (by total length, left), also the river with the greatest final erosion rate, and the river with the least final erosion rate (right) limited to simulations with an initial erosion rate of 2.4 ha/yr/km.

Figure 35: Two rivers within 0.1 standard deviations of the average final length and erosion rate.

Figure 36: Two other rivers within 0.1 standard deviations of the average final length and erosion rate.

```
length: min=121111.733427, max=245477.926265, mean=164197.810949, std=18801.315324
erate: min=0.609788, max=10.922526, mean=2.045091, std=1.106808

21 entries within 0.100000 stds of mean length and erate:
Sorted by length:
   i              file         length  maxwidth0            depth             flow             diam            sdist           erate0
----- ------------------- ---------------- ----------- ---------------- ---------------- ---------------- ---------------- ----------------
    1          run0093.mnrr   165978.351001        500         2.750000      1400.000000         0.000750         1.250000         1.800000
    2          run2865.mnrr   165704.539125        800         3.250000      1200.000000         0.001250         1.250000         1.800000
    3          run1109.mnrr   165578.722902        600         3.000000       800.000000         0.001250         1.000000         1.800000
    4          run2187.mnrr   165358.440019        700         3.500000      1200.000000         0.000750         0.750000         3.600000
    5          run1313.mnrr   165318.164738        600         3.250000      1000.000000         0.001250         1.000000         1.800000
    6          run1494.mnrr   165286.179166        600         3.500000       800.000000         0.001250         1.000000         2.400000
    7          run1567.mnrr   164471.722314        700         2.750000      1200.000000         0.000500         1.000000         3.600000
    8          run2211.mnrr   164236.967117        700         3.500000       800.000000         0.001000         0.750000         3.600000
    9          run0373.mnrr   164232.258206        500         3.000000      1400.000000         0.001250         0.750000         1.800000
   10          run2335.mnrr   164116.967355        800         2.750000      1200.000000         0.000500         1.000000         3.600000
   11          run1077.mnrr   163838.353242        600         3.000000      1000.000000         0.001000         1.250000         1.800000
   12          run0137.mnrr   163693.819152        500         2.750000      1400.000000         0.001000         1.000000         1.800000
   13          run2046.mnrr   163352.270533        700         3.250000      1200.000000         0.001000         1.000000         2.400000
   14          run2167.mnrr   162958.503200        700         3.500000       800.000000         0.000750         1.000000         3.600000
   15          run2441.mnrr   162808.497691        800         2.750000      1400.000000         0.001000         1.000000         1.800000
   16          run1203.mnrr   162769.984850        600         3.250000       800.000000         0.000750         0.750000         3.600000
   17          run1798.mnrr   162721.572855        700         3.000000      1000.000000         0.000750         1.250000         2.400000
   18          run1450.mnrr   162650.741448        600         3.500000       800.000000         0.001000         1.250000         2.400000
   19          run1042.mnrr   162556.591619        600         3.000000      1200.000000         0.000750         1.250000         2.400000
   20          run0949.mnrr   162543.981306        600         2.750000      1400.000000         0.001250         0.750000         1.800000
   21          run1179.mnrr   162506.110740        600         3.250000      1200.000000         0.000500         0.750000         3.600000

Sorted by erate:
   i              file          erate  maxwidth0            depth             flow             diam            sdist           erate0
----- ------------------- ---------------- ----------- ---------------- ---------------- ---------------- ---------------- ----------------
    1          run2187.mnrr        2.147791        700         3.500000      1200.000000         0.000750         0.750000         3.600000
    2          run1450.mnrr        2.129999        600         3.500000       800.000000         0.001000         1.250000         2.400000
    3          run1567.mnrr        2.129232        700         2.750000      1200.000000         0.000500         1.000000         3.600000
    4          run1798.mnrr        2.128249        700         3.000000      1000.000000         0.000750         1.250000         2.400000
    5          run1179.mnrr        2.116560        600         3.250000      1200.000000         0.000500         0.750000         3.600000
    6          run2335.mnrr        2.109599        800         2.750000      1200.000000         0.000500         1.000000         3.600000
    7          run1494.mnrr        2.088894        600         3.500000       800.000000         0.001250         1.000000         2.400000
    8          run1109.mnrr        2.085901        600         3.000000       800.000000         0.001250         1.000000         1.800000
    9          run0949.mnrr        2.074946        600         2.750000      1400.000000         0.001250         0.750000         1.800000
   10          run0373.mnrr        2.072935        500         3.000000      1400.000000         0.001250         0.750000         1.800000
   11          run0137.mnrr        2.067125        500         2.750000      1400.000000         0.001000         1.000000         1.800000
   12          run2211.mnrr        2.052708        700         3.500000       800.000000         0.001000         0.750000         3.600000
   13          run1042.mnrr        2.051317        600         3.000000      1200.000000         0.000750         1.250000         2.400000
   14          run2167.mnrr        2.035231        700         3.500000       800.000000         0.000750         1.000000         3.600000
   15          run1203.mnrr        2.018962        600         3.250000       800.000000         0.000750         0.750000         3.600000
   16          run1313.mnrr        2.002006        600         3.250000      1000.000000         0.001250         1.000000         1.800000
   17          run1077.mnrr        1.982914        600         3.000000      1000.000000         0.001000         1.250000         1.800000
   18          run2441.mnrr        1.975375        800         2.750000      1400.000000         0.001000         1.000000         1.800000
   19          run2046.mnrr        1.966225        700         3.250000      1200.000000         0.001000         1.000000         2.400000
   20          run0093.mnrr        1.961223        500         2.750000      1400.000000         0.000750         1.250000         1.800000
   21          run2865.mnrr        1.939741        800         3.250000      1200.000000         0.001250         1.250000         1.800000
```

Table 7: Database entries showing all simulations which are within 0.1 standard deviations of the final average length and also the final average erosion rate, sorted first by length and then by final erosion rate.

4.3 Histograms and 2/3d regressions

The database program can also extract and plot:

　　* Histograms of any input or output variable.
　　* 2-dimensional or 3-dimensional relationships between any 2 or 3 input and/or output variables.
　　* Linear regressions and correlation coefficients of these relationships.

On the next page are histograms of a few input and output variables for all simulations. Note the differences between the initial and final erosion rates, and between the final river length and the total length, which includes the length of all excised cutoffs. Although the JP89 model maintains a fixed river width at each point, the average width can change when new points are interpolated between existing points, and when cutoffs are removed. It is also interesting to note that the wider rivers tend to promote more variation in width over time, whereas the narrower rivers tend to stay nearer to the same width throughout time.
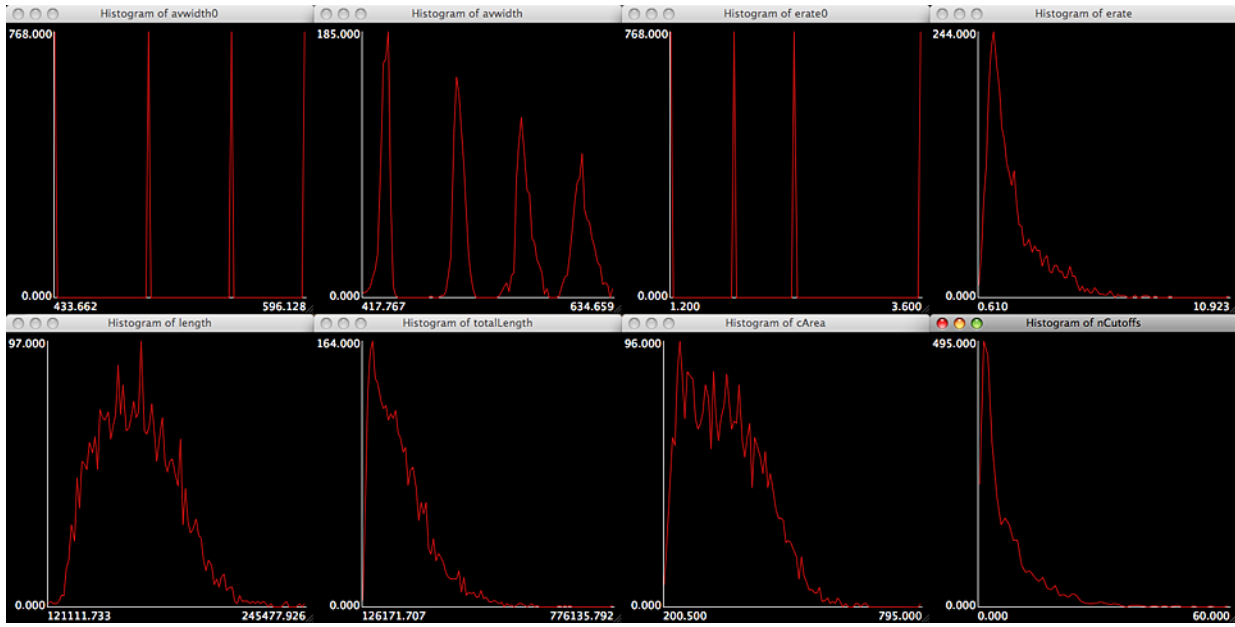
Figure 37: Histograms of simulation variables.

Below are some 2-dimensional plots of 3 output variables vs. river length and vs. total length. The values of a (intercept) and b (slope) show the best-fit lines, and the values of r (the Pearson product-moment correlation coefficient) show the goodness of fit. These plots can also add color to show a third dimension, in this case flow. Note that if river length is replaced by the total length including cutoffs, the distributions change and the linear fits become much better. Thus, the scattered 'cloud' which is superimposed on the top line of plots is due to cutoffs reducing the length of the river. Also notice the contrary influence of increased flow, which tends to make rivers more active, but also shorter.

Figure 38: Output variables vs. length, total length, and flow.

Shown next are the relationships between 5 output variables and all input parameters. These plots are generally unsurprising, showing trends which have already been predicted by test runs performed before the large population of simulations.

Figure 39: Output variables vs. input parameters.

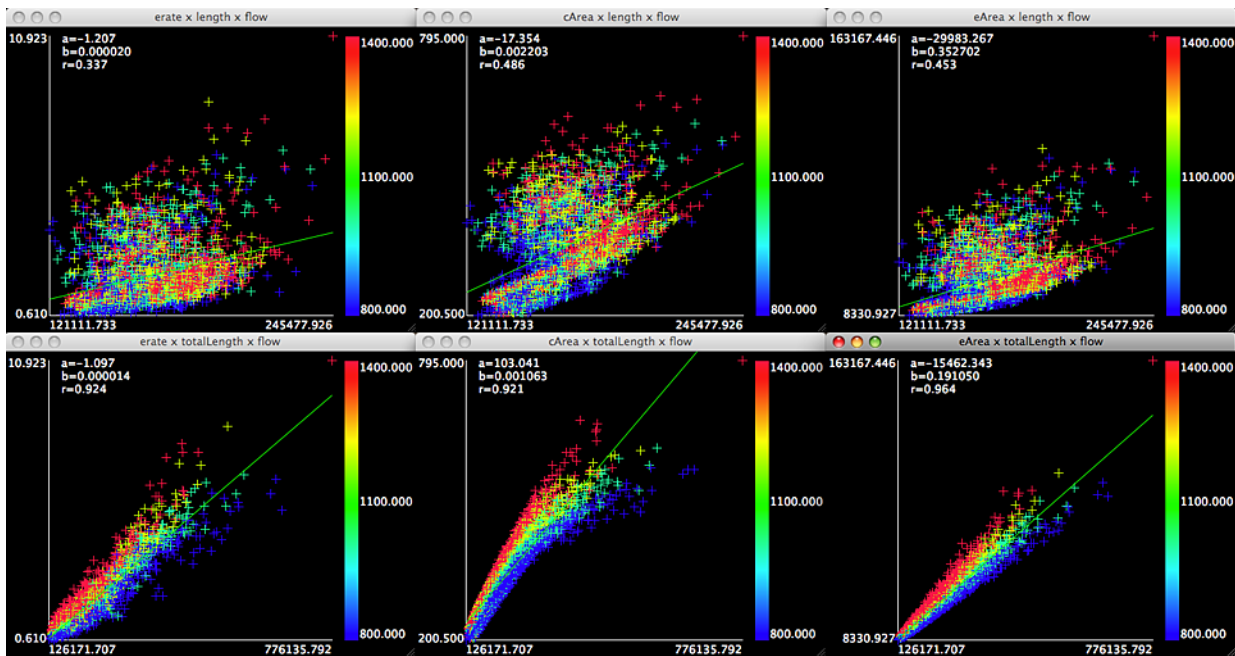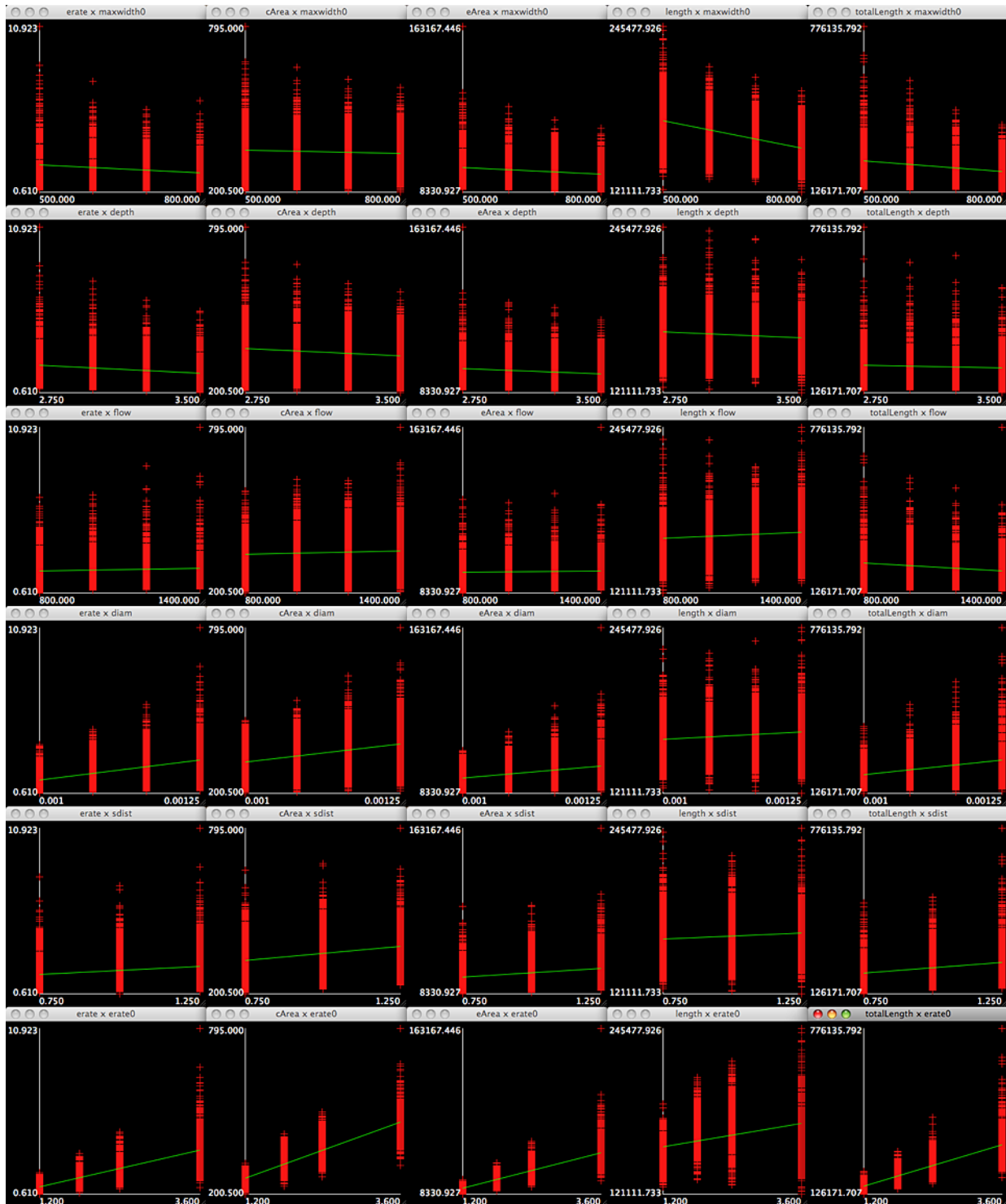Finally shown are relationships between output variables and average width, final erosion rate, and flow. Note again the contrary effect of increased flow, which tends to produce narrower rivers in each case.
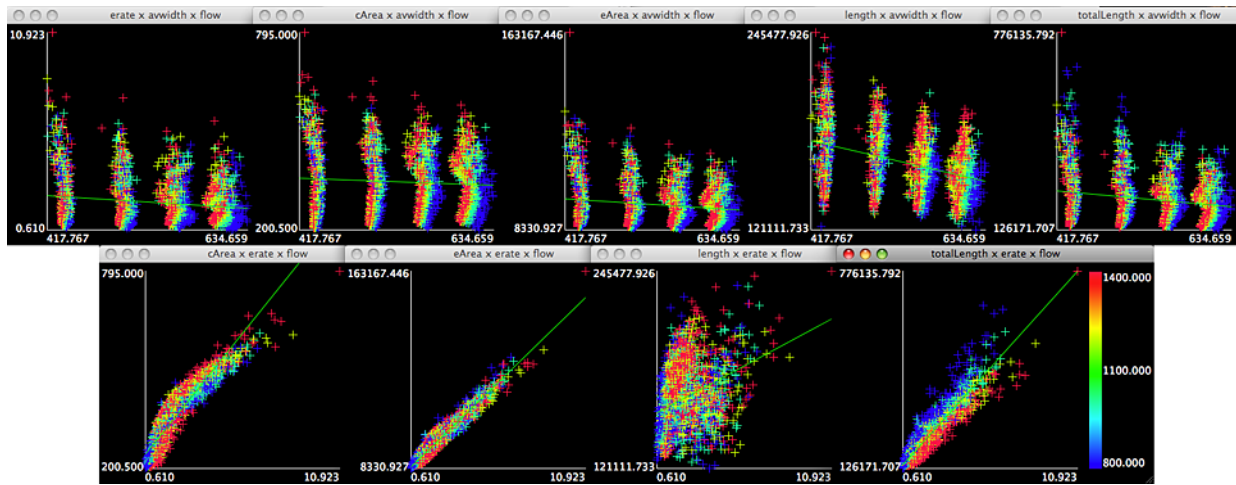

Figure 40: Output variables vs. average width, final erosion rate, and flow.

All these plots inspire two general observations:

1. There appears to be a downward trend in all output variables with respect to increased width and depth, and an upward trend with respect to increased bed particle size, curvature summation distance, and initial erosion rate. The response to flow is mixed, although generally counter-intuitive, as increased flow tends to generate shorter, narrower, rivers.

2. There are strong positive trends in final erosion rate, area coverage, and cumulative eroded area with respect to total river length. However, although the correlation between these variables and river length without cutoffs is less positive and strong, it appears that almost all river lengths can be generated from fairly low values of initial erosion rate, depending on the other input parameters. Or, put another way, increased erosion rate does not necessarily generate monotonically increasing river length. This is likely due to the increased number of cutoffs which are also associated with high erosion rates, and which limit the growth of river length by their periodic removal.

4.4 Common coverage & cumulative erosion

For this study, the most important result is the 2-dimensional common coverage array of the aggregate river, created from the area coverage and residence time arrays of individual rivers, which shows the fraction of all simulations which reach, occupy, or pass through different points in the valley during the next 100 years. Also important is the 2-dimensional array showing the average cumulative erosion at different points in the valley over the next 100 years.

The common coverage array shows the fraction of all simulated rivers that occupy points (125x125 m squares) in the valley at least once over 100 years. In the plots which follow, this value goes from 1.0, shown in red, which indicates points where 100% of all 3072 simulated rivers have gone, to 0.5, shown in green, which indicates points where 50% of all simulated rivers (1536) have gone, to a minimum non-zero value of

0.000326, shown in dark blue, which indicates points where only one simulated river has gone, to 0.0, shown in black (or not at all on the transparent overlays), which indicates all other points where no river has gone. These values can also be interpreted as the probabilities of each point being reached by the actual river over this time period. The limits of specific probability values, shown as contours and interpreted as the likelihood of the actual river migrating this far from its original position, are considered to be the '100 year migration corridor' of the river at that confidence level.

The average cumulative erosion is plotted as hectares per $(0.5 \text{ km})^2 = 0.25 \text{ km}^2$. Note that 0.25 km^2 is 25 ha, so that points showing more than 25 ha total erosion were, on average, visited by the aggregate river more than once. Also note that the cumulative erosion is the total continuously summed (after each 0.25 year time step) erosion at a point, not the difference between the final and initial land areas adjacent to the river. Thus, the simulated river could stay mostly in one place and meander very slightly, and it would continue to erode surface area, possibly beyond the capacity of the landscape to provide sediment.

In this study, it is assumed that surface runoff and transfer, or some other mechanism, will continue to provide sediment necessary to satisfy any cumulative erosion. Finally, note that in the JP89 model, erosion of material from one bank of the river equals deposition of material on the other bank. Therefore, the average cumulative erosion is also a measure of the deposition or turnover of new sediment in the valley, and of the general activity of the river at specific (x, y) points.

Although the common coverage and cumulative erosion arrays are acquired at a resolution of 500 x 500 m squares, they were interpolated by a factor of 4x to yield an effective resolution of 125 x 125 m. The interpolation was performed in two stages: first an interpolation by 2x followed by 2d smoothing of the result, and then another interpolation by 2x followed by additional smoothing. This process does not actually add any information to the calculations, but it does make the resulting surface more aesthetically pleasing to the eye, it allows the extraction of smoother contour lines for limiting values, and it makes it possible to more accurately estimate the 2d locations where there are fractional changes in the values of the arrays.

These arrays can be plotted on a blank background, on a grid of lines at 1 km, 500 m, 250 m, or 125 m resolution, or on either the topographic map or satellite image mosaics. For this study, plotting these arrays on the maps and satellite images is most useful, as it allows the migration of the river to be seen in the context of the geographic and man-made features of the valley. Arrays can be overlaid on a background image using any opacity between 0.0 and 1.0, so that features of the maps and satellite images can also be seen. Contour lines can be extracted at any value between 0.0 and 1.0 for the common coverage array, or between 0.0 and the maximum eroded area for cumulative erosion. One or more of the simulated rivers, and/or the location of target areas within the valley, can also be overlaid on these plots as required.

The common coverage arrays have also been calculated at intervals of 10 years during the simulation time, and can be plotted in sequence to show the progression of the aggregate river across the valley. In the plots that follow, approximate areas contained within each of the 100 year common coverage contour lines are also displayed. The initial area of the full-width digitized river (average width = 747.84 m, length = 95353.75 m) is about 71.31 km^2, although all of the width-limited simulations used in this study start with less than this area. As a comparison to the full-simulation results, common coverage and cumulative erosion arrays are also shown for only those simulations that were initialized at 2.4 ha/yr/km.
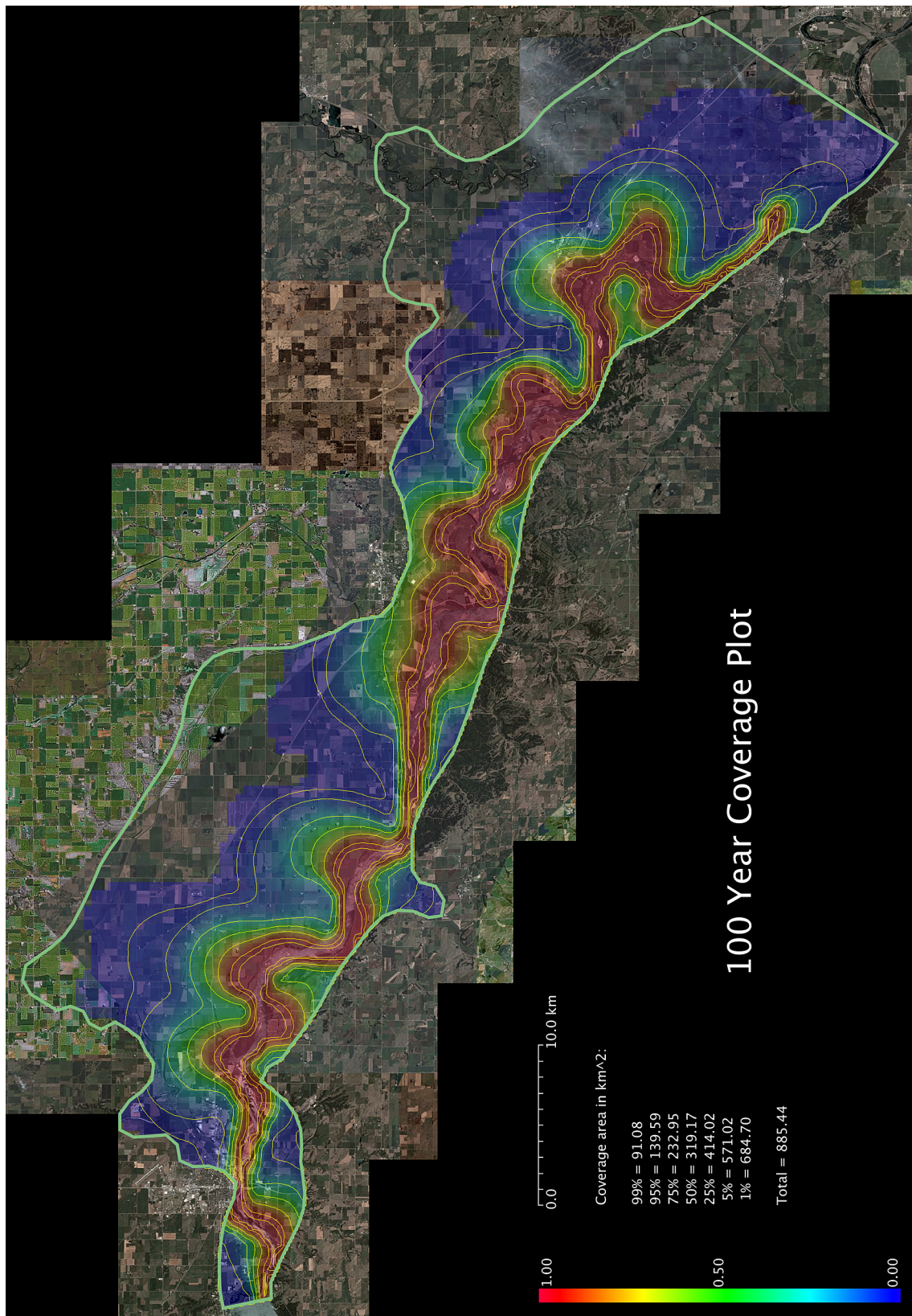
Figure 41: The common coverage array of 3072 river simulations overlaid on the satellite image mosaic, with contours showing the migration ranges of 99%, 95%, 75%, 50%, 25%, 5%, and 1% of all rivers.

Figure 42: The common coverage array of 3072 river simulations overlaid on the topographic map mosaic, with contours showing the migration ranges of 99%, 95%, 75%, 50%, 25%, 5%, and 1% of all rivers.

100 Year Coverage Plot

10.0 km

0.0

Coverage area in km^2:

99% = 91.08
95% = 139.59
75% = 232.95
50% = 319.17
25% = 414.02
5% = 571.02
1% = 684.70

Total = 885.44

1.00   0.50   0.00

Figure 43: The common coverage array at 10 year intervals overlaid on the satellite image mosaic, with contours showing the migration ranges of 95%, 50%, and 5% of all rivers.
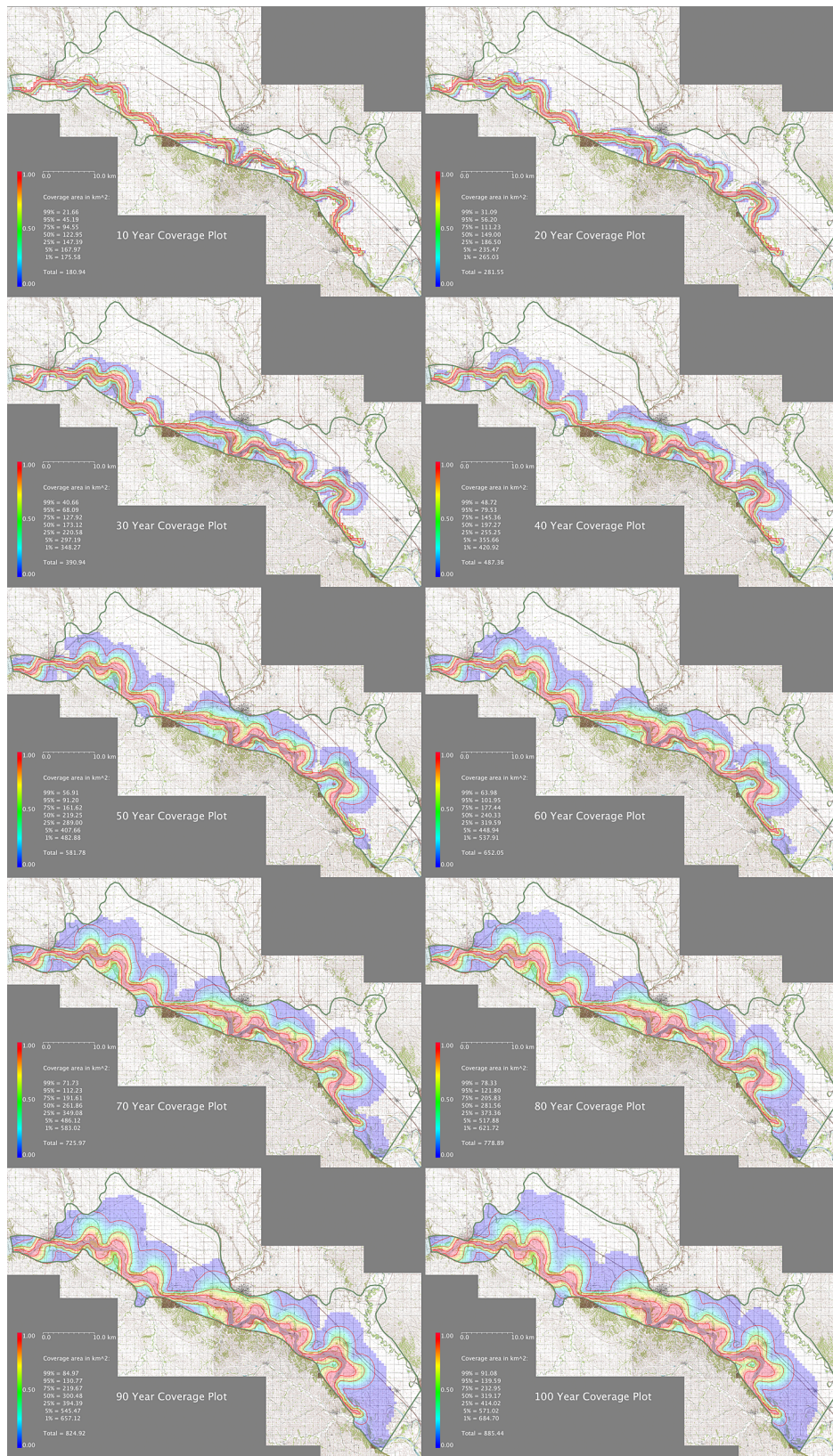
Figure 44: The common coverage array at 10 year intervals overlaid on the topographic map mosaic, with contours showing the migration ranges of 95%, 50%, and 5% of all rivers.
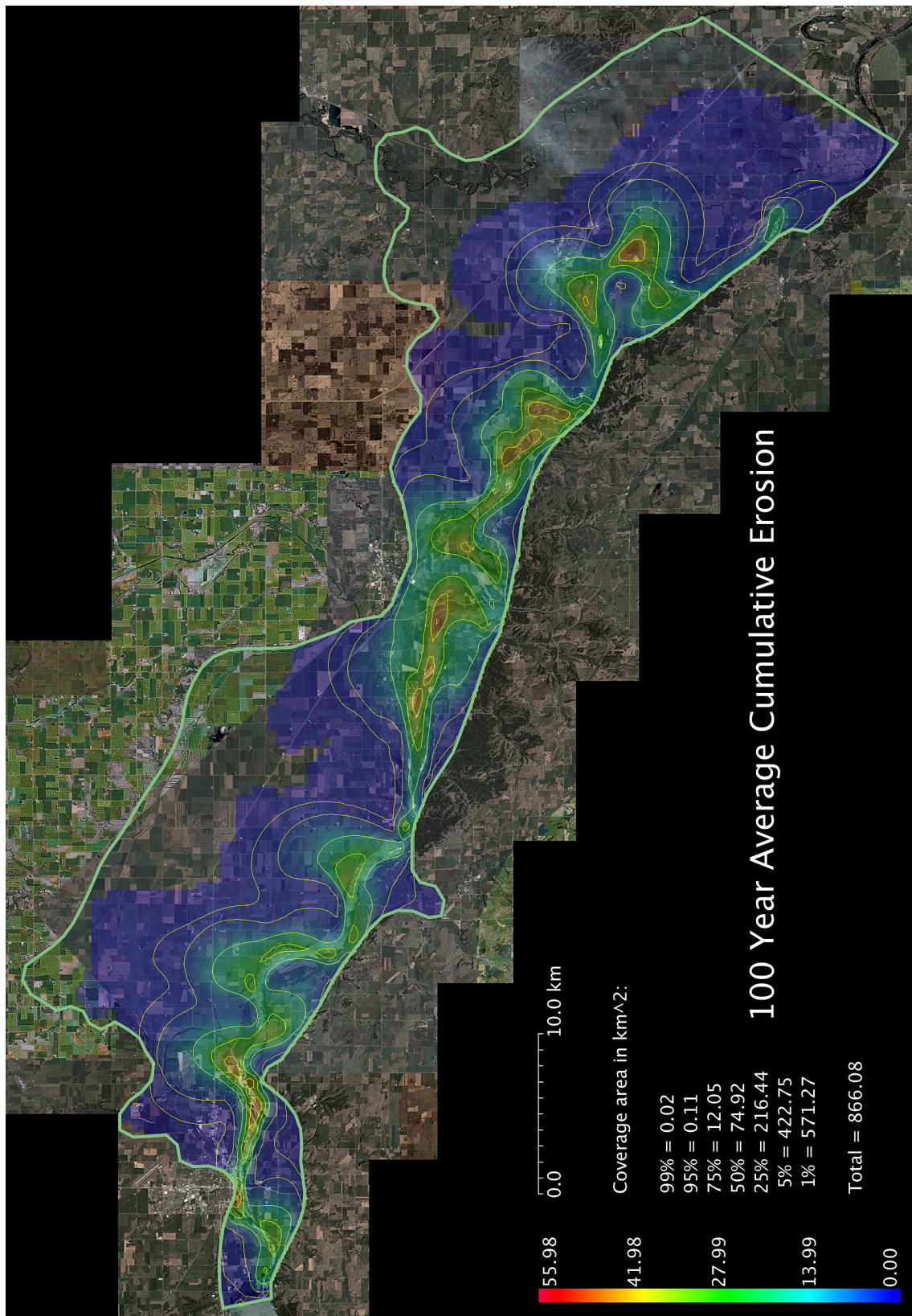
Figure 45: The average cumulative erosion in hectares of 3072 river simulations overlaid on the satellite image mosaic, with contours showing the areas having 99%, 95%, 75%, 50%, 25%, 5%, and 1% of the maximum erosion.

Figure 46: The average cumulative erosion in hectares of 3072 river simulations overlaid on the topographic map mosaic, with contours showing the areas having 99%, 95%, 75%, 50%, 25%, 5%, and 1% of the maximum erosion.

Figure 47: The common coverage array of 768 river simulations having an initial erosion rate of 2.4 ha/yr/km overlaid on the satellite image mosaic, with contours showing the migration ranges of 99%, 95%, 75%, 50%, 25%, 5%, and 1% of all rivers.

Figure 48: The average cumulative erosion in hectares of 768 river simulations having an initial erosion rate of 2.4 ha/yr/km overlaid on the topographic map mosaic, with contours showing the areas having 95%, 75%, 50%, 25%, 5%, and 1% of the maximum erosion.

4.4.1 Coverage with respect to parameter subsets

The full population of 3072 simulations performed includes runs which were initialized at all discrete values of the 6 input paramters {width, depth, flow, particle diameter, curvature summation distance, erosion rate}, and the common coverage arrays shown above are calculated from this set of results. However, by calculating additional common coverage arrays for subsets of simulations which were generated by ranges of input parameters having specific constant values, it is possible to define the '100 year migration corridor' under different conditions and assumptions. Nevertheless, while these individual subsets do show marked differences in coverage for values which are somewhat less than 1.0, they do not significantly change the shape of the 'core' set of points reached by most rivers at values of 0.99, 0.95, or slightly below.

The plots below show differences in the 100 year common coverage for subsets of runs which have fixed values of each of the 6 different input parameters, arranged in sequences of these values. Therefore, they do not represent new information about the simulations, but are a filtering of the full output so as to look for trends in the results, as indicated by differences in the 99% to 1% contour lines of the coverage as the input parameters change. Numerical values estimating the coverage area contained within each set of contour lines are also shown.

* The first set of plots show differences in coverage with respect to maximum attenuated river width. While the coverage at 95% and 75% of all rivers increases monotonically with width, the coverage at 99% peaks at 700 m, the coverage at 50% peaks at 600 m, and all other coverage percentages (including the total coverage) decrease monotonically with increased river width, suggesting that, on average, the farthest migrating rivers are neither too narrow nor too wide.

* The next set of plots show coverage with respect to river depth. In all percentages of simulations, the coverage decreases monotonically with increasing depth.

* The next set of plots show coverage with respect to flow. All percentages of rivers >= 25% peak at either 1000 or 1200 m^3/s, while all percentages <= 5% increase monotonically with increasing flow, suggesting that while the highest flow does produce the farthest ranging rivers as individuals, the migration range of most rivers is greatest for a more moderate flow.

* The next set of plots show coverage with respect to bed particle diameter. In this case again, all percentage areas increase with increasing particle size.

* The next set of plots show coverage with respect to upstream summation distance (in local river widths). This clearly indicates that the coverage increases, and is somewhat sensitive to, the amount of upstream river geometry that affects the lateral migration at any point.

* Finally, as expected, the major contributing parameter to all coverage areas appears to be the initial erosion rate. During the simulation, the erosion rate is not maintained or adjusted, and may become either higher or lower than its initial value for any particular river. Nevertheless, this seems to be the primary variable responsible for variations in coverage.

These trends suggest that management strategies designed to affect specific parameters might be useful in attempts to control the migration of the river, either overall or within localized areas.
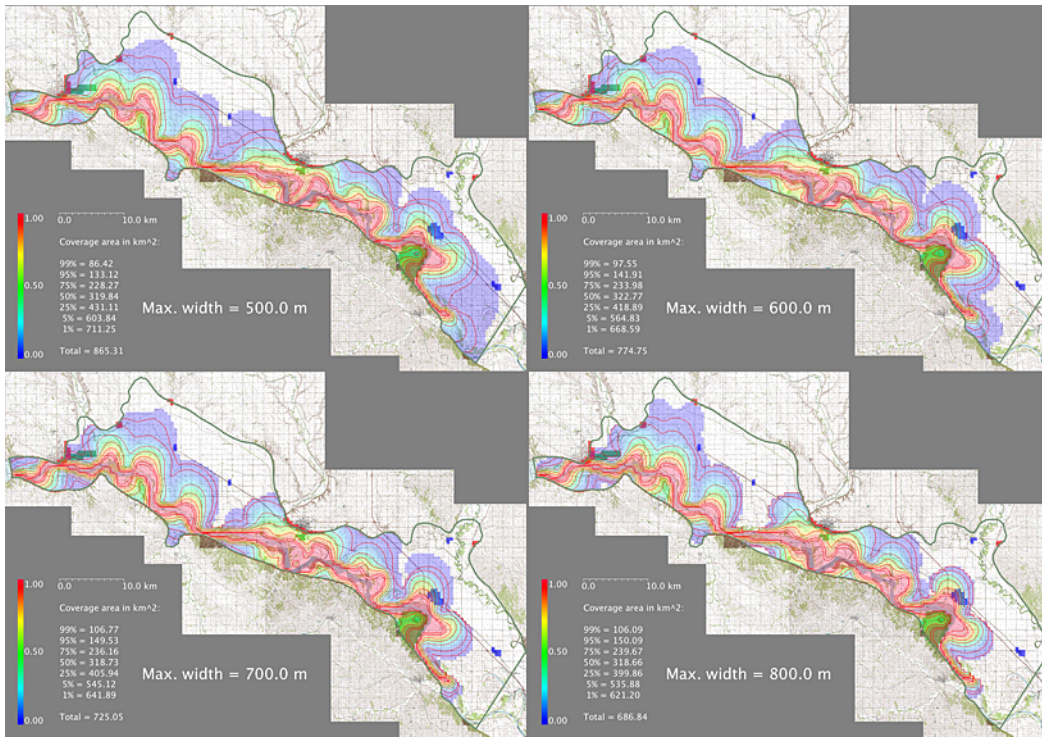
Figure 49: Variation in the common coverage array of 3072 river simulations with respect to maximum width, overlaid on the topographic map mosaic, with contours showing the migration ranges of 99%, 95%, 75%, 50%, 25%, 5%, and 1% of all rivers, and with 13 target areas also shown.
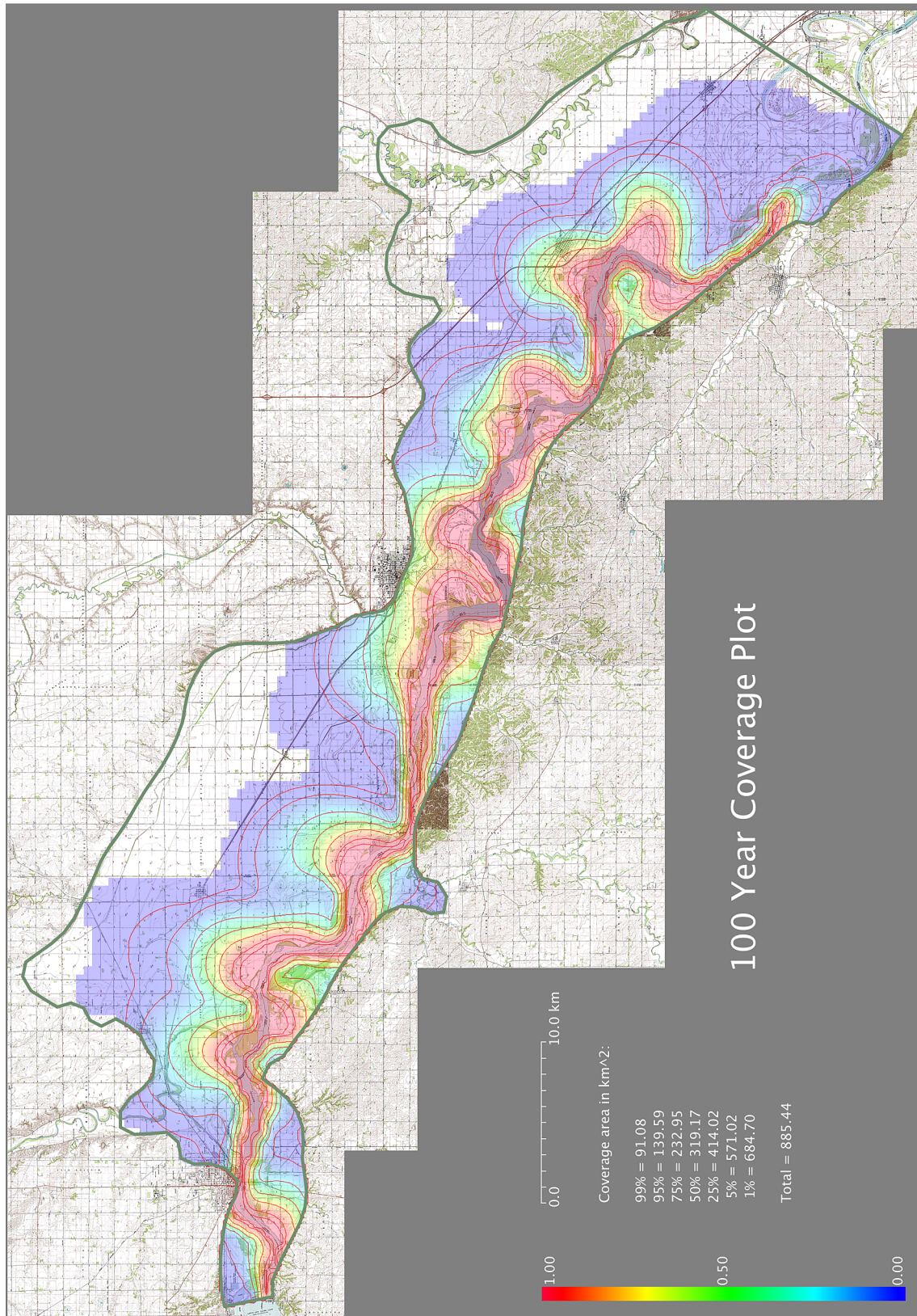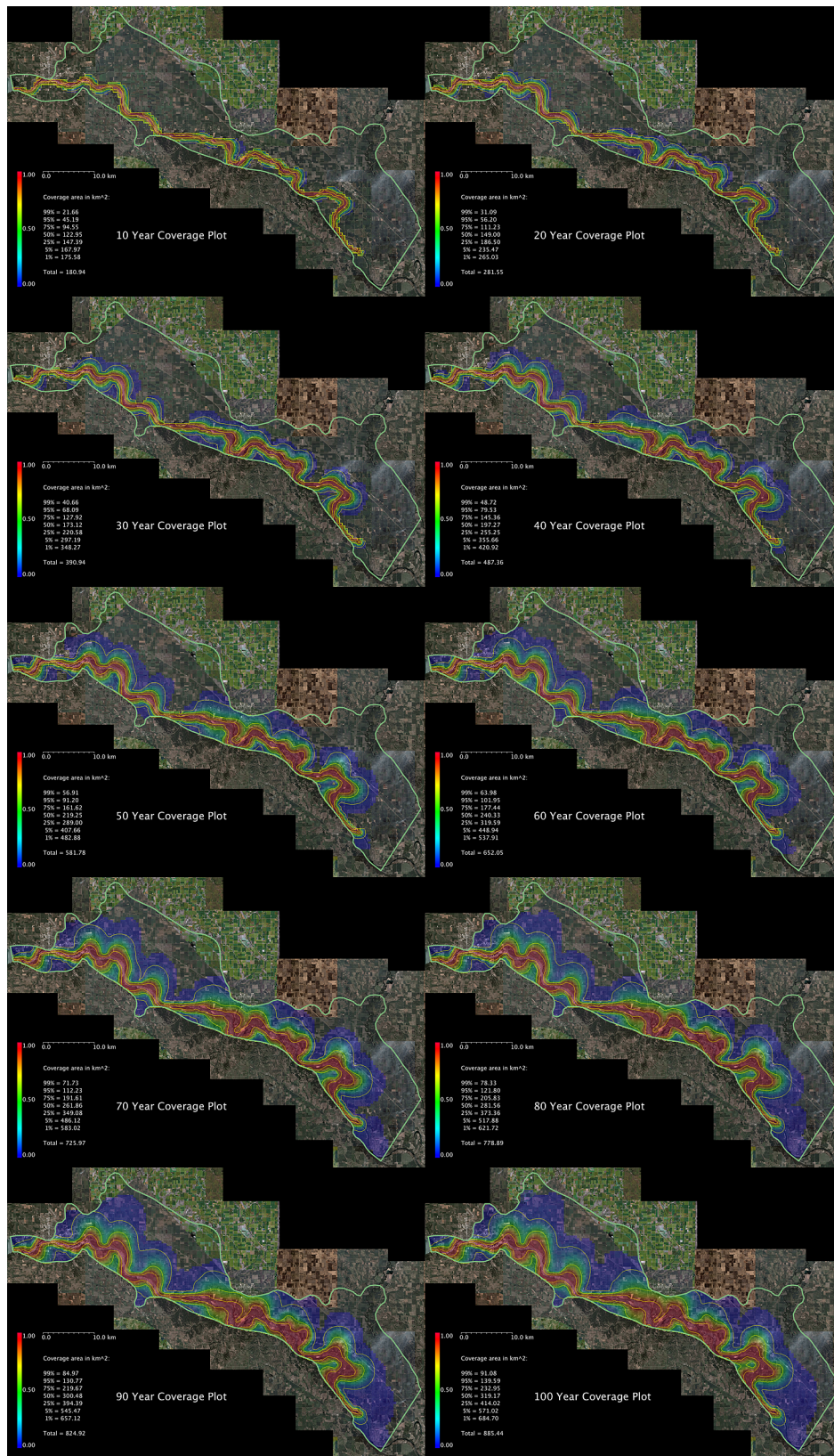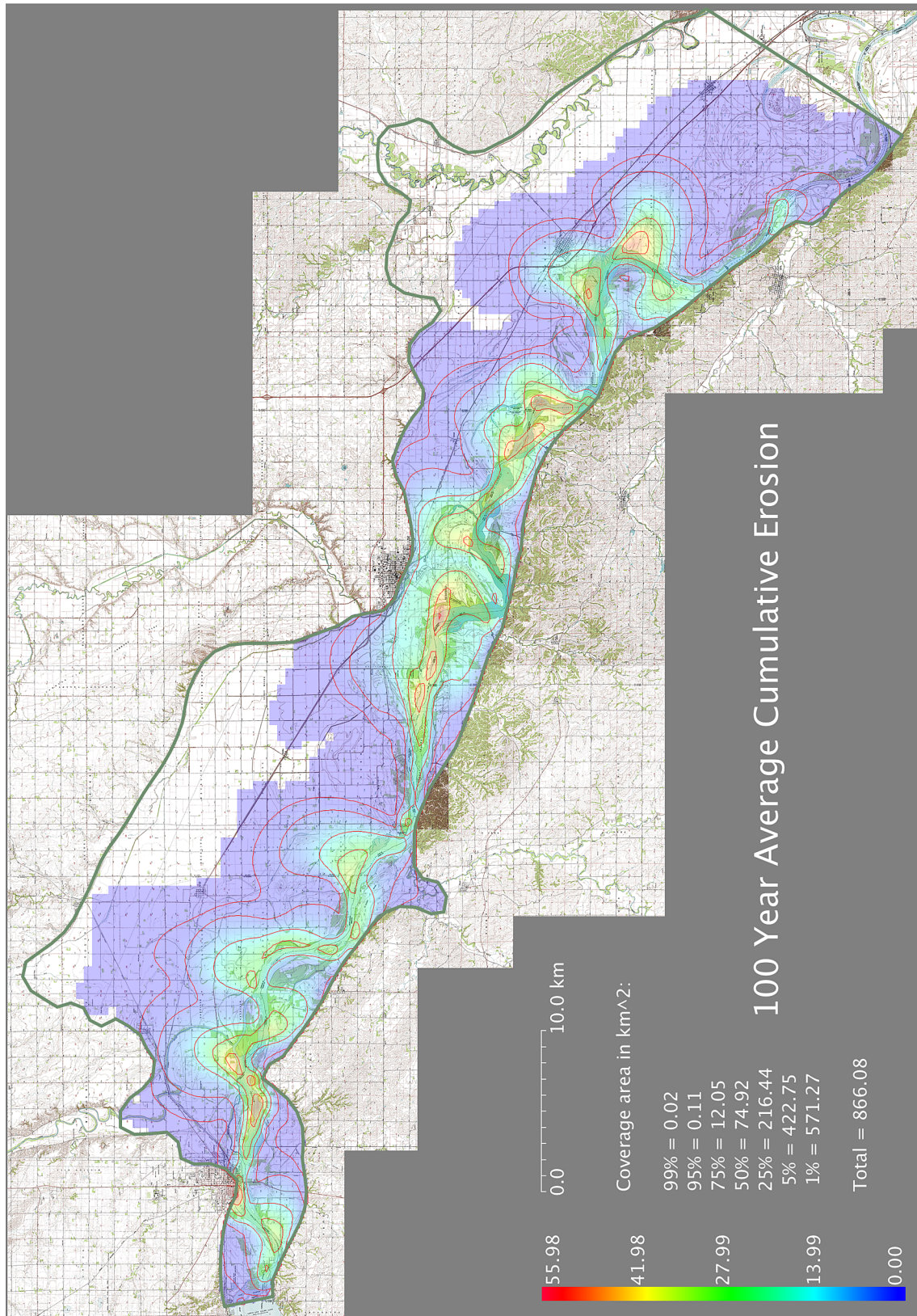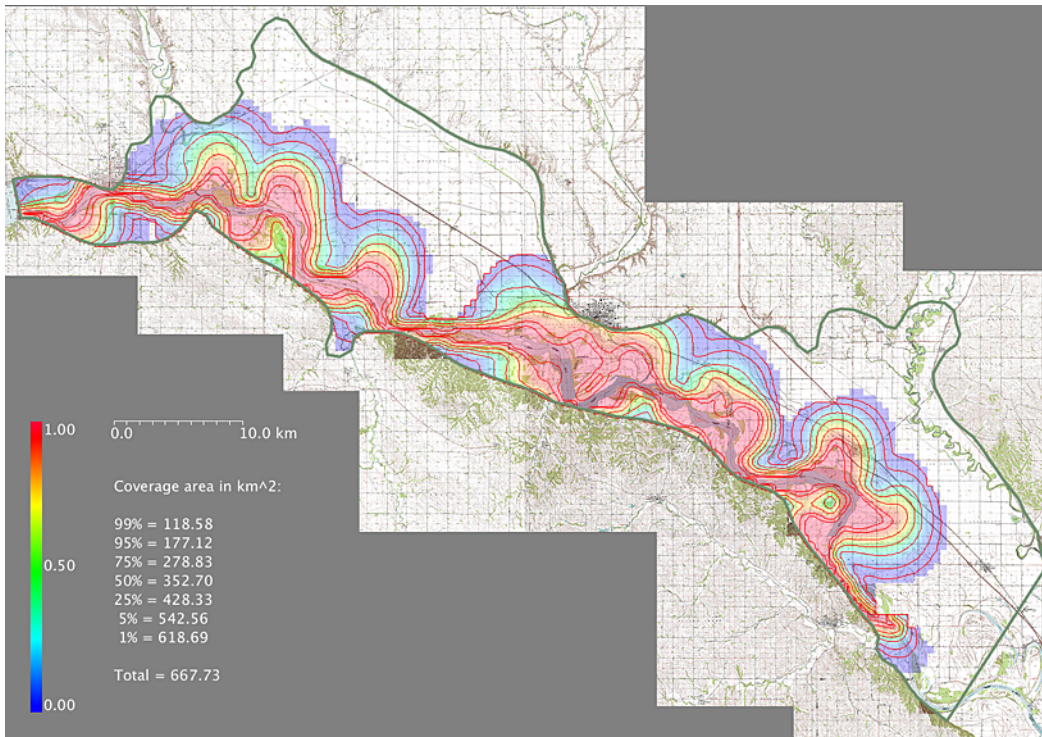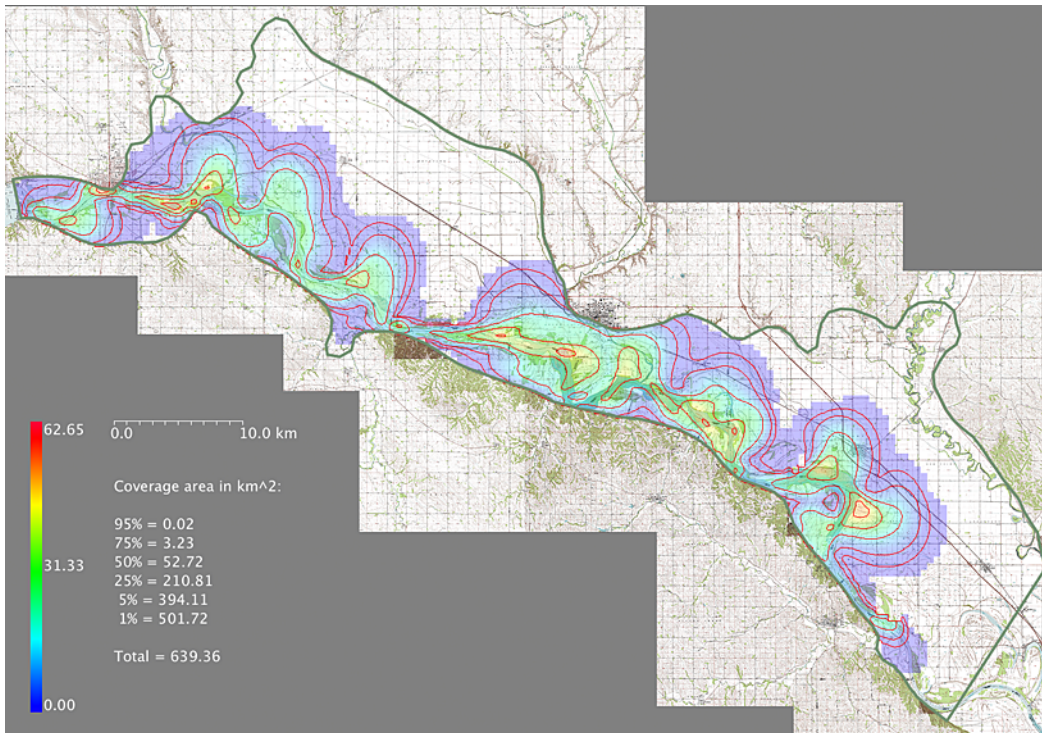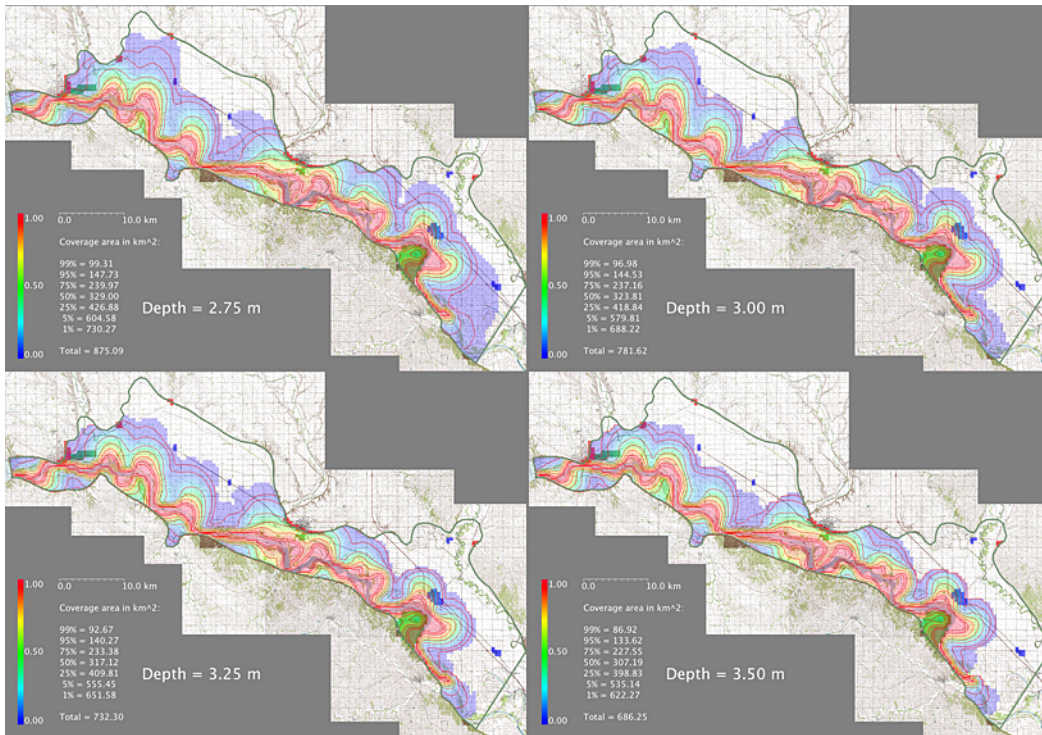

Figure 50: Variation in the common coverage array of 3072 river simulations with respect to depth, overlaid on the topographic map mosaic, with contours showing the migration ranges of 99%, 95%, 75%, 50%, 25%, 5%, and 1% of all rivers, and with 13 target areas also shown.
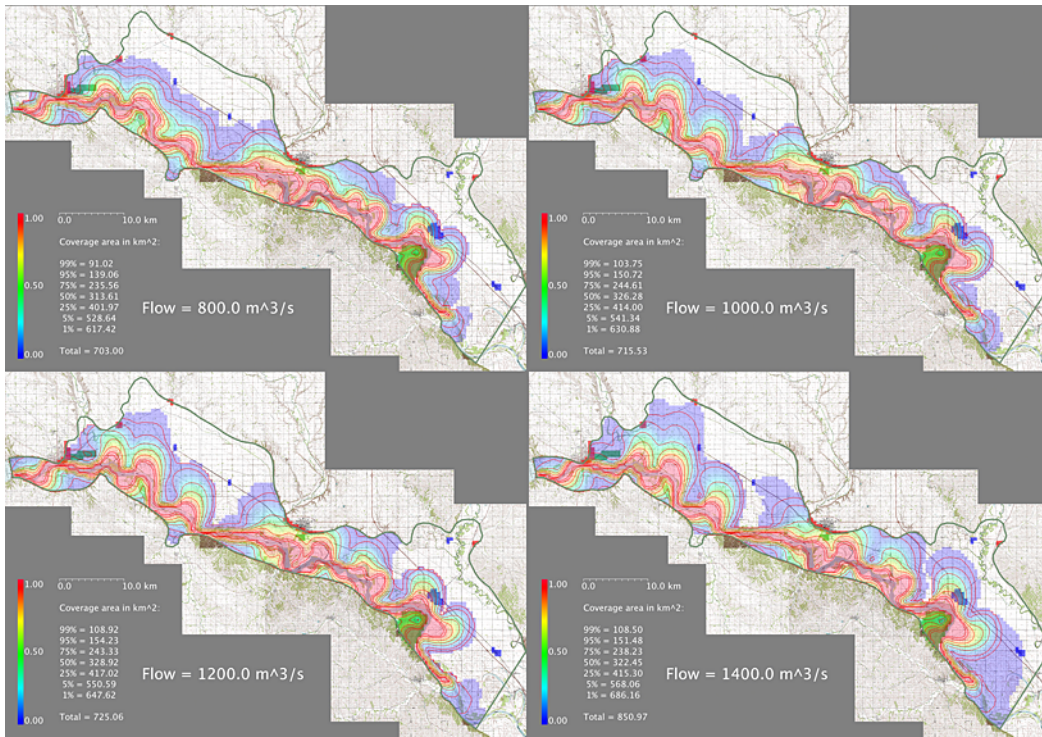
Figure 51: Variation in the common coverage array of 3072 river simulations with respect to flow, overlaid on the topographic map mosaic, with contours showing the migration ranges of 99%, 95%, 75%, 50%, 25%, 5%, and 1% of all rivers, and with 13 target areas also shown.
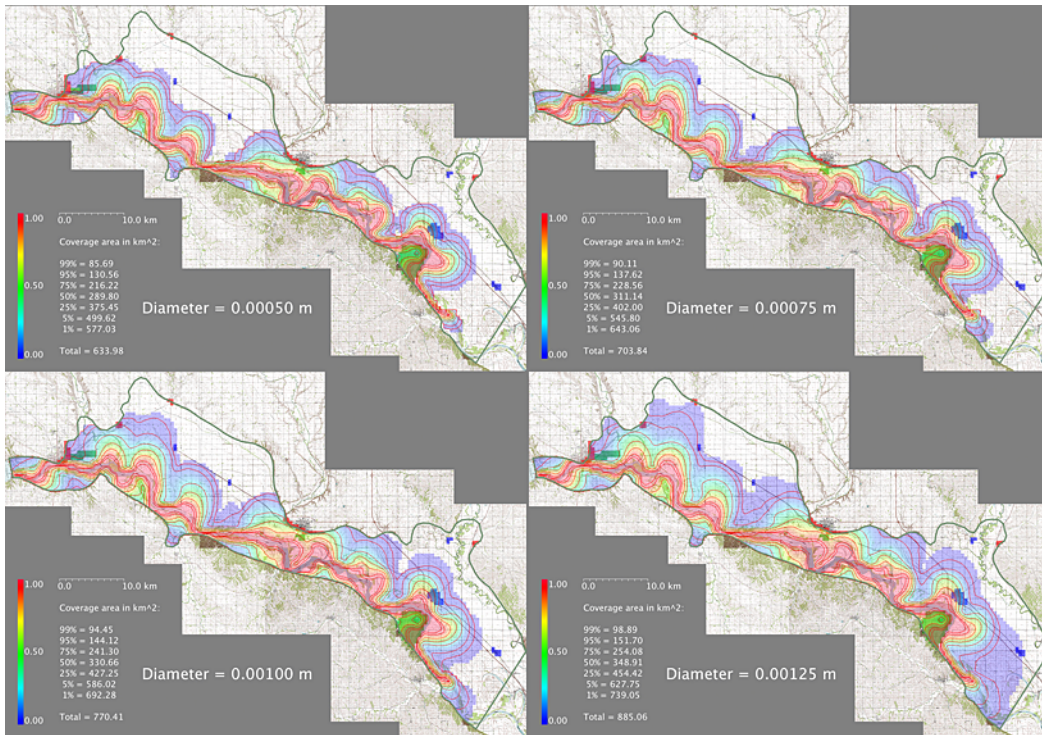
Figure 52: Variation in the common coverage array of 3072 river simulations with respect to bed particle diameter, overlaid on the topographic map mosaic, with contours showing the migration ranges of 99%, 95%, 75%, 50%, 25%, 5%, and 1% of all rivers, and with 13 target areas also shown.
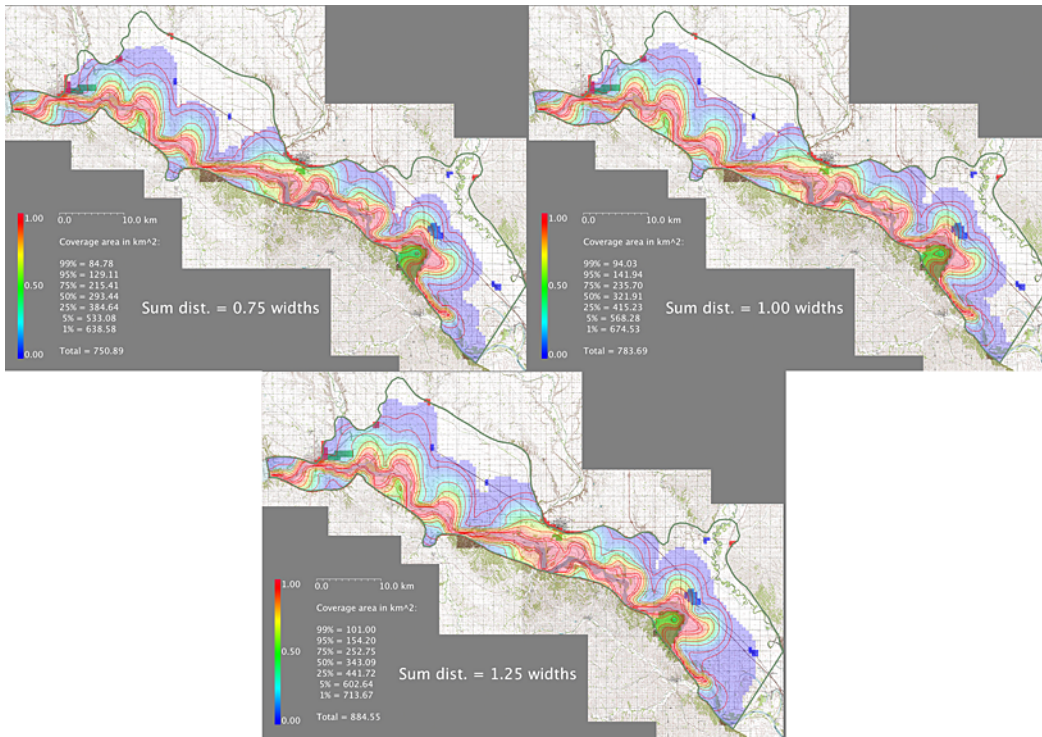
Figure 53: Variation in the common coverage array of 3072 river simulations with respect to curvature summation distance, overlaid on the topographic map mosaic, with contours showing the migration ranges of 99%, 95%, 75%, 50%, 25%, 5%, and 1% of all rivers, and with 13 target areas also shown.
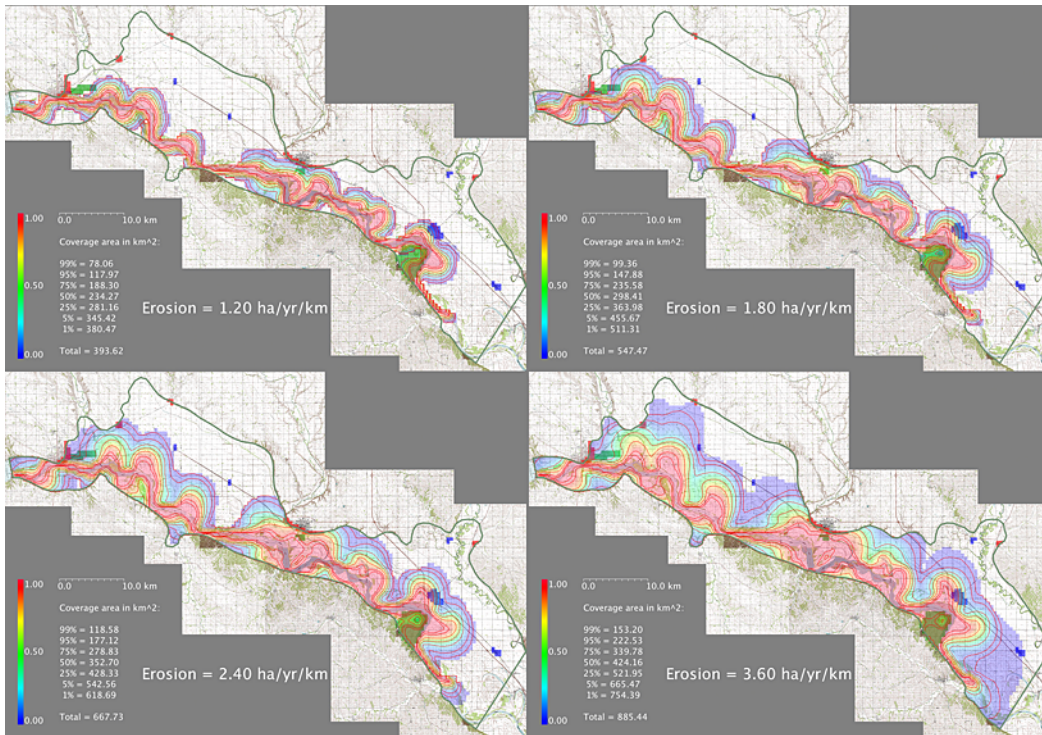
Figure 54: Variation in the common coverage array of 3072 river simulations with respect to initial erosion rate, overlaid on the topographic map mosaic, with contours showing the migration ranges of 99%, 95%, 75%, 50%, 25%, 5%, and 1% of all rivers, and with 13 target areas also shown.

4.5 Target invasion

On the next pages are statistics showing the minimum, maximum, and mean 100 year percent coverages of the 13 targets listed in section 3.4.9. Each of these values is based on the number of 500 x 500 m grid cells of a target which are occupied by each of the simulated rivers at any time during the simulation, divided by the total number of grid cells in that target. Also shown are statistics showing the minimum, maximum, and mean arrival times of the aggregate river at each of these targets. These values are based on the first time each of the simulated rivers reaches a specific target (if at all), at a resolution of 10 year intervals. Values of -1 indicate that a target was not reached by any river. Finally shown are statistics showing the percent coverages and arrival times at each target for the 6 input parameter sequence subsets of all simulations listed in section 4.4.1.

4.5.1 Example rivers reaching specific targets

Below, and on the next pages, are examples of the first simulated river (out of the total population of 3072) that reaches each of 8 of the 13 targets listed in section 3.4.9 (and also the shortest river if several reach the target at the same time). Note that 4 targets (Meckling, Richland, Volin, and Westfield) are not reached by any rivers, although Meckling and Volin are 'grazed' by at least one river. All rivers start within the bounds of Ponca State Park, but vary in their ability to erode additional area from this target. In all cases, the final 100 year configuration of the example river is shown, so that the part of the river first reaching the specific target may exist as a cutoff, rather than the main channel, at the end of the simulation.
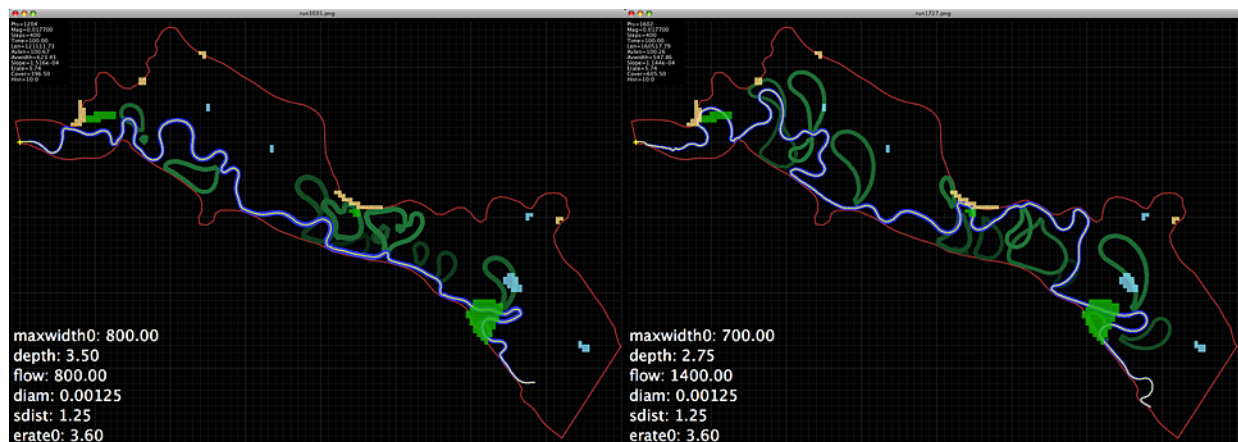
Figure 55: (Left) the shortest (121.11 km) of the first rivers to reach Elk Point (in 30 years); (right) the shortest (160.52 km) of the first rivers to reach Gayville (in 80 years).

```
Percent of target area occupied during simulation:
          stat    Elk Point         Gayville  Harold Davidson       Jefferson         Meckling      Mission Hill Ponca state park
---------------- ---------------- ---------------- ---------------- ---------------- ---------------- ---------------- ----------------
          min:    0.000000         0.000000         0.000000         0.000000         0.000000         0.000000         0.306667
          max:    1.000000         1.000000         1.000000         0.666667         0.000000         1.000000         1.000000
          mean:   0.463886         0.002930         0.710417         0.000217         0.000000         0.036133         0.761714

Time rivers reach specific targets (years):
          stat    Elk Point         Gayville  Harold Davidson       Jefferson         Meckling      Mission Hill Ponca state park
---------------- ---------------- ---------------- ---------------- ---------------- ---------------- ---------------- ----------------
          min:    30.000000        80.000000        20.000000        100.000000       -1.000000        60.000000        0.000000
          max:    100.000000       100.000000       100.000000       100.000000       -1.000000        100.000000       0.000000
          mean:   61.805444        91.000000        60.371257        100.000000       -1.000000        85.773810        0.000000

Percent of target area occupied during simulation (mean):
          case    Elk Point         Gayville  Harold Davidson       Jefferson         Meckling      Mission Hill Ponca state park
------------------ ---------------- ---------------- ---------------- ---------------- ---------------- ---------------- ----------------
  maxwidth0=500.00  0.279948         0.002604         0.695833         0.000868         0.000000         0.028971         0.710729
  maxwidth0=600.00  0.372472         0.001953         0.712760         0.000000         0.000000         0.026693         0.755486
  maxwidth0=700.00  0.518689         0.002604         0.653125         0.000000         0.000000         0.041016         0.782118
  maxwidth0=800.00  0.684436         0.004557         0.779948         0.000000         0.000000         0.047852         0.798524

     depth=2.75     0.553462         0.011719         0.725260         0.000868         0.000000         0.058268         0.773420
     depth=3.00     0.491039         0.000000         0.717448         0.000000         0.000000         0.041341         0.770104
     depth=3.25     0.429458         0.000000         0.706510         0.000000         0.000000         0.032878         0.761476
     depth=3.50     0.381587         0.000000         0.692448         0.000000         0.000000         0.012044         0.741858

     diam=0.00050   0.359222         0.000000         0.605729         0.000000         0.000000         0.006836         0.696858
     diam=0.00075   0.446078         0.000651         0.690625         0.000000         0.000000         0.027344         0.747969
     diam=0.00100   0.504749         0.003255         0.749219         0.000000         0.000000         0.043945         0.785469
     diam=0.00125   0.545496         0.007812         0.796094         0.000868         0.000000         0.066406         0.816563

     flow=800.00    0.285922         0.000000         0.751042         0.000000         0.000000         0.000651         0.755104
     flow=1000.00   0.403952         0.000000         0.739844         0.000000         0.000000         0.006185         0.788524
     flow=1200.00   0.538909         0.000000         0.687500         0.000000         0.000000         0.054036         0.770781
     flow=1400.00   0.626762         0.011719         0.663281         0.000868         0.000000         0.083659         0.732448

     sdist=0.75     0.394187         0.000977         0.629492         0.000000         0.000000         0.007324         0.705885
     sdist=1.00     0.474035         0.000977         0.720703         0.000000         0.000000         0.037109         0.766849
     sdist=1.25     0.523437         0.006836         0.781055         0.000651         0.000000         0.063965         0.812409

     erate0=1.20    0.097580         0.000000         0.209375         0.000000         0.000000         0.000000         0.507569
     erate0=1.80    0.429151         0.000000         0.720573         0.000000         0.000000         0.000000         0.718455
     erate0=2.40    0.624770         0.000000         0.920052         0.000000         0.000000         0.021484         0.861806
     erate0=3.60    0.704044         0.011719         0.991667         0.000868         0.000000         0.123047         0.959028

Time rivers reach specific targets (mean years):
          case    Elk Point         Gayville  Harold Davidson       Jefferson         Meckling      Mission Hill Ponca state park
------------------ ---------------- ---------------- ---------------- ---------------- ---------------- ---------------- ----------------
  maxwidth0=500.00  69.630435        90.000000        59.423077        100.000000       -1.000000        81.714286        0.000000
  maxwidth0=600.00  65.384615        95.000000        56.672078        -1.000000        -1.000000        83.142857        0.000000
  maxwidth0=700.00  59.927431        85.000000        62.922297        -1.000000        -1.000000        87.073171        0.000000
  maxwidth0=800.00  55.885486        92.500000        62.392273        -1.000000        -1.000000        88.947368        0.000000

     depth=2.75     60.876133        91.000000        61.001616        100.000000       -1.000000        85.312500        0.000000
     depth=3.00     61.625000        -1.000000        60.845295        -1.000000        -1.000000        85.600000        0.000000
     depth=3.25     62.120718        -1.000000        60.096308        -1.000000        -1.000000        87.142857        0.000000
     depth=3.50     62.727273        -1.000000        59.559748        -1.000000        -1.000000        85.263158        0.000000

     diam=0.00050   66.283662        -1.000000        64.010601        -1.000000        -1.000000        98.333333        0.000000
     diam=0.00075   62.878049        100.000000       61.491086        -1.000000        -1.000000        90.000000        0.000000
     diam=0.00100   60.536810        96.666667        59.278034        -1.000000        -1.000000        85.918367        0.000000
     diam=0.00125   58.353116        86.666667        57.332340        100.000000       -1.000000        81.866667        0.000000

     flow=800.00    62.794918        -1.000000        56.384840        -1.000000        -1.000000        70.000000        0.000000
     flow=1000.00   61.690590        -1.000000        58.657407        -1.000000        -1.000000        91.250000        0.000000
     flow=1200.00   61.398176        -1.000000        62.181208        -1.000000        -1.000000        84.558824        0.000000
     flow=1400.00   61.495468        91.000000        65.182609        100.000000       -1.000000        86.373626        0.000000

     sdist=0.75     65.549598        100.000000       64.682540        -1.000000        -1.000000        94.000000        0.000000
     sdist=1.00     62.152047        90.000000        59.644550        -1.000000        -1.000000        87.833333        0.000000
     sdist=1.25     58.361204        90.000000        57.447514        100.000000       -1.000000        83.118280        0.000000

     erate0=1.20    90.057971        -1.000000        87.087719        -1.000000        -1.000000        -1.000000        0.000000
     erate0=1.80    73.089552        -1.000000        73.797101        -1.000000        -1.000000        -1.000000        0.000000
     erate0=2.40    58.697422        -1.000000        58.805774        -1.000000        -1.000000        96.153846        0.000000
     erate0=3.60    41.675603        91.000000        39.947917        100.000000       -1.000000        83.873239        0.000000
```

Table 8: Percent of targets covered during 100 years and time targets are reached by all simulations (-1 means never), and by subsets of simulations having input parameters set to specific values.

```
Percent of target area occupied during simulation:
            stat      Richland Vermillion shore     Volin shore        Westfield      Yankton east     Yankton SD50
---------------- ---------------- ---------------- ---------------- ---------------- ---------------- ----------------
            min:     0.000000         0.000000         0.000000         0.000000         0.000000         0.000000
            max:     0.000000         1.000000         0.000000         0.000000         1.000000         1.000000
           mean:     0.000000         0.383195         0.000000         0.000000         0.132138         0.060366

Time rivers reach specific targets (years):
            stat      Richland Vermillion shore     Volin shore        Westfield      Yankton east     Yankton SD50
---------------- ---------------- ---------------- ---------------- ---------------- ---------------- ----------------
            min:    -1.000000        30.000000        -1.000000        -1.000000        10.000000        30.000000
            max:    -1.000000       100.000000        -1.000000        -1.000000       100.000000       100.000000
           mean:    -1.000000        69.011387        -1.000000        -1.000000        17.254174        71.926864

Percent of target area occupied during simulation (mean):
            case      Richland Vermillion shore     Volin shore        Westfield      Yankton east     Yankton SD50
-------------------- ---------------- ---------------- ---------------- ---------------- ---------------- ----------------
  maxwidth0=500.00     0.000000         0.308594         0.000000         0.000000         0.098586         0.124349
  maxwidth0=600.00     0.000000         0.394301         0.000000         0.000000         0.094215         0.077546
  maxwidth0=700.00     0.000000         0.394914         0.000000         0.000000         0.147972         0.027705
  maxwidth0=800.00     0.000000         0.434972         0.000000         0.000000         0.187779         0.011863

       depth=2.75     0.000000         0.427160         0.000000         0.000000         0.163504         0.061198
       depth=3.00     0.000000         0.405254         0.000000         0.000000         0.142578         0.061126
       depth=3.25     0.000000         0.367877         0.000000         0.000000         0.118676         0.058521
       depth=3.50     0.000000         0.332491         0.000000         0.000000         0.103795         0.060619

     diam=0.00050     0.000000         0.252911         0.000000         0.000000         0.113467         0.030816
     diam=0.00075     0.000000         0.354013         0.000000         0.000000         0.120815         0.042028
     diam=0.00100     0.000000         0.433594         0.000000         0.000000         0.137742         0.065683
     diam=0.00125     0.000000         0.492264         0.000000         0.000000         0.156529         0.102937

      flow=800.00     0.000000         0.310892         0.000000         0.000000         0.077753         0.124928
     flow=1000.00     0.000000         0.397289         0.000000         0.000000         0.108073         0.053675
     flow=1200.00     0.000000         0.425781         0.000000         0.000000         0.148344         0.020761
     flow=1400.00     0.000000         0.398820         0.000000         0.000000         0.194382         0.042101

       sdist=0.75     0.000000         0.297449         0.000000         0.000000         0.111816         0.039063
       sdist=1.00     0.000000         0.396025         0.000000         0.000000         0.134975         0.055447
       sdist=1.25     0.000000         0.456112         0.000000         0.000000         0.149623         0.086589

      erate0=1.20     0.000000         0.004366         0.000000         0.000000         0.135510         0.002170
      erate0=1.80     0.000000         0.215380         0.000000         0.000000         0.119048         0.024089
      erate0=2.40     0.000000         0.525352         0.000000         0.000000         0.104725         0.053313
      erate0=3.60     0.000000         0.787684         0.000000         0.000000         0.169271         0.161892

Time rivers reach specific targets (mean years):
            case      Richland Vermillion shore     Volin shore        Westfield      Yankton east     Yankton SD50
-------------------- ---------------- ---------------- ---------------- ---------------- ---------------- ----------------
  maxwidth0=500.00    -1.000000        69.952941        -1.000000        -1.000000        12.638655        67.756410
  maxwidth0=600.00    -1.000000        67.316103        -1.000000        -1.000000        15.203252        70.382979
  maxwidth0=700.00    -1.000000        69.258475        -1.000000        -1.000000        18.294036        79.677419
  maxwidth0=800.00    -1.000000        69.642857        -1.000000        -1.000000        21.518325        89.500000

       depth=2.75    -1.000000        68.863198        -1.000000        -1.000000        14.455172        74.936709
       depth=3.00    -1.000000        69.257028        -1.000000        -1.000000        15.940171        70.473373
       depth=3.25    -1.000000        68.771552        -1.000000        -1.000000        17.981791        72.251309
       depth=3.50    -1.000000        69.157428        -1.000000        -1.000000        21.313629        70.414508

     diam=0.00050    -1.000000        74.526854        -1.000000        -1.000000        17.187500        73.095238
     diam=0.00075    -1.000000        70.365591        -1.000000        -1.000000        17.366071        71.666667
     diam=0.00100    -1.000000        67.658349        -1.000000        -1.000000        17.090103        72.105263
     diam=0.00125    -1.000000        65.261261        -1.000000        -1.000000        17.373887        71.346939

      flow=800.00    -1.000000        66.152174        -1.000000        -1.000000        30.169133        66.857923
     flow=1000.00    -1.000000        67.721022        -1.000000        -1.000000        18.263386        69.735450
     flow=1200.00    -1.000000        70.226804        -1.000000        -1.000000        13.735256        85.970149
     flow=1400.00    -1.000000        71.903766        -1.000000        -1.000000        11.888021        86.853933

       sdist=0.75    -1.000000        73.530499        -1.000000        -1.000000        18.534279        72.972973
       sdist=1.00    -1.000000        69.655689        -1.000000        -1.000000        17.335491        72.343096
       sdist=1.25    -1.000000        65.034578        -1.000000        -1.000000        15.997831        70.905923

      erate0=1.20    -1.000000        97.307692        -1.000000        -1.000000        24.884058        94.500000
      erate0=1.80    -1.000000        87.707006        -1.000000        -1.000000        17.054598        83.333333
      erate0=2.40    -1.000000        73.959828        -1.000000        -1.000000        13.942161        73.936170
      erate0=3.60    -1.000000        51.409214        -1.000000        -1.000000        12.730061        66.052632
```

Table 9: Percent of targets covered during 100 years and time targets are reached by all simulations (-1 means never), and by subsets of simulations having input parameters set to specific values.

Figure 56: (Left) the shortest (121.11 km) of the first rivers to reach Harold Davidson Field (in 20 years); (right) the only (245.48 km) river to reach Jefferson (in 100 years).
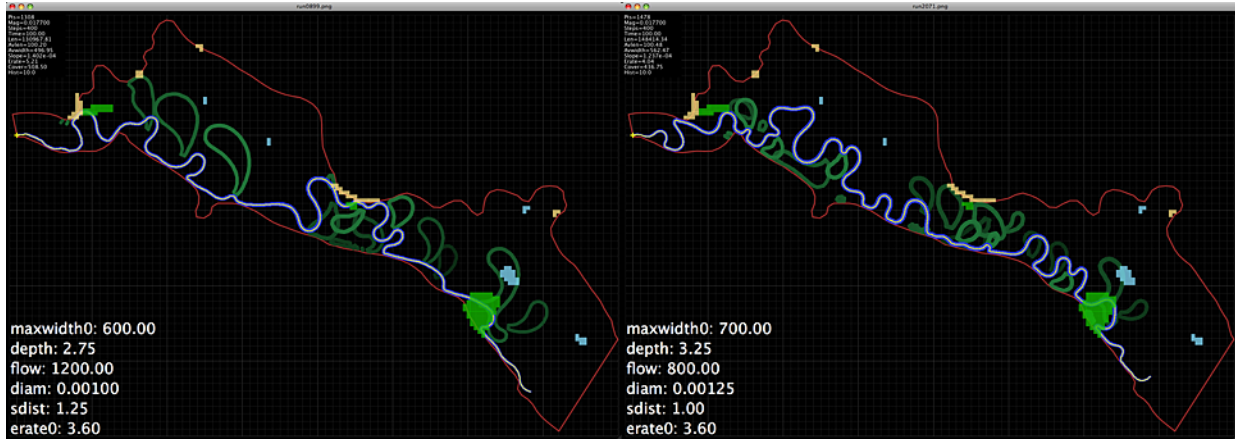

Figure 57: (Left) the shortest (130.97 km) of the first rivers to reach Mission Hill (in 60 years); (right) the shortest (148.41 km) of the first rivers to reach Vermillion (in 30 years).
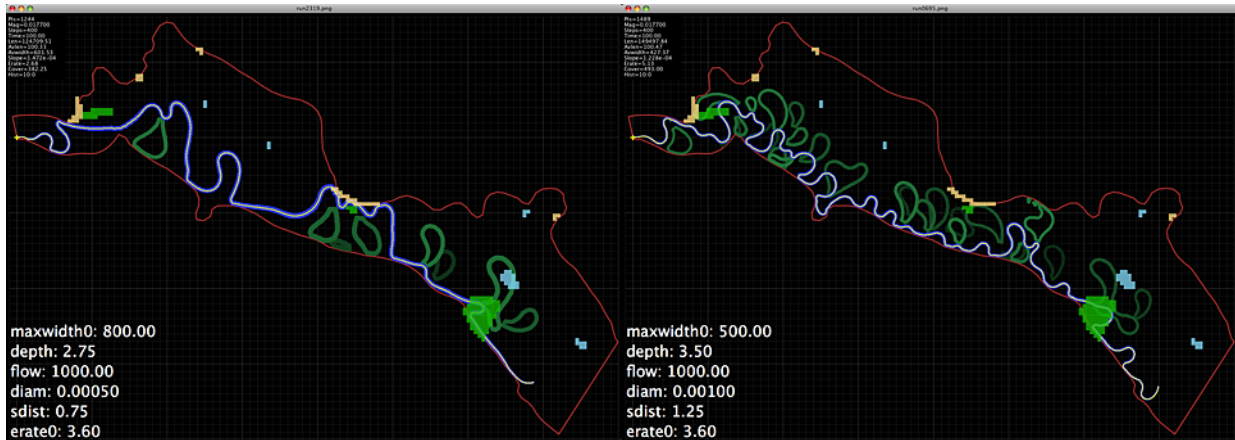

Figure 58: (Left) the shortest (124.71 km) of the first rivers to reach East Yankton (in 10 years); (right) the shortest (149.50 km) of the first rivers to reach Yankton along SD50 (in 30 years).

4.6 Comparison of JP89 and CS results

On the following pages are statistics and plots from the Circumferential Speed simulation database of 540 rivers, showing both extreme and nominal river examples, and the 100 year common coverage and average cumulative erosion of the entire set. Note in these cases that the longest, most active, and greatest area rivers are now distinct from one another (in contrast to the JP89 results), and that the CS rivers do not suffer from the oscillation instability which is common to the wider, less active, JP89 rivers (see section 4.6.1 below). Also note that the CS simulations were not run using an initial erosion rate of 3.6 ha/yr/km, as 1.2 - 2.4 ha/yr/km were deemed sufficient. Although the purpose of the present study was to concentrate on the use of and the results from the JP89 meandering model, some comparisons between the final coverage arrays of the two meandering methods are noteworthy:

* The 540 Circumferential Speed runs, when combined, produce a common coverage plot which is very similar in appearance to that of the 3072 Johannesson-Parker 1989 simulations.

* The JP89 maximum coverage area is 21% greater than the corresponding CS maximum coverage area. This may be due simply to the inclusion of simulations having initial erosion rates of 3.6 ha/yr/km in the JP89 runs.

* However, all other CS percent coverages (from 99% to 1%) are larger than the corresponding JP89 percentage area, even though they represent simulations performed at lower erosion rates.

This suggests that although more of the 'core' CS rivers tend to migrate farther, on average, from their original positions than do their JP89 counterparts, the CS rivers considered as a whole do not, and there is less variation to the 'migration corridor' than in the JP89 results. Two potential explanations for these observations might be that:

1. Although the standard deviation in both river length and erosion rate of all CS rivers is greater than the standard deviation of JP89 river length and erosion rate, the ratio of standard deviation to mean of both these variables is greater for the JP89 population. This may indicate that the process which generated the population with the higher ratio is in some sense 'more random'. Certainly, the process which generated the JP89 simulations is 'more complex' in terms of the equations and computer code used.

2. Many of the JP89 rivers decrease their erosion rates during the course of the simulation, whereas all of the CS rivers increased their erosion rates. The initial and final distributions of erosion rates of the JP89 runs (shown in section 4.3) and the CS runs (not shown) indicate that while both initial distributions are discrete, the JP89 final distribution has a narrow, sharp peak and a wide range of values in the exponential 'skirt', while the CS final distribution is considerably more closely and uniformly distributed.

It is not our intention to dwell particularly upon the Circumferential Speed results, as this meandering method represents a considerably 'less physical' model. We have included it only as a check to confirm that the Johannesson-Parker 1989 results appear to be reasonable for this category of models which are based on speed differences on opposing banks of the river.

```
Sorting by length...
Top 5 entries:
    i                 file           length    maxwidth0             depth             diam             flow            sdist           erate0
----- -------------------- ---------------- ----------- ----------------- ---------------- ---------------- ---------------- ----------------
    1           run5061.mnrr    241664.023926          500         3.000000          0.001000      1200.000000         1.250000         1.800000
    2           run5029.mnrr    235876.747113          500         2.750000          0.001000      1400.000000         0.750000         2.400000
    3           run5154.mnrr    229563.323450          600         2.750000          0.001000      1200.000000         0.750000         1.800000
    4           run5217.mnrr    229438.040702          600         3.250000          0.001000      1000.000000         0.750000         1.800000
    5           run5163.mnrr    229191.817973          600         2.750000          0.001000      1400.000000         0.750000         1.800000

Bottom 5 entries:
    i                 file           length    maxwidth0             depth             diam             flow            sdist           erate0
----- -------------------- ---------------- ----------- ----------------- ---------------- ---------------- ---------------- ----------------
    1           run5463.mnrr    146383.265702          800         3.000000          0.001000      1200.000000         1.000000         1.800000
    2           run5427.mnrr    144649.148812          800         2.750000          0.001000      1200.000000         1.000000         1.800000
    3           run5446.mnrr    142953.297626          800         3.000000          0.001000       800.000000         1.000000         2.400000
    4           run5365.mnrr    141156.906170          700         3.250000          0.001000      1200.000000         1.000000         2.400000
    5           run5302.mnrr    136861.301604          700         2.750000          0.001000      1400.000000         1.000000         2.400000

Sorting by totalLength...
Top 5 entries:
    i                 file      totalLength    maxwidth0             depth             diam             flow            sdist           erate0
----- -------------------- ---------------- ----------- ----------------- ---------------- ---------------- ---------------- ----------------
    1           run5125.mnrr    983425.118468          500         3.500000          0.001000      1000.000000         1.250000         2.400000
    2           run5134.mnrr    978498.984176          500         3.500000          0.001000      1200.000000         1.250000         2.400000
    3           run5008.mnrr    978112.313243          500         2.750000          0.001000       800.000000         1.250000         2.400000
    4           run5017.mnrr    973867.707984          500         2.750000          0.001000      1000.000000         1.250000         2.400000
    5           run5089.mnrr    968416.290172          500         3.250000          0.001000      1000.000000         1.250000         2.400000

Bottom 5 entries:
    i                 file      totalLength    maxwidth0             depth             diam             flow            sdist           erate0
----- -------------------- ---------------- ----------- ----------------- ---------------- ---------------- ---------------- ----------------
    1           run5504.mnrr    177873.564453          800         3.250000          0.001000      1400.000000         0.750000         1.200000
    2           run5459.mnrr    177852.215155          800         3.000000          0.001000      1200.000000         0.750000         1.200000
    3           run5522.mnrr    177852.215120          800         3.500000          0.001000      1000.000000         0.750000         1.200000
    4           run5486.mnrr    177848.909939          800         3.250000          0.001000      1000.000000         0.750000         1.200000
    5           run5477.mnrr    177844.516502          800         3.250000          0.001000       800.000000         0.750000         1.200000

Sorting by erate...
Top 5 entries:
    i                 file            erate    maxwidth0             depth             diam             flow            sdist           erate0
----- -------------------- ---------------- ----------- ----------------- ---------------- ---------------- ---------------- ----------------
    1           run5125.mnrr         7.129977          500         3.500000          0.001000      1000.000000         1.250000         2.400000
    2           run5098.mnrr         6.944018          500         3.250000          0.001000      1200.000000         1.250000         2.400000
    3           run5089.mnrr         6.879741          500         3.250000          0.001000      1000.000000         1.250000         2.400000
    4           run5062.mnrr         6.784955          500         3.000000          0.001000      1200.000000         1.250000         2.400000
    5           run5044.mnrr         6.664453          500         3.000000          0.001000       800.000000         1.250000         2.400000

Bottom 5 entries:
    i                 file            erate    maxwidth0             depth             diam             flow            sdist           erate0
----- -------------------- ---------------- ----------- ----------------- ---------------- ---------------- ---------------- ----------------
    1           run5270.mnrr         1.597992          700         2.750000          0.001000       800.000000         0.750000         1.200000
    2           run5333.mnrr         1.597952          700         3.000000          0.001000      1400.000000         0.750000         1.200000
    3           run5387.mnrr         1.597938          700         3.500000          0.001000      1000.000000         0.750000         1.200000
    4           run5315.mnrr         1.597738          700         3.000000          0.001000      1000.000000         0.750000         1.200000
    5           run5351.mnrr         1.597547          700         3.250000          0.001000      1000.000000         0.750000         1.200000

Sorting by cArea...
Top 5 entries:
    i                 file            cArea    maxwidth0             depth             diam             flow            sdist           erate0
----- -------------------- ---------------- ----------- ----------------- ---------------- ---------------- ---------------- ----------------
    1           run5278.mnrr       615.750000          700         2.750000          0.001000       800.000000         1.250000         2.400000
    2           run5350.mnrr       615.750000          700         3.250000          0.001000       800.000000         1.250000         2.400000
    3           run5314.mnrr       611.500000          700         3.000000          0.001000       800.000000         1.250000         2.400000
    4           run5296.mnrr       611.000000          700         2.750000          0.001000      1200.000000         1.250000         2.400000
    5           run5368.mnrr       611.000000          700         3.250000          0.001000      1200.000000         1.250000         2.400000

Bottom 5 entries:
    i                 file            cArea    maxwidth0             depth             diam             flow            sdist           erate0
----- -------------------- ---------------- ----------- ----------------- ---------------- ---------------- ---------------- ----------------
    1           run5531.mnrr       275.750000          800         3.500000          0.001000      1200.000000         0.750000         1.200000
    2           run5441.mnrr       275.500000          800         3.000000          0.001000       800.000000         0.750000         1.200000
    3           run5414.mnrr       275.250000          800         2.750000          0.001000      1000.000000         0.750000         1.200000
    4           run5432.mnrr       275.250000          800         2.750000          0.001000      1400.000000         0.750000         1.200000
    5           run5495.mnrr       275.250000          800         3.250000          0.001000      1200.000000         0.750000         1.200000
```

Table 10: Circumferential Speed results sorted by river length (m), total river length (including cutoffs), final erosion rate (ha/yr/km), and total coverage area (km^2). The top (greatest) and bottom (least) five entries are shown for each variable. Note that the same river (#5125) is the top entry by total length and erosion rate, but that all other top and bottom entries are now distinct, as opposed to the JP89 results.
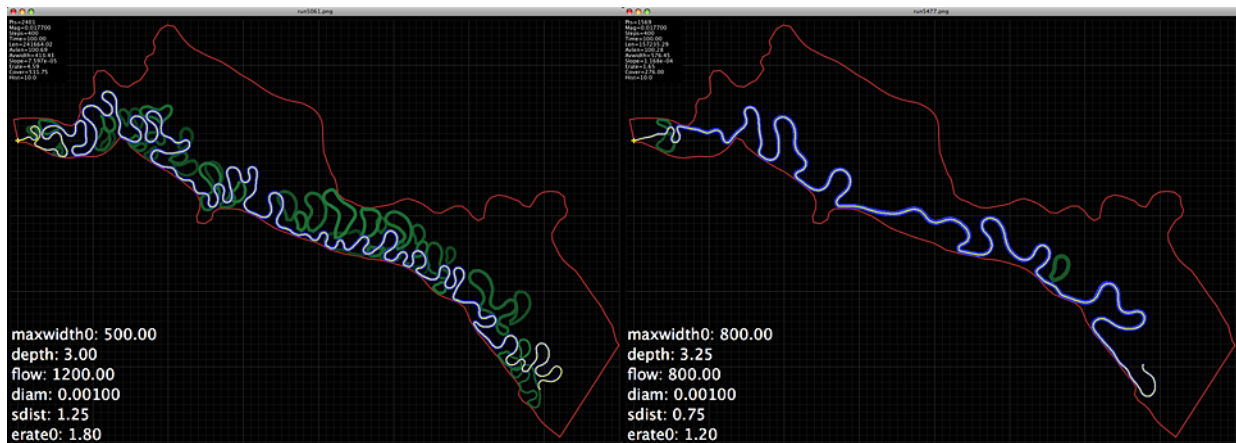
Figure 59: The longest (left) and shortest total length (right) Circumferential Speed rivers.

Figure 60: The Circumferential Speed river with the greatest coverage area (left), and a more 'nominal' example within 0.1 standard deviations of the average length and erosion rate.

```
length: min=136861.301604, max=241664.023926, mean=185450.211953, std=19185.135621
erate: min=1.597547, max=7.129977, mean=3.682848, std=1.434533
11 entries within 0.100000 stds of mean length and erate: Sorted by length:
```

Sorted by length:

i	file	length	maxwidth0	depth	flow	diam	sdist	erate0
1	run5373.mnrr	187231.061085	700	3.250000	1200.000000	0.001000	1.000000	1.800000
2	run5292.mnrr	186698.921741	700	2.750000	1200.000000	0.001000	1.000000	1.800000
3	run5328.mnrr	186530.234307	700	3.000000	1200.000000	0.001000	1.000000	1.800000
4	run5355.mnrr	186094.193047	700	3.250000	1000.000000	0.001000	1.000000	1.800000
5	run5364.mnrr	185959.635729	700	3.250000	1200.000000	0.001000	1.000000	1.800000
6	run5310.mnrr	185276.831475	700	3.000000	800.000000	0.001000	1.000000	1.800000
7	run5319.mnrr	185105.200638	700	3.000000	1000.000000	0.001000	1.000000	1.800000
8	run5391.mnrr	184591.943066	700	3.500000	1000.000000	0.001000	1.000000	1.800000
9	run5274.mnrr	184259.225592	700	2.750000	800.000000	0.001000	1.000000	1.800000
10	run5301.mnrr	183999.965286	700	2.750000	1400.000000	0.001000	1.000000	1.800000
11	run5337.mnrr	183549.724821	700	3.000000	1400.000000	0.001000	1.000000	1.800000

Sorted by erate:

i	file	erate	maxwidth0	depth	flow	diam	sdist	erate0
1	run5310.mnrr	3.828120	700	3.000000	800.000000	0.001000	1.000000	1.800000
2	run5292.mnrr	3.798892	700	2.750000	1200.000000	0.001000	1.000000	1.800000
3	run5355.mnrr	3.788126	700	3.250000	1000.000000	0.001000	1.000000	1.800000
4	run5319.mnrr	3.775528	700	3.000000	1000.000000	0.001000	1.000000	1.800000
5	run5328.mnrr	3.769140	700	3.000000	1200.000000	0.001000	1.000000	1.800000
6	run5373.mnrr	3.761057	700	3.250000	1400.000000	0.001000	1.000000	1.800000
7	run5301.mnrr	3.760422	700	2.750000	1400.000000	0.001000	1.000000	1.800000
8	run5364.mnrr	3.760175	700	3.250000	1200.000000	0.001000	1.000000	1.800000
9	run5274.mnrr	3.729479	700	2.750000	800.000000	0.001000	1.000000	1.800000
10	run5337.mnrr	3.720908	700	3.000000	1400.000000	0.001000	1.000000	1.800000
11	run5391.mnrr	3.704230	700	3.500000	1000.000000	0.001000	1.000000	1.800000

Table 11: Circumferential Speed results showing all simulations which are within 0.1 standard deviations of the final average length and also the final average erosion rate, sorted first by length and then by final erosion rate.
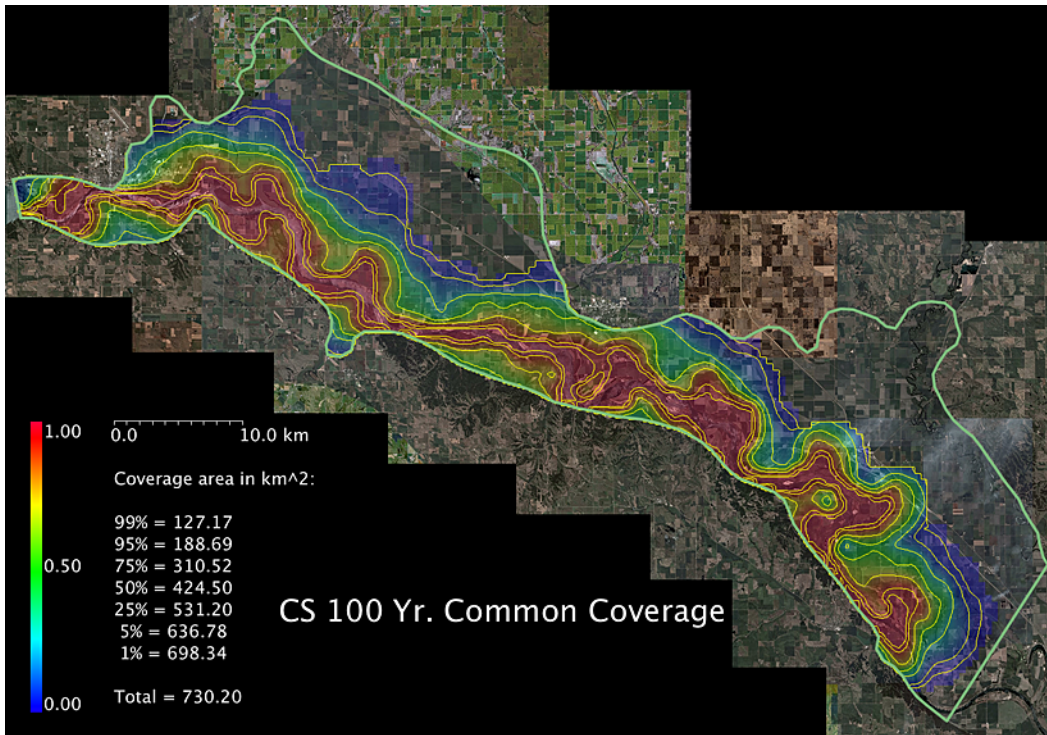
Figure 61: The common coverage array of 540 Circumferential Speed simulations overlaid on the satellite image mosaic, with contours showing the migration ranges of 99%, 95%, 75%, 50%, 25%, 5%, and 1% of all rivers.
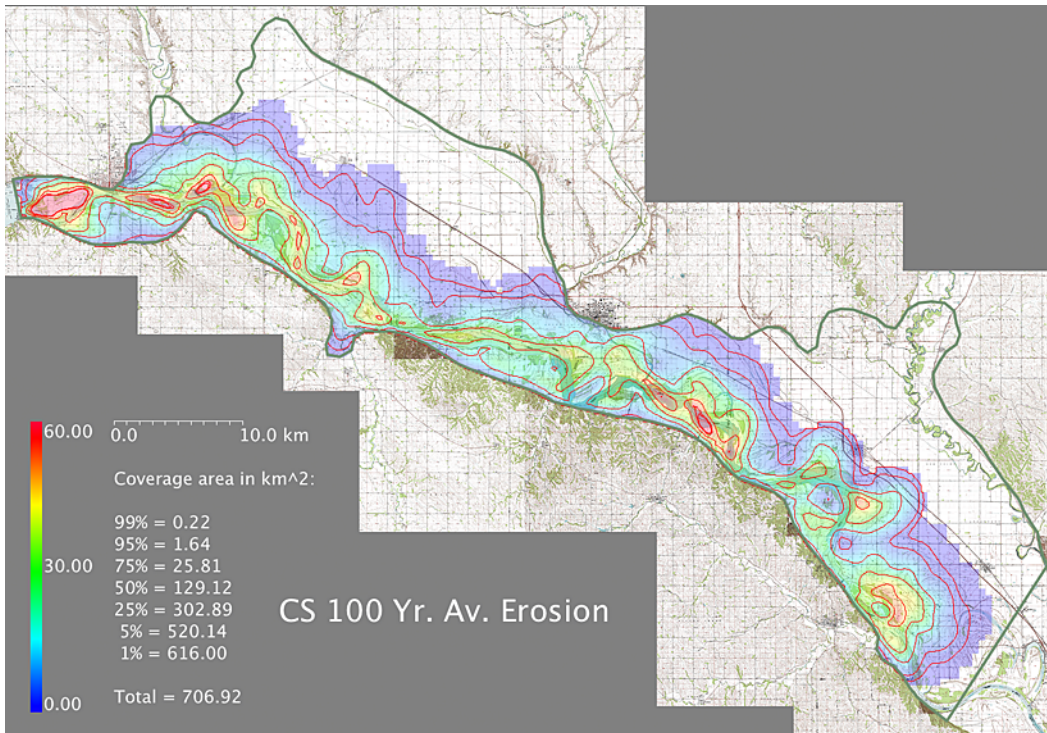
Figure 62: The average cumulative erosion in hectares of 540 Circumferential Speed simulations overlaid on the topographic map mosaic, with contours showing the areas having 99%, 95%, 75%, 50%, 25%, 5%, and 1% of the maximum erosion.

4.6.1 Instabilities

We have already remarked that several of the JP89 simulations show instabilities consisting of a short sequence of equal-amplitude and equal-wavelength oscillations, usually near to the inlet end of the river. We have speculated as to the possible causes of these instabilities in section 3.4.2.3, but we do not actually know the reason for them. They appear to be a resonance caused by the interaction of the JP89 method with the local river width and other parameters, as they usually occur only for wider, less active rivers.

We have also noted previously that the JP89 method often needs to 'get up to speed' with a downstream distance of several km from the inlet before the u1b values stabilize and proper meandering behavior sets in. This suggests that a phase delay in the integral equations may be responsible for causing constructive interference at some particular frequency of motion at a particular downstream distance, again due to a unique combination of river width and activity. The overall effect is that the water seems to 'bounce back and forth' from one bank to another until the conditions of resonance cease to affect the migration.

Rather than attempt to debug this situation --if at all possible-- we have elected to leave the instabilites as they are for 2 reasons:

1. They don't seem to affect the downstream shape of the river once they die out.
2. They only occur with visible effect in a small fraction of the simulations.

Below is a histogram of the maximum lengths of these instabilities (the number of sequential oscillations) found in all 3072 JP89 simulations, and a plot of instability length vs. the erosion rate and vs. maximum width. Note that instabilities occur predominantly at the lowest erosion rates, and the greatest widths.
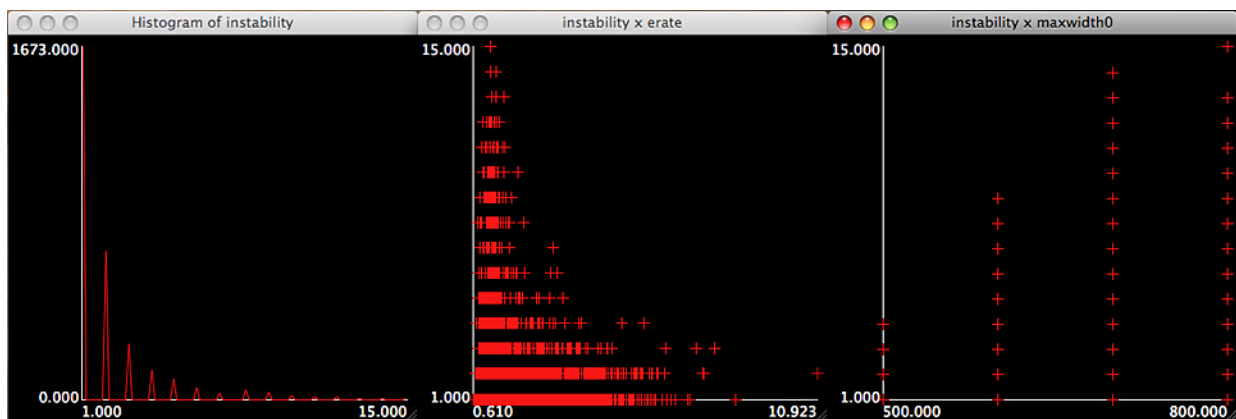
Figure 63: Histogram of all instabilities, and instabilities with respect to erosion rate and maximum width.

```
Top 10 instabilities:
  i           file  instability        erate  maxwidth0          depth            flow           diam          sdist         erate0
--- --------------  -----------  -----------  ---------  -------------  --------------  -------------  -------------  -------------
  1    run2572.mnrr           15     1.158797        800       3.000000     1200.000000       0.000750       1.000000       1.200000
  2    run1820.mnrr           14     1.310471        700       3.000000     1400.000000       0.000750       1.250000       1.200000
  3    run2000.mnrr           14     1.163723        700       3.250000     1200.000000       0.000750       1.250000       1.200000
  4    run1588.mnrr           13     1.185810        700       2.750000      800.000000       0.000750       1.000000       1.200000
  5    run2449.mnrr           13     1.535519        800       2.750000      800.000000       0.001250       0.750000       1.800000
  6    run2588.mnrr           13     1.305311        800       3.000000     1400.000000       0.000750       1.250000       1.200000
  7    run1636.mnrr           12     1.286136        700       2.750000      800.000000       0.001000       1.000000       1.200000
  8    run1741.mnrr           12     1.070309        700       3.000000     1000.000000       0.000500       0.750000       1.800000
  9    run1922.mnrr           12     1.403860        700       3.250000      800.000000       0.000500       0.750000       2.400000
 10    run1964.mnrr           12     1.115818        700       3.250000     1400.000000       0.000500       1.250000       1.200000
```

Table 12: 10 rivers having the greatest number of instabilities.

Shown below are the number and fraction of all simulations having instabilities up to a given length. Note that there are no rivers with zero instabilities. Two rivers having instabilities of length 4 (which are virtually invisible to the eye) are also plotted below. These cases account for more than 90% of all simulations.

Figure 64: Single river with the most instabilities (15, left), one example of 1673 rivers with only 1 instability (right).

```
Instabilities <= 15: 3072 (100.00 %)
Instabilities <= 14: 3071 (99.97 %)
Instabilities <= 13: 3069 (99.90 %)
Instabilities <= 12: 3066 (99.80 %)
Instabilities <= 11: 3055 (99.45 %)
Instabilities <= 10: 3041 (98.99 %)
Instabilities <=  9: 3022 (98.37 %)
Instabilities <=  8: 2990 (97.33 %)
Instabilities <=  7: 2948 (95.96 %)
Instabilities <=  6: 2919 (95.02 %)
Instabilities <=  5: 2866 (93.29 %)
Instabilities <=  4: 2772 (90.23 %)
Instabilities <=  3: 2637 (85.84 %)
Instabilities <=  2: 2373 (77.25 %)
Instabilities <=  1: 1673 (54.46 %)
Instabilities <=  0:    0 (0.00 %)
```

Table 13: Number and percentage of all simulations having specific numbers of instabilties, or less.

Figure 65: Two rivers (out of 2772) with 4 instabilities.

For this study, we would have liked to be able to reproduce a range of river simulations that, with the appropriate choices of input paramters, could be made to resemble the MNRR as it was 115 years ago, before human intervention and management began to change and constrain its shape, and which could also be made to resemble the river as it is today, using the same physical model. The basic shape of the 59-mile segment of the MNRR hasn't changed all that much in 115 years, although it has lost much of the braiding, multiple channels, and larger loops it had then, and it appears today as like a somewhat tamer sibling of its former self. Nevertheless, we felt that it should be possible to capture the range of the geometry and the dynamics of both rivers using different simulations which were only variations of the same model.
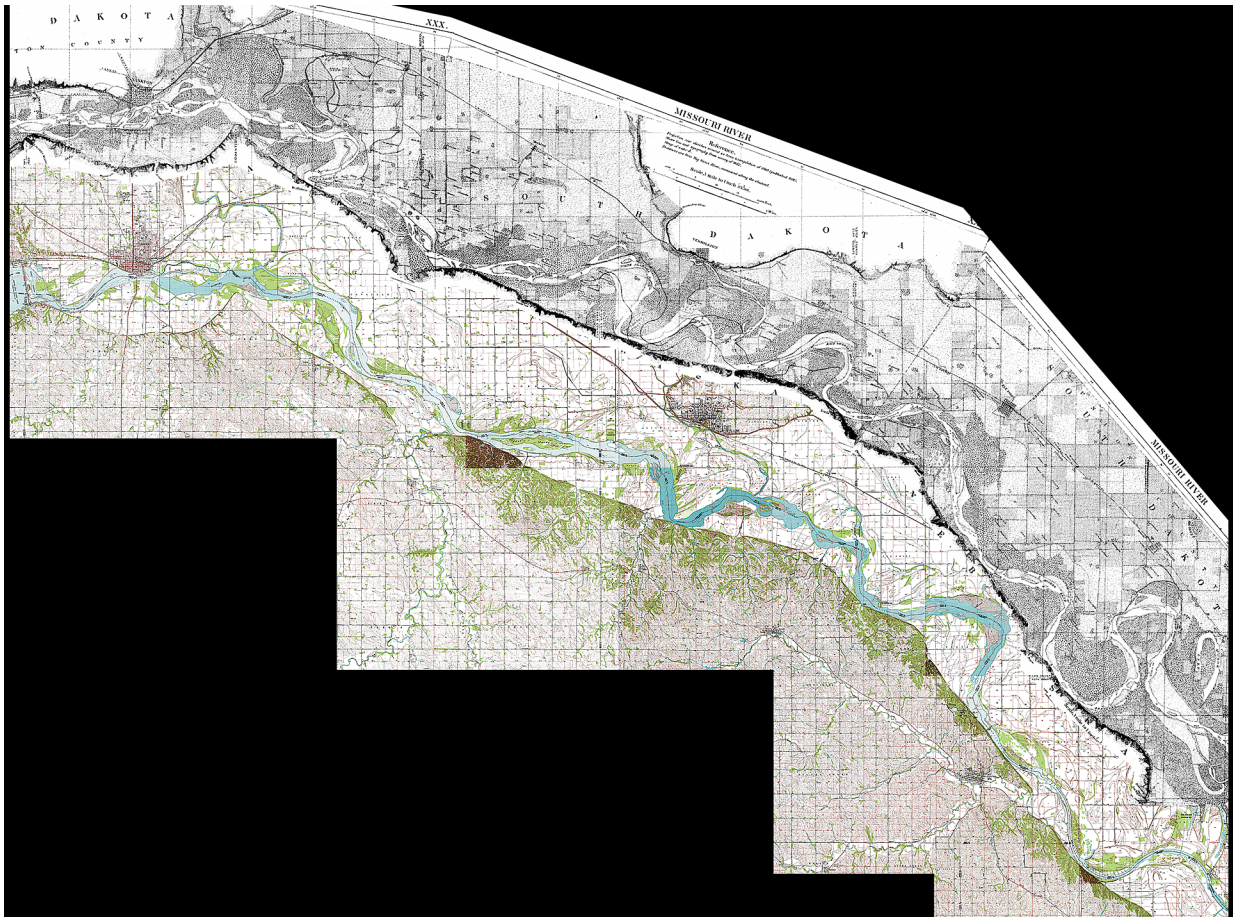
Figure 66: The 59-mile segment of the MNRR as it was during the 1890s and during recent time. Mosaic made from Missouri River Commission maps at http://aa179.cr.usgs.gov/1894maps/.

Single-channel meandering models which make use of uniform channel width and bed material, and only rudimentary use of variation in bank resistance to lateral migration, such as the Johannesson-Parker 1989 model employed in this study, are the current 'state of the art' in channel migration models. Such physical models represent a significant improvement over simpler approaches that ignore channel dynamism and make use of geometry alone. Models that ignore such dynamism are suitable only for highly constrained channels with hardened banks and are typically of limited usefulness in the context of wild and scenic rivers such as the MNRR, because dynamic channels are the norm rather than the exception for these rivers.

Nevertheless, the JP89 method does not really produce simulation results that look much like the MNRR, neither of today nor of 115 years ago. This model does produce somewhat 'river-like' meandering loops, compound bends, and cutoffs, but they don't have the same 'flavor' as the features found in the MNRR, and are considerably more 'generic' looking. Given a selection of images of real rivers to choose from, and a set of JP89 simulations produced with different input parameters, it would be difficult if not impossible to match simulations to reality in any one-to-one systematic way, and candidates for such matches would not be particularly convincing. Other meandering methods (for example, the Circumferential Speed method) produce similarly disappointing results.

When we originally compared observations of the MNRR from the maps and satellite images to initial tests of the meandering methods, we predicted that the JP89 method would not produce very realistic simulations for this river. It is clear from the maps and images that the MNRR violates both the requirements and the basic principles of the JP89 method: that the flow is always faster on the outside radius of curves, and that material is always eroded there and then deposited on the inside radius. The MNRR is generally very wide, has very unsymmetric banks, a very non-linear bed depth profile, and often a shallower bed depth at the outside radius of curves, where material has accumulated rather than eroded. This may follow partly from the hypothesis that the primary flow is confined to a narrow off-center region which is not well delineated by the actual banks, especially in wide segments of the river.

Nevertheless, by virtue of using a range of different input parameter combinations, the JP89 method can produce a wide variety of river geometries which we thought were sufficient for the 'proof of concept' of this project, namely that predictions about the MNRR could be made by using a large population of simulations. These predictions would employ many simulations (e.g., thousands) over a constrained parameter space and would thereby also provide 99% to 1% confidence limits on the predicted quantities, specifically the range of migratory motion of the actual river. Such confidence limits aim to provide practical estimates of reasonable uncertainty for future resource managers, but the disadvantage of this approach is that these limits provide an incomplete picture of the process of river migration because of the inability of state-of-the-art models to adequately capture important aspects of reality.

Within the population of runs, simulations performed at the nominal erosion rate of 1.2 ha/yr/km are not very revealing, as the range of migration is quite low, and the rivers produced generate few if any new loops or cutoffs, whereas comparisons of the 1890 and 1959-1996 maps indicate that the river should migrate by several km or more on average at each point, and produce a dozen or so new loops and cutoffs during 100 years. However, simulations with exaggerated migration rates of 2x to 3x the nominal rate are of considerable visual interest, even if they do represent potential overestimates of the river motion during the next century. Making use of such exaggerated simulations might be called a 'dramatization' of the evolution of the river over the next 100 years, or, an indication of what might happen if circumstances conspired to create and sustain greater than average migration rates which were not adequately managed by human intervention.

By combining individual simulations which are clearly underestimates of the likely river migration, and others which are clearly overestimates of that motion, as well as many more which are neither, it becomes possible to delineate at what point the evolution of the river becomes untenable, and therefore potentially dangerous to established human habitation and other property. The "100 year migration corridor" visualizations of section 4.4 are quite compelling, not only because they are actually interesting, but because

some parts of the river appear quite "wilder" than others, with wider migration-prone areas, often in just those locations where we might expect them to be --especially near the extrema of current bends. The fact that the locations of these wider areas in the common coverage array are consistent with our expectations is an indication that the methodology has succeeded. Furthermore, the fact that there are regions of both wider and narrower migration indicates that river managers must look past a simplistic, uniform-width buffer management strategy.

5.2 Appropriateness of meandering methods chosen

Although it is a 'physical' method, we are not completely happy with the Johannesson-Parker 1989 meandering model, especially for use on the MNRR, and are somewhat disappointed that such a complex model involving 2 second-order integral equations performs so poorly. On the other hand, we are pleased that such a simple meandering method as Circumferential Speed works well to generate typical meandering behavior from geometry alone, but we acknowledge the need for a more realsitic method that makes use of the necessary physics. Perhaps there is a way to combine the two. Our intuition is that the best practical method will be a simple physical model which may also be second-order in either integration or differentiation, but our bias given our experience during this study is toward a mass, force, and acceleration-based model rather than, or perhaps in combination with, one based on bank flow speed.

Now that we have created an efficient way to test different meandering models, it seems natural to try some others in the context of simulating the migration of the MNRR. However, we suspect that, based on the outcome of this project, it will not be possible to find the 'one true' meandering model which is best above all others under all circumstances, but that it might be possible to modify or extend an existing model (like JP89) sufficiently to fit measured data for the MNRR. To do so, we would need access to depth, flow, and bed composition data far in excess of the detail that we have now. One of us (Jacobson) has access to contemporary hydraulic data and additional historical data for the river, which would enable us to model variations in flow over the simulation time. During this study, depth was set to a constant for the entire river, but we require access to more complex bathymetric data and models in order to properly model the channel and bed, which should also include cross-stream depth profiles, as it is evident from the maps and satellite images that the MNRR is definitely not an idealized trapezoidal channel.

Furthermore, in many places the width of the river which is calculated from the digitized banks is likely to be considerably in excess of the actual flow width, due to the presence of bars and other shallow areas, and the deep flowing thalweg may be far from the calculated centerline. In the simulations performed for this study, we have 'clipped' the river width to a maximum value of 800 m and below, partly because we think that this is more representative of the actual meandering width, especially in segments where we have disregarded islands, shallows, and multiple channels in the digitization (although the JP89 model also crashes for larger widths). We hypothesize that the water surface and bank widths are a deceptive kind of 'event horizon' which hide the fast-flowing, narrow, submerged conduits which are actually responsible for sediment exchange and river migration. A consequence of this hypothesis is that there may be another sinuous planform beneath the visible planform, and that the surface width of the river may be just the 'hull' or 'envelope' indicating the range of the active submerged planform.

We believe that the single-thread meandering model used in this study is clearly not adequate to accurately

represent a river such as the MNRR, primarily because:

1. It reduces the geometry of the river to a single idealized channel defined by a centerline and width and having a trapezoidal cross-section.

2. It does not track the transport of sediment within the water from where it is eroded from the banks or bottom to where it is eventually deposited downstream.

3. It does not provide appropriate feedback mechanisms whereby the erosion and deposition of sediment changes the geometry of both the river bed and the flow.

We propose to develop a meandering model which takes these issues into consideration, by (a) modeling the cross-stream depth and flow profiles as other than linear gradients so as to better represent both shallow, slow-moving flows near the banks and faster, deeper flows away from the banks, (b) tracking, at least on a cross-sectional basis of stream distance s, the transport of sediment within the downstream flow, and (c) changing the geometry via erosion and accumulation of each bank independently of one another, rather than as a single idealized centerline, width, and flow. We further hypothesize that there may be several narrow, eroding, and sediment carrying 'cores' submerged within the observable banks and water surface of the MNRR, and that these multiple threads are responsible for the actual geometry and dynamics of the river.

To accomplish this will require modifying the meandering program:

* To represent the river as a macroscopic entity and extended 3-dimensional system rather than as a purely 1-d idealized geometric object.

* To incude support for variable widths and depths, depth and flow speed profiles, and the inclusion of islands and bars in the stream, separated by a small number of short alternate paths (e.g. 'chutes').

* To interface and integrate the river banks and bed, and the meandering motion of both, with the surrounding topography.

To accomplish these goals, we propose to combine the vector-based meandering models we have been using in this study (which are based on a serial discretization of river coordinates which can migrate continuously across an xy domain) with a grid-based domain which represents the banks, surrounding terrain, and submerged bed. This hybrid approach might allow us to avoid the necessity of keeping track of the bank coordinates (and all the computational bookkeeping this entails) as bifurcations, islands, chutes, and braids, etc... form, while one or more contiguous high-speed cores flow and meander across the submerged grid in a manner similar to which the single river does at the surface in the current simulation. This might also allow us to model the depth of the water at each {x, y} point, so that shallows could form away from the active threads.

Initially, threads would not interact with one another, as if they were distributed in 3-dimensional space, which would avoid additional computational bookkeeping. Threads would meander via two potentially different processes: one when they are away from the banks and surrounded by water, and another when they contact and erode the banks --the key difference being that while fully submerged the resistance to migration would be considerably less than when contacting a bank. This might promote the 'meander within a

meander' patterns we hypothesize leading to the formation of larger surface loops out of smaller submerged loops, and to the overall migration of the composite channels, and the appearance and disappearance of bars and other shallow areas, as a collaborative effect of these threads.

5.3 Material properties of simulation domain

In this section we want to say a bit more about three decisions that were made concerning some of the material properties of the river, the valley, and the boundary, apart from the values of the physical input parameters which were chosen to generate the large population of simulations used in this study. These involve some simplifications which were made and which probably have had no adverse effects on the results, but we wanted to anticipate questions that might arise due to these decisions. The three decisions were to:

1. Fix the inlet end of the river, but not the outlet at Kensler's Bend. This has often resulted in making the 'tail' of the river look qualitatively different from the rest of the simulated river. There are two basic reasons for this difference:

   A. The Ponca end of the river is less than 300 m wide (whereas the average is over 700 m) and is not fixed. Therefore it naturally migrates with more activity, and as it lengthens, additional intermediate points are added with the same smaller width. This effect accumulates over 100 years, often resulting in long thin tails on the rivers at that end. However, although the activity of the Ponca end of the river might be higher than average, and the resulting geometry more sinuous, this does not seem to have affected its migration range or coverage area, which is similar to the rest of the river.

   B. As we have already noted, it is an adverse property of the Johannesson-Parker 1989 method (a double integral based on the distance s) that the downstream end of the river usually meanders more than the upstream end due to higher than average far bank speed perturbations, generally with increasing activity along s. Conversely, we had also wondered why points on the river near to the inlet end were moving so little, and were often taking on a linear or circular geometry rather than the normal meandering loop shape. This is due to the lower than average far bank speed perturbations at that end of the river.

   As an alternative, we could fix both ends of the river, although this would not solve the problem of higher than normal u1b values near the outlet end. Another alternative might be to truncate the river once the width narrows at the Ponca end, and thereby eliminate the elongated 'tail' before it has a chance to form. Our preference, however, was to see what this end would do if it were not constrained by the concrete walls and dikes of Kensler's Bend. From looking at the 1890 maps, and the legacy oxbows in the 1957-1996 maps and 2006 satellite images, it appears that this is the part of the MNRR where most of the meandering motion occurs.

2. Model the erodibility of the surrounding valley as a homogenous constant everywhere, and base that erodibility on the measured erosion rate. Most likely, there is a way to account for differences in material within the valley and to infer quantitative differences in those materials from published information. However, this would have required significant additional work and was not thought to be appropriate for this stage of the project. Currently the valley is modeled as a flat homogenous surface having isotropic and

constant material properties. Actually, these properties are just inferred from the average erosion rate of the river, rather than being calculated distinctly at each point.

We have accumulated 2-dimensional arrays showing where, when, and how much erosion takes place at each point in the valley. An estimate of the cumulative material eroded from any point in the valley is also available and plotted along with the common coverage array in section 4.4. It would be possible to set the migration rate to different values (or percentages of the same initial calibrated value) at different points within the valley, including points near to the boundary walls, so that there could be programmed regions of higher or lower erodibility. However, this would represent additional complexity over and above the base scenario we wished to perform for this project. Now that we have performed and analyzed the homogenous base case, such variations of material properties in {x, y}, or in time, would be appropriate for an additional study.

3. Limit the migration of the river to within 'hard' boundary walls which enclose the valley. As discussed in (2) above, there is probably a way to have some finite erodibility at the valley margins. However, at present the boundary walls are both 'hard' and 'impermeable'. That is, all points which migrate outside the boundary, or to within 1/2 river width of the boundary, are moved back inside the boundary and at least 1/2 width away from it, along a vector perpendicular to the closest segment of the boundary. We have taken some steps to try to ameliorate the adverse effects of the straight line segments of the boundary which induce zero curvature in near river segments (for example, by allowing the river to maintain some variation in width up to a maximum amount).

The boundary is homogenous everywhere, although in reality there are two types of limit: the high valley walls which are primarily to the south which do form an impenetrable barrier over a 100 year timescale, and the 1200' topographic line to the north and up several canyons which break up the north walls. Although the river could potentially erode past the 1200' line, it is unlikely to do so, and is unlikely to reach this line, within 100 years. Also, the inlet is well below this elevation (at 1163.91'), so that such erosion would create well-defined cliffs which are not in evidence in either the 1890 or 1957+ maps. Nevertheless, making both the boundary and the interior of the valley heterogenous in their material properties would be a logical next step as part of an additional project.

5.4 Indications for future research --
5.4.1 Separability of simulation framework, meandering methods, and database of results

In this section we wish to reiterate the modularity of the software which was written for this project, both at the program level and at the code level. The programs which were created can be divided into 3 classes:

I. General purpose programs which could potentially be used in other projects:

1. Digitizing river (or other) coordinates; calculating river centerline and width.
2. Displaying Digital Elevation Models (DEMs) as images.
3. Displaying DEMs as 3d surfaces.
4. Converting {longitude, latitude} to {x, y} coordinates.

II. Programs which were designed specifically for simulating meandering rivers which may have been digitized using program (1) above:

5. Testing meandering methods.
6. Simulating one instance of the MNRR or another river. (This program can also run multiple instances through the use of command files.)

III. Special purpose programs which could be adapted for analyzing the results of other simulation projects:

7. Accumulating information to construct the river database.
8. Performing queries on the river database.

In particular, we wish to point out that:

* Programs (1-4) could easily be adapted for other GIS projects by a scientific programmer who is familiar with Python.

* The meandering code used in programs (5) and (6) is quite modular, and so could be (and was) replaced with other code performing a similar function and using the same programming interface without modifying the main programs.

* Although program (7) was designed to collect information that was specific to the simulations that were performed for this study, program (8) could, with minor modifications, be used with other database tables to provide a structured query and analysis interface, including the ability to create graphical output of results. This program in particular is potentially adaptable for use in a remote, client-server architecture, such as from a web-based Python program over an Internet connection, accessed from a browser such as Firefox.

While these programs are all available for use by interested parties from the website listed in section 2.4, there was insufficient time available during this project to make them 'user friendly' to individuals who are not familiar with Python programming. Nevertheless, modifications to improve general accessibility and utility would be well worth a modest investment during a subsequent project.

5.4.2 Variation of input, domain, and boundary parameters

Although 3612 different combinations of input parameters were used to generate the large population of simulations used in this study, there were many simplifications performed to select these values. For example, whereas the width of the river was accurately measured from the digitized banks, it was discovered that this information could not be used with the Johannesson-Parker 1989 meandering model, and the width had to be attenuated to a maximum of 800 m. This was not seen as a significant problem, however, as for independent reasons it was surmised that the full width of the digitized banks were in excess of the actual meandering channel. Further studies would presumably benefit from the ability to make use of the original geometric information without modification, should a suitable meandering method capable of utilizing it be employed.

In addition, the depth, flow, bed grain diameter, and other input parameters were all held constant over the entire length of the river for the duration of the simulation. While the erosion rate was allowed to vary during the course of the simulations, it was initialized to a specific average value for the entire river at the beginning

of each simulation. These simplifications were not considered to be deleterious to the present study, which was intended primarily as a 'proof of concept' of the possibility of predicting a migration corridor from available information and contemporary meandering models. Nevertheless, further studies would benefit from the ability to:

* Vary the input parameters both along the length of the river and also during the course of the simulation. In particular, seasonal or planned variations in water flow should be permitted to see what effect they have on migration, and what time delay between changes in flow and changes in the resulting migration might exist. Variations in flow could either be pre-programmed as part of the simulation, made while the simulation was in progress from the user interface, or modeled as stochastic effects of weather or other unforseen events. Similarly, river depth and the other input parameters should be allowed to vary in both space and time. Currently the {x, y} coordinates and width of the river are specified as columns of text input data. It would be a logical extension of this format to specify the depth, grain size, or any other input parameter which varies according to stream length in this manner as well.

* Vary the material properties of the valley. As stated in section 5.3, the erodibility of the valley is currently the same constant value everywhere. The next step would be to specify different values as either continuous variables over {x} and {y} locations, or as a set of discrete values at individual points, along specific curves, or within enclosed regions in the valley to represent artificial fortifications or other devices/structures designed to retard or promote erosion and thereby alter the motion of the river. These values could also be pre-programmed to change in a systematic way with respect to time in order to, for example, model seasonal variations in erodibility due to temperature, surface water content and runoff, or ground cover and vegetation, or they could be modeled as discrete extraordinary events.

* Vary the material properties of the boundary. The location, elevation, and erodibility of the simulation boundary could be varied by pre-programming or user interaction during the simulation in order to answer 'what if' questions about the potential range of motion of the river based on existing limits such as bedrock, or proposed limits such as new concrete walls or wing dykes. Using a technique similar to that employed in the current study, many slightly different simulations could again be performed to see what aggregate, probabilistic effects proposed changes to the valley boundary, or from the addition of other boundary elements within the valley, might have on river migration. Some boundaries could be allowed to remain 'hard', providing impassable limits to migration as they do in the current study, while others are made 'soft' in the sense that they would permit partial or controlled inundation of the river based on variable material properties.

5.4.3 Alternate meandering methods

To meet the requirements of the proposed meandering method discussed in section 5.2, we might take one of the following development paths:

1. Continue to use current 'state of the art' meandering models such as Johannesson-Parker 1989, but attempt to modify or extend them in exceptional ways to work correctly with non-ideal rivers such as the MNRR.

2. Create a new class of meandering methods which attempt a priori to better capture the physics of migratory motion within a new set of differential or integral equations which can be 'tuned'

for use with a wide variety of different rivers such as the MNRR.

3. Combine an existing meandering method with a new simulation framework so that the existing code can be reused in new modular ways and becomes part of the overall simulation, and which may interact with additional elements of the simulation to create a collaborative effect which better models a river such as the MNRR.

We have elected to pursue the third path, since we already have working code that performs well for its task, and since the modifications which we feel make sense to capture the essence of the MNRR and its underlying dynamics are a logical extension of the work we have already completed.

5.4.3.1 Multiple threads

As an indication of the next logical research step to take after the current study, we have spent two weeks working on a simple 'multiple-thread' river simulation. This new program:

* Represents the simulation domain by a square grid of points, and the river bed by a 3d surface showing the depth of the water at each grid point.

* Makes use of one or more narrow, independently meandering threads of flow, all of which are submerged within the observable banks and surface of the river, and which migrate via one of the existing models.

* Estimates sediment erosion from and re-deposition to the river bed by a simple exponential mechanism.

Although this is an initial, simplistic attempt, it is sufficient to demonstrate how the combined, synergetic effect of several discrete threads of flow might produce geometry and dynamics which are closer to what are seen in the MNRR, including:

* Multiple channels, bifurcation and merging of channels.
* 'Braiding' (a complex and changing interwoven surface pattern).
* Islands and chutes.
* More naturally sculpted 3d basins.
* Deposition of sediment to form shallows and bars.

To begin to explore the ideas listed above, we created a very simple multiple thread simulation program derived from the MNRR simulation program used in this study. It combines the vector-based meandering approach we have been using with a grid-based background which represents the depth of the river at every point (or, in this case, in every 50x50 m square). Threads meander according to the model of simple curvature (see section 3.4.2.1). At present, threads interact only through the common depth of the water (see discussion below). The migration rate of each point on a thread is based on the depth of the water at that point and in its immediate neighborhood. When a thread is surrounded by water of the same depth, it can migrate at the maximum rate allowed by its curvature. However, when the depth to one side (based on the depth of the next grid-cell in the direction of meandering) is less than that of the thread (possibly being dry land), the migration rate is attenuated by a non-linear function.

The shape of this function is based on the following ideas:

* Migration should be easiest (fastest) when the thread is surrounded by water at the same depth, and more difficult (slower, but not zero) when there is dry land to one side.

* Migration should be near the maximum rate when the depth to one or both sides of the thread is similar to the thread depth, and progressively slower as the depth decreases. Depths near to zero should retard migration nearly as much as dry land.
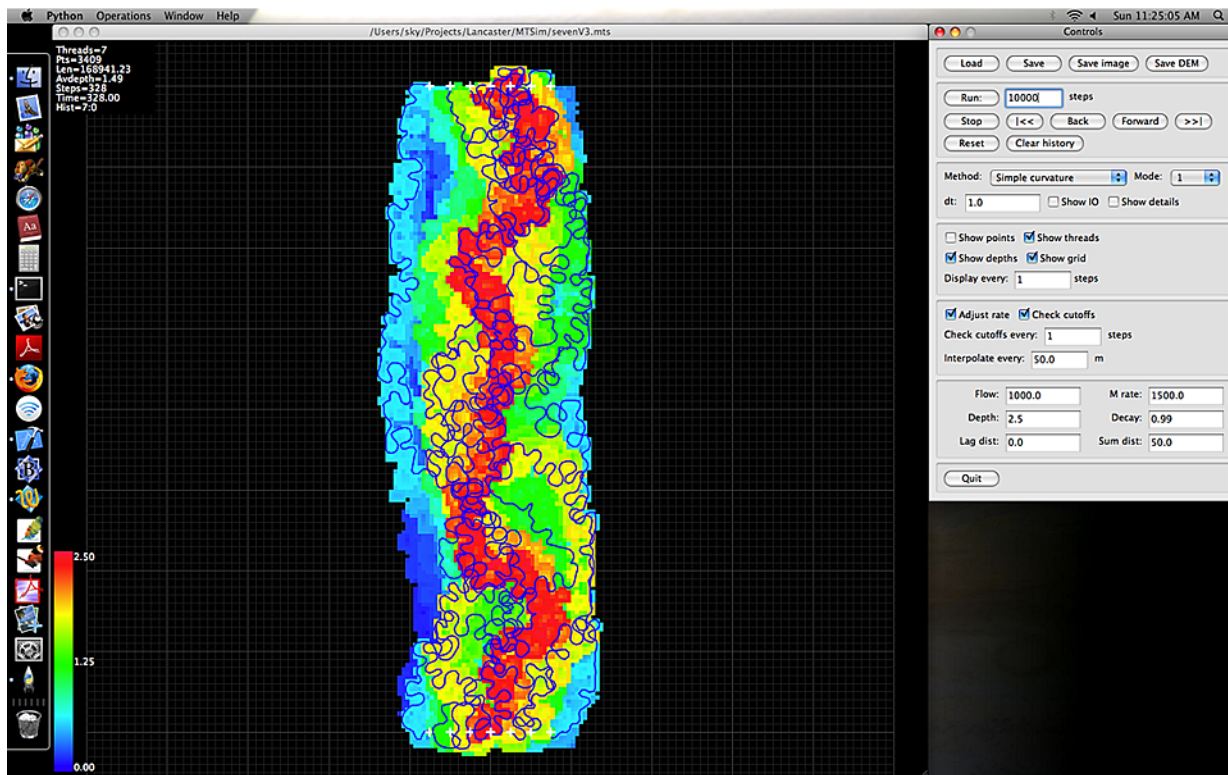

Figure 67: Multiple thread river simulation program.
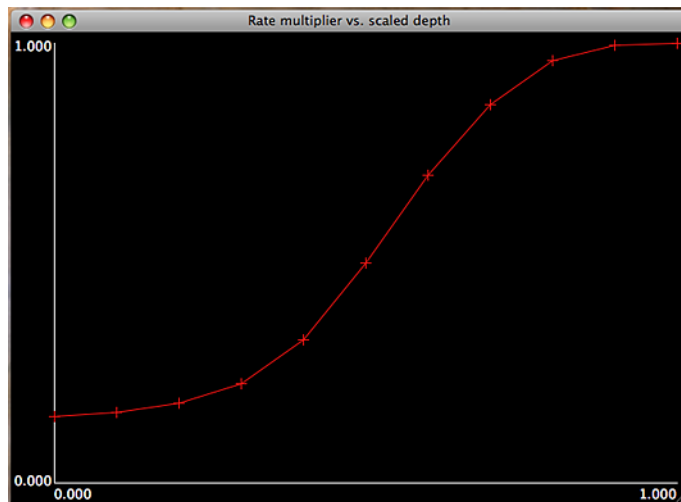
Figure 68: Non-linear function mapping water depth to thread migration rate.

It would be easy to substitute another function which maps depth to migration rate, in order to see what the effect of different functions might be. We are not modeling sediment transport directly, yet. Migrating threads 'scour' the river bed to their depth in each grid-cell that they occupy. The depths of cells not currently occupied by a thread 'decay' at a constant exponential rate, typically 0.99 (i.e. depth(x, y, t + dt) = depth(x, y, t) * 0.99). This serves to simulate re-sedimentation without having to perform all the computational bookkeeping which would otherwise be required.

In the plots that follow, loop cutoffs are removed as they happen, but are not accumulated since they occur within water. Both endpoints of each thread are fixed, as if they were connected to additional contiguous upstream and downstream segments of the river. Each square of the drawn grid is 100 m per side, although the depth and motion is calculated for every 50 x 50 m sub-square. The threads are 25 m wide. Actually, the distances are unimportant, since the particular meandering model used (simple curvature) does not make use of scaled physical quantities (e.g. flow volume), but only geometry. After each motion step, all threads are re-interpolated at 50 m resolution using circular arcs. In general, the length of each thread continues to increase during the simulation, except when cutoffs are removed.
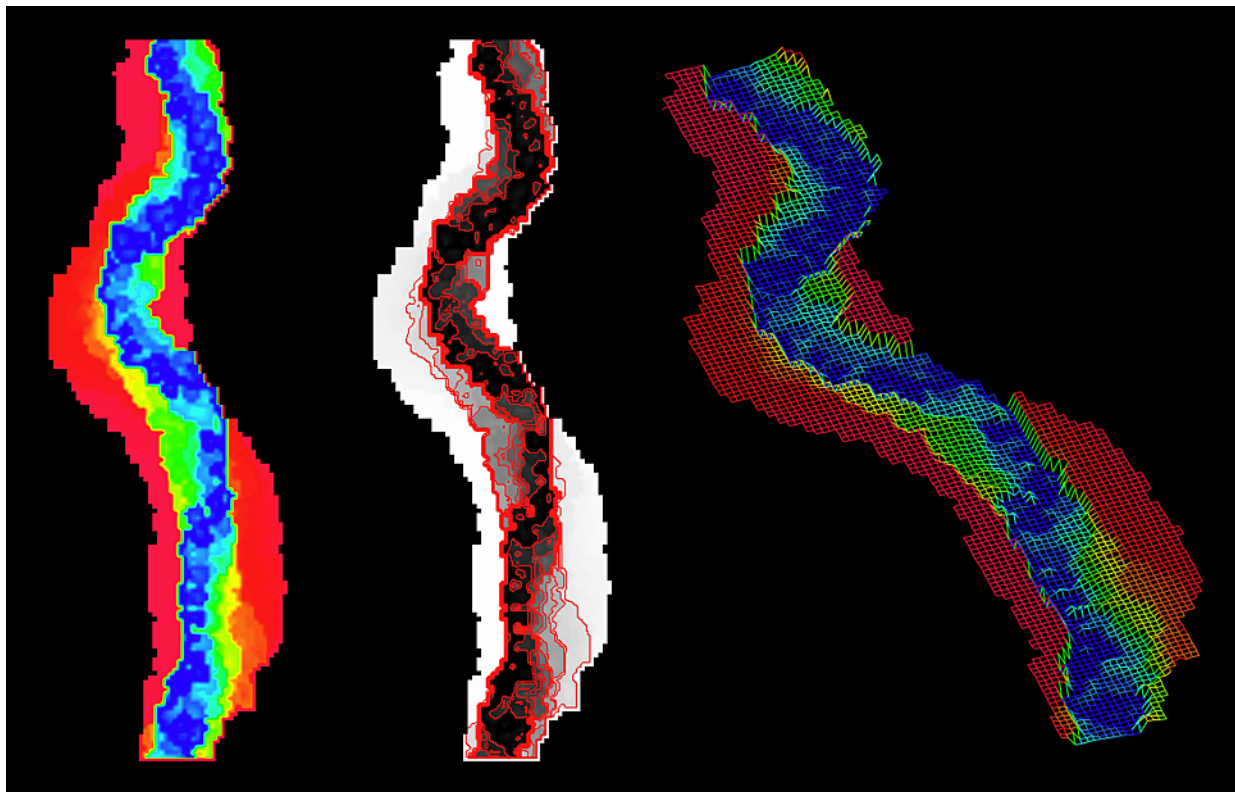
Figure 69: Single thread 'meander within a meander' pattern.

Each thread's migration rate is constrained at each point along its length by the non-linear attenuation function, depending on the depth of the water in the cells toward which the thread wishes to meander cross-stream. Therefore, it is easier (faster) for the thread to meander toward deeper water, and more difficult (slower) for the thread to meander toward shallower water, or dry land, leading to a preferential deepening of the middle of the channel. The depth of each cell occupied by the thread is set to 2.5 m, while the depths of all unoccupied cells decrease to depth(x, y, t) * 0.99 every dt, simulating the effect of re-sedimenting the river bed and banks. Currently no effort is made to keep track of or to balance the amount of sediment removed by

the thread, or replaced by the decay effect.

Shown above is an example of a single thread simulation plotted as a color Digital Elevation Model (DEM), a monochrome DEM with contour lines every 0.25 m, and as a 3d wire frame. Each DEM has been interpolated by 4x from the original 50 m grid, so that the resolution is 12.5 m (1/2 the thread width). The color of the background indicates depth (red = 0, blue = 2.5 m). A single thead with depth-restricted motion and continuous re-sedimentation will in general produce a gently meandering channel. Note that there are 2 kinds of migration going on, each at a different scale:

1. The migration of the submerged thread, which in this case is simply a constant times the local curvature of the thread, where the value of the constant changes according to the depth of the water.

2. The overall migration of the eroded chanel, which is in general both wider and considerably less sinuous than that of the thread.

The meandering of the channel in (2) is not the result of any specifically programmed meandering model, but is an indirect, aggregate, emergent process resulting from the underlying interaction of the thread and the surrounding bed and banks. Shown below are two steps from the same simulation in which 3 threads of equal depth were initialized on 'mostly straight' lines having slight random perturbations, 500 m apart. The final step configuration is also shown with depth contours and in 3d.
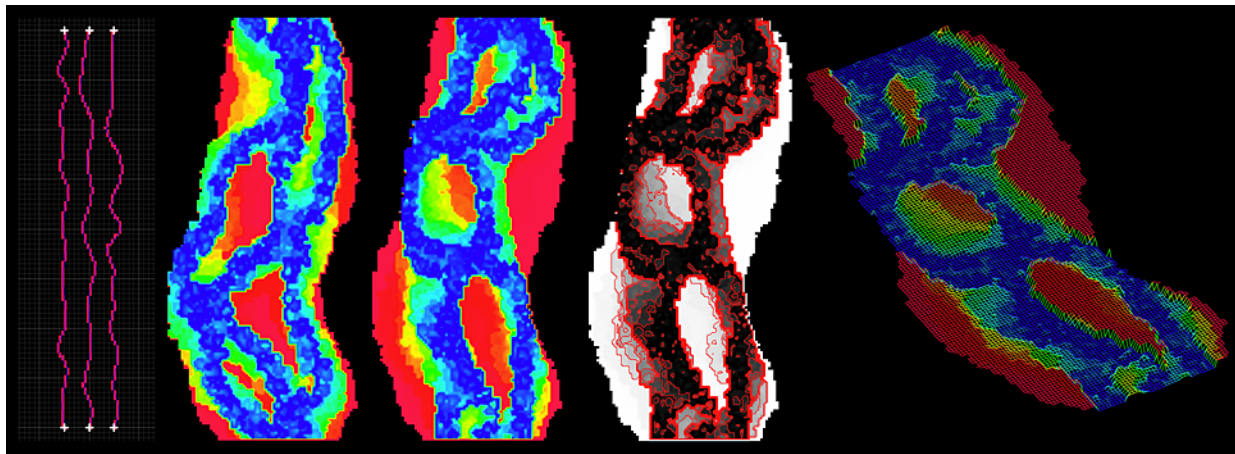
Figure 70: 3 threads forming islands and braids.

The 3 threads migrate independently of one another, and interact only through the depth background. Nevertheless, there is a tendency for threads to synergistically merge and separate due to their combined effect on the depth of the bed, and to create a braided pattern which changes over time. Note that the overall effect of several threads is to create a wide system of braids or multiple channels and islands which itself gently meanders across the landscape. Simulations were also performed with 5 independent threads having the same depth, and which yielded similar braid/island patterns.

Threads don't all need to be at the same depth, and we expect that multiple threads in a real river would be distributed in {x, y, z} space, so that they can pass one another without touching (in the current simulations, thread pair intersections are simply ignored). In the 5 thread simulation shown below, threads are created

with the following depths: {0.833 m, 1.666 m, 2.5 m, 1.666 m, 0.833 m}. Threads maintain a constant depth, and migrate at the maximum rate if the current depth is equal to or greater than their own. This adds an additional level of synergy, as a shallow thread can 'piggyback' over a deeper thread and move at the maximum rate while the deeper thread is attenuated by scouring the bottom. These threads have also been created 250 m apart (10x their width) rather than at 500 m. Simulations using threads at different depths have, in general (a) a single discernable thalweg, and (b) a more naturally sculpted basin.
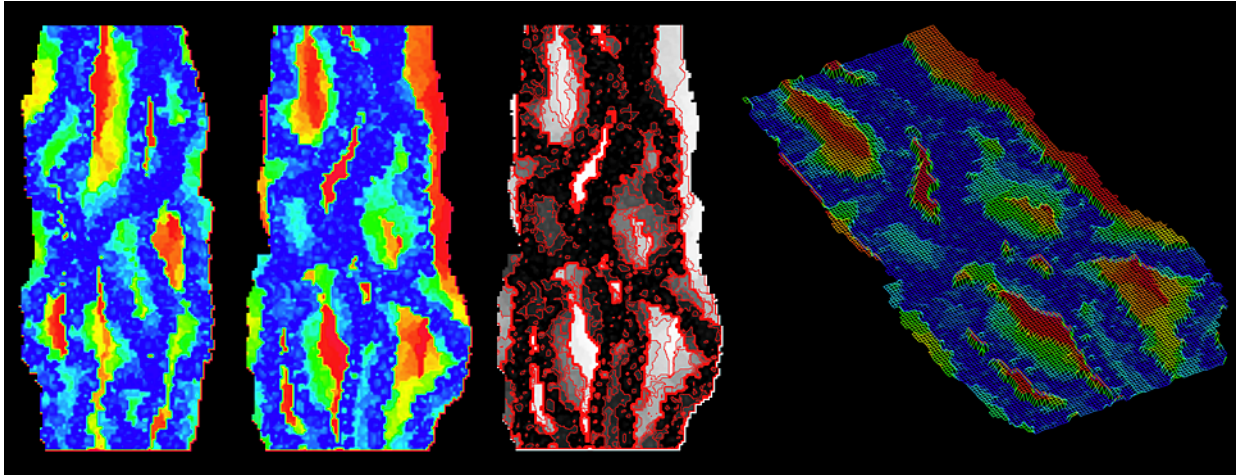
Figure 71: 5 threads forming multiple channels and complex shallows.
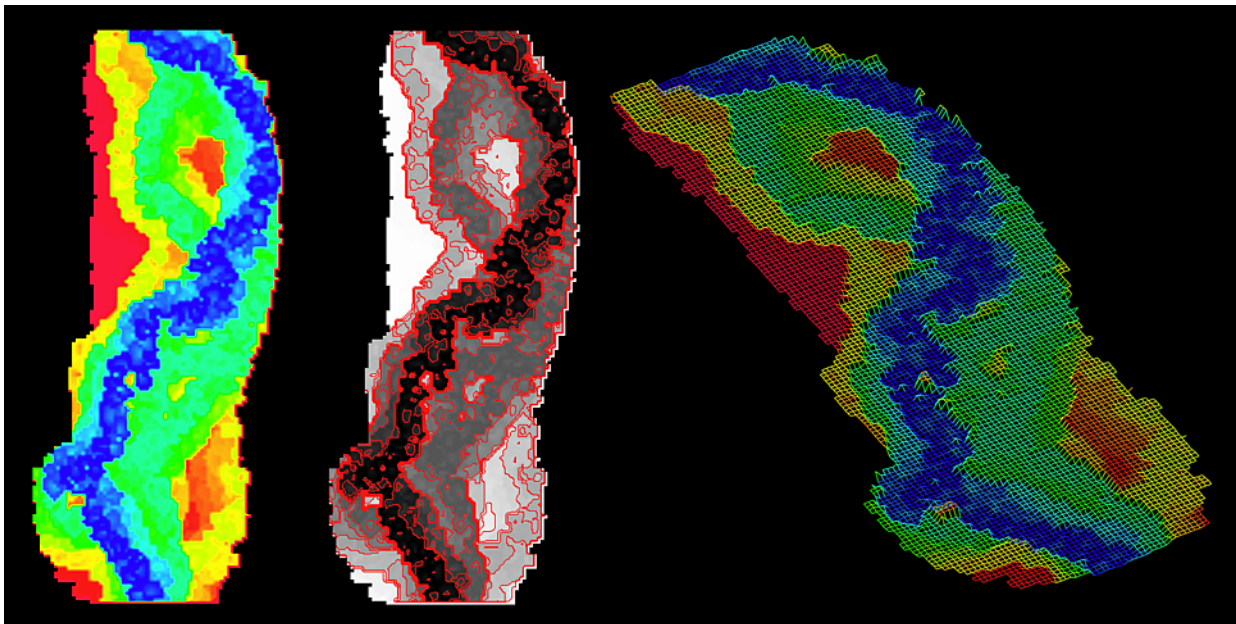
Figure 72: 5 threads of different depths forming single thalweg and sculpted basin.

The multiple-thread simulations shown here are the simplest we could think of that make use of some of the work we have already done, and that we could reasonably accomplish in only 2 weeks. Obvious improvements to these might include the following:

* The threads need to meander by some physical mechanism other than simple curvature. Actually, there should probably be two such mechanisms: one when the thread is submerged and another when it is

eroding a bank. The latter might be one of the speed-based methods such as JP89, etc... However, the mechanism for meandering within the submerged flow should probably be based on force rather than speed, in that a 'tube of water flowing within water' which creates expanding loops must:

A. Perform work as its loops increase in size (as the changing radius entails a centripetal force which acts through a distance (the changing radius)). The energy for this expansion could come from 3 sources:

   1. The speed (kinetic energy) of the flow could slow, which, for an incompressible flow such as water, would require an increase in thread radius (cross-sectional area), moving against a depth pressure which would require an additional loss of speed, and cause the thread to 'die out' quite quickly. Since we are positing long-distance-stable threads, this is not a tenable mechanism, and we are 'axiomatically' requiring the thread speed to remain constant or nearly so throughout its length.

   2. The thread could become colder (thermal energy). Actually, we suspect that this does happen, and we would like to see some relevant observations of flow speed, temperature, and depth of actual river threads.

   3. Primarily, the energy for thread motion comes from the gravitational (potential energy) difference between the river inlet and outlet. All of the simulations shown above were performed on a completely flat level plane, and assumed that the specified rate of water flow could be maintained by whatever means necessary.

B. Support a change in linear momentum wherever the thread of moving water changes direction, which must be accompanied by a change in momentum of the surrounding water (by conservation of momentum), which would in turn affect the flow field downstream. This is similar to the rationale used in the JP89 paper for describing the cause of the secondary helical vortex, but the effects must be tracked well away from the location of the thread causing them.

C. Support changes in the angular momentum of each curved, expanding thread loop, which must be accompanied by a torque at right angles to that momentum: i.e. such a thread must be forced either to be twisted, or at least to be tilted and thereby change depth at one end or the other, along any length which is both curved and accelerating (in direction), and changing in radius. This is a prediction made in addition to those proposed in the JP89 paper. (Actually, the JP89 paper is incorrect in that it predicts a torque and helical flow based on a transfer of linear to angular momentum. Correctly, the torque is only applied when there is a change in angular momentum, at the beginning and end of each bend, or when the bend changes size or orientation.)

* The threads should interact with one another. Threads could cut off one another, or they could 'cross over' like chromosomes do at their points of intersection (in which segments of threads would be exchanged). We know of no hydrodynamic reason why threads might attract or repel one another like electrical currents flowing through wires, but perhaps there is a way for them to close distance and merge along short segments. Threads must also be allowed to bifurcate and join again.

* The threads should very their depth over both time and distance, based on some mechanism which is different from that of {xy} meandering. Currently, threads maintain a specific depth, without good reason.

Actual threads should be able to change their depth depending on bed geometry and other conditions (e.g. temperature and pressure, or the torque described above). However, we suspect that the mechanism for varying thread depth in z is different from that of thread migration in x and y. Nevertheless, a suitable physical process should be sought.

* Thread velocity should be used to extrapolate a 'flow field' over the entire depth domain, which should in turn be used to calculate sediment pickup, transport, and downflow accumulation. For example, previous and unrelated work by one of us (Sky Coyote) has been used to calculate the flow of the atmosphere on Venus from Earth-based telescope images. A similar procedure could be used to calculate the vector flow (direction and magnitude) at every {x, y} or {x, y, z} point in the river basin, both near to and away from the individual threads. With this information, additional vector field calculations concerning localized sediment buildup and removal, vorticity, and departure from laminar flow could be performed, or a solution to the Navier-Stokes equations could be performed.
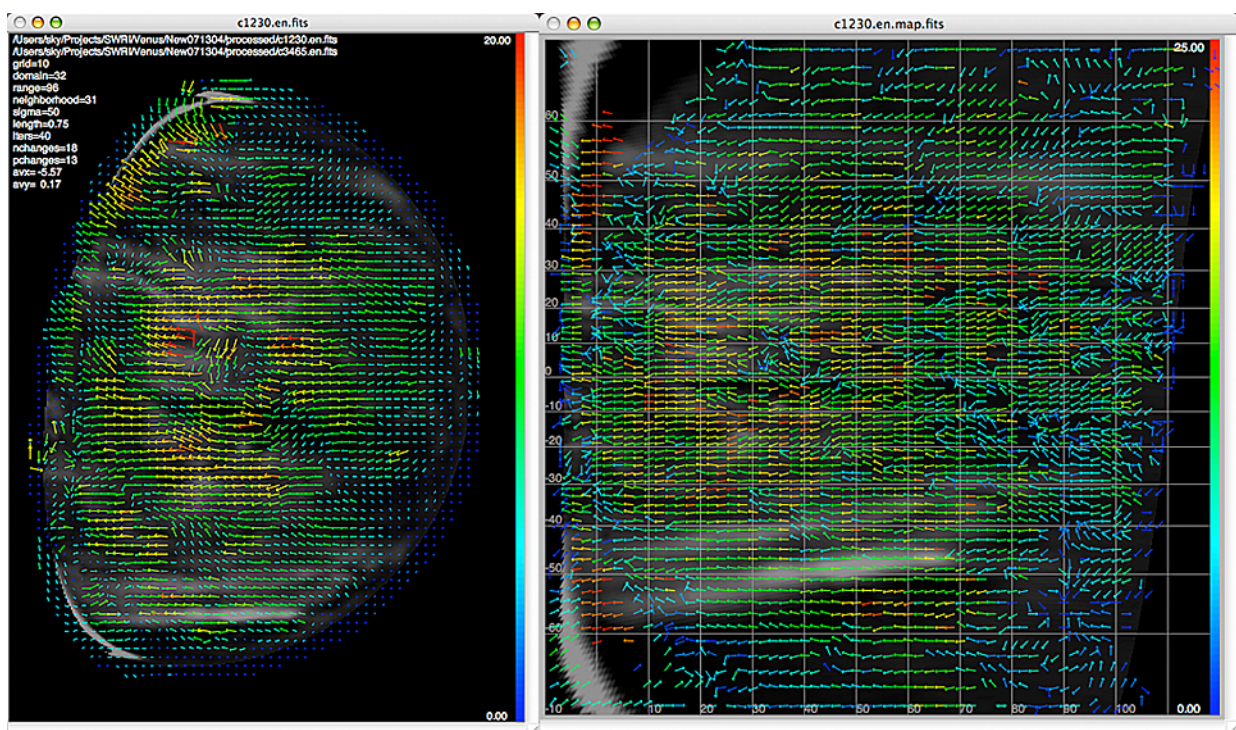
Figure 73: Vector map of cloud motion field on Venus.

* The 3d geometry of the river basin should be initialized with real bathymetric data acquired from the 59-mile segment of the MNRR. This data should include the positions of existing islands and bars, both submerged and on the surface. For initial test purposes, it is not necessary to digitize the entire length of the river from Gavins Pt. Dam to Kensler's Bend, but perhaps two or three representative full-width segments which are a few kilometers in length. If possible, 3d digitization should be performed at a resolution of about 10 m, although artificial bed and bank surfaces can be interpolated at this resolution if data is not available for all parts of the study areas. Once the simulation has been properly initialized according to the flow volumes, water sediment content, and other physical parameters appropriate to these segments of the river, the evolution of the simulation should be tracked and compared to the actual changes which can be observed in the river over timescales of from several weeks to several months, and feedback about agreement or disparity between the simulation and reality used to correct the model as it is in operation.

6.0 Conclusion

In this study we feel we have demonstrated the 'proof of concept' that a quantitative prediction can be made about the probable 100 year migration range, location, and area of the 59-mile segment of the Missouri National Recreational River, even though the meandering model used to make this prediction is not adequate to realistically simulate the detailed motion of the actual river over that time scale. Although state-of-the-art models such as Johannesson-Parker 1989 are capable of producing generic meandering behavior, they are not sufficiently specific nor detailed enough to model an actual river as complicated as the MNRR, in spite of their mathematical and physical complexity. Moreover, the basic characteristic geometry and dynamics of meandering behavior can be generated by much simpler, non-physical models which produce similar results, sugesting that the complexity of the equations used in such models does not add any significant improvement to their output.

We have attempted to use a holistic and synergetic approach to solving the main problem of this study, in that we have constructed our solution as the interaction of many individual parts (individual simulations), none of which was sufficient on its own to yield an answer, but each of which contributed a small but important part to the overall solution. Our solution reflects this methodology in that it is actually an ensemble of several different solutions, each of which is revealed by looking at the different conditions, assumptions, and input parameters which govern the underlying river system. These solutions stretch across both space (which indicate the migration ranges of fractional subsets of the aggregate solution at different confidence levels), and across time (which indicate the progression of these subsets as they migrate across the river valley during 100 years), but also across physical parameters such as width, depth, flow, and bed particle size, which in principle can be affected by human action. We have also identified the most important physical parameter responsible for the range of migration: the continuous real-time erosion rate. Although this result is not surprising, it does corroborate in a quantitative way what was only suspected (or assumed) qualitatively.

Our solution is also surprising, or at least intriguing, in that it demonstrates that the migration of the river over time does not occur at a constant rate along its length, but is instead dependent upon the local geometry and material conditions to produce distinctly different results at different places. The prediction not only of the average migration of the river, but also of the variation of that migration along its length, was an unexpected bonus to the work, as it allows differential management strategies and allocation of resources to target specific problem areas. Another important result of our solution is that it indicates, again at different confidence levels, specific regions within the river valley which are susceptible to danger from the advancing river, when they are likely to encounter this danger, and which other regions are immune from such danger. Two potential economic questions which might be answered as consequences of this information are (1) the locations where currently land-locked property will become 'prime riverfront property' during the next few years, and (2) the locations where dry land currently well away from the river may eventually be subsumed. Ecological decisions of the same kind can be applied to the management of new and existing habitats along the river, and to the planning and preparation for future habitats which may not exist for several years. Common features of our solution that are important to both sets of decisions are that it is quantitative, specific in locale, and long-term.

The methodology we have developed for this study could equally be applied to other migrating rivers, anywhere in the world. The 'defect' of the techniques we have used here --that the meandering models are

not specific enough to model the MNRR as a unique entity-- becomes an advantage when applied to other, considerably varied rivers and locations by virtue of the multiple simulation framework. Nevertheless, our own interest lies in the development of a more successful model which is specific to the evolution of the MNRR --one that makes use of the 3d geometry of the river bed and banks including all of the channels, chutes, braids, islands, and bars which interact to create this geometry, and that also takes into consideration the 3d flow of water and transport of sediment from point to point along this geometry in a simple but meaningful way. We believe that simple mechanisms, the use of accurately measured observational data, and frequent feedback about the correspondence (or the lack thereof) between simulation and reality are more important to the creation of a useful model than are complicated equations and overly-inclusive, but potentially inapplicable, physics.

This has been both an interesting and a worthwhile project on which to work for the past year. We sincerely hope that our work can be of value not only to the current generation of managers, researchers, and river-dwellers (both human and otherwise) along the MNRR, but also to several generations to come during the next century.

7.0 Acknowledgments

8.0 Bibliography

The following references represent not only sources of information used during this study, but also additional, interesting reading about the MNRR and river simulations in general.

1. Elliott, C. M., and R. B. Jacobson (2006), Geomorphic classification and assessment of channel dynamics in the Missouri National Recreational River, South Dakota and Nebraska, USGS Scientific Investigations Report 2006-5313. Geotechnical report of morphology and material properties of the MNRR. Many interesting tables, figures, and images. Lots of useful information.

2. Google Earth (website). http://earth.google.com/. Excellent source of free high quality images of the MNRR and elsewere.

3. Ikeda, S., G. Parker, and K. Sawai (1981), Bend theory of river meanders. Part 1. Linear development. Journal of Fluid Mechanics, Vol. 112, 363-377. Seminal work on mathematics of river meandering.

4. Johannesson, H., and G. Parker (1989), Velocity redistribution in meandering rivers, Journal of Hydraulic Engineering, Vol. 115, No. 8. Mathematics of river meandering. The main meandering model used in this study. Builds on the model of Ikeda (1981) above.

5. Lancaster, S. T., and R. L. Bras (2002), A simple model of river meandering and its comparison to natural channels. Hydrological Processes 16, 1-26. Mathematics of river meandering.

6. Lancaster, S. T. (1998), A nonlinear river meandering model and its incorporation in a landscape

evolution model. PhD thesis, MIT. Mathematics of river meandering.

7. Missouri River Commission Maps (website). http://aa179.cr.usgs.gov/1894maps/. 1890s maps of the MNRR.

8. National Parks Conservation Association (website), Missouri National Recreational River, http://www. npca.org/stateoftheparks/lewis_clark_trail/mnrr.html. Information about the MNRR from an ecological viewpoint.

9. National Park Service, Missouri National Recreational River, 59-mile reach guide (website). http://www. nps.gov/mnrr/59guide.htm. General introduction to and facts about the MNRR.

10. Python (website). http://www.python.org. Your first stop for everything Python. All scientists should know how to program in Python, and should use it in their daily work.

11. USGS National Map (website). http://nationalmap.gov/. Digital elevation models (DEMs) of the entire US available for downloading as data.

12. USGS National water information system, Missouri River at Yankton SD (website). http://waterdata. usgs.gov/ne/nwis/dv/?site_no=06467500&referred_module=sw. MNRR water gauge height near inlet.

13. USGS National water information system, Missouri River at Sioux City IA (website). http://waterdata. usgs.gov/ne/nwis/dv/?site_no=06486000&agency_cd=USGS& referred_module=sw. MNRR water gauge height near outlet.

14. USGS store (website). http://store.usgs.gov/. Free topographic and other maps for downloading.

15. Wikipedia, Missouri River (website). http://en.wikipedia.org/wiki/Missouri_river. General introduction to the Missouri River with history and many useful facts.

16. WxPython (website). http://www.wxpython.org. Cross-platform graphics library for Python.